



CZECH TECHNICAL UNIVERSITY IN PRAGUE

---

Faculty of mechanical engineering

Department of Automotive, Combustion Engine and Railway Engineering

Virtual design of powertrain components under consideration  
of construction space and NVH requirements

Master thesis

Study program: Master of Automotive Engineering

Field of study: Advanced Powertrains

Company supervisor: Dipl.-Ing. Christian Meissner

University supervisor: Ing. Ondřej Miláček

Helen Hedrichová

---

**Prague 2018**

## I. Personal and study details

Student's name: **Hedrichová Helen** Personal ID number: **408689**  
Faculty / Institute: **Faculty of Mechanical Engineering**  
Department / Institute: **Department of Automotive, Combustion Engine and Railway Engineering**  
Study program: **Master of Automotive Engineering**  
Branch of study: **Advanced Powertrains**

## II. Master's thesis details

Master's thesis title in English:

**Virtual design of powertrain components under consideration of construction space and NVH requirements**

Master's thesis title in Czech:

**Optimalizace členů pohonného řetězce automobilu s ohledem na zástavbový prostor, hluk a vibrace**

Guidelines:

Focus of the master thesis is the method development for virtual design of a sample side shaft and dual-mass flywheel for a plug-in hybrid with front-wheel drive under consideration of the available construction space, stress and NVH requirements by determining and optimizing key parameters and the final creation of a calculation algorithm. Tasks:

- Research about half shafts, types, dimensioning, dual-mass flywheels, types, characteristics, key parameters, function, impact and behavior for different operating conditions
- Description of NVH in hybrid vehicles under different operating conditions
- DMF design and calculation (especially bow springs) with respect to installation space limits
- Induction to NVH evaluation methodology in 1D mbs (defining meaningful phys. quantities, evaluation method)
- Creation of hybrid powertrain as 1D torsional mbs model with characteristic properties. Modal analysis.
- Time domain analysis of pertinent operating conditions of hybrid powertrain (engine start, idle drive/rattle, load change, part/full load drive) and its NVH conformable evaluation. DMF optimization to improve behavior in operating conditions

Bibliography / sources:

\_\_\_\_\_

Name and workplace of master's thesis supervisor:

**Ing. Ondřej Miláček, Department of Automotive, Combustion Engine and Railway Engineering, FME**

Name and workplace of second master's thesis supervisor or consultant:

\_\_\_\_\_

Date of master's thesis assignment: **20.03.2018** Deadline for master's thesis submission: **20.08.2018**

Assignment valid until: \_\_\_\_\_

\_\_\_\_\_  
Ing. Ondřej Miláček  
Supervisor's signature

\_\_\_\_\_  
doc. Ing. Oldřich Vitek, Ph.D.  
Head of departments signature

\_\_\_\_\_  
prof. Ing. Michael Valášek, DrSc.  
Dean's signature

## III. Assignment receipt

The student acknowledges that the master's thesis is an individual work. The student must produce her thesis without the assistance of others, with the exception of provided consultations. Within the master's thesis, the author must state the names of consultants and include a list of references.

\_\_\_\_\_  
Date of assignment receipt

\_\_\_\_\_  
Student's signature

Statutory Declaration

I declare that I have developed and written the enclosed Master Thesis completely by myself, and have not used sources or means without declaration in the text. Any thoughts from others or literal quotations are clearly marked. The Master Thesis was not used in the same or in a similar version to achieve an academic grading or is being published elsewhere

In Prague, the 19<sup>th</sup> August 2018

.....

## Acknowledgements

I would first like to thank my thesis advisor in the company IAV M.Sc. Arndt Meyer for the first part and Dipl.-Ing. Christian Meissner for his great support during the second part of the thesis, for his objective and calm manner in all situations. He was always opened whenever I ran into a trouble spot or had questions about my writing.

I would also like to thank Ing. Ondřej Miláček, my advisor of the Faculty of mechanical engineering at CTU in Prague, for his quick responses and valuable contributions and notes to the master thesis which were steering me in the right direction when necessary.

Finally I must express gratitude to Dipl.-Ing. Soeren Franke, who gave me the chance to write the work within the company IAV and even though having little time by himself, spent long moments reviewing my work and giving me advice.

## Abstract

This Master thesis focuses on the virtual design of powertrain components under consideration of construction space and NVH requirements. In the first part of the thesis an introduction of hybrid vehicles, half shafts and dual-mass flywheels can be found. Calculation for a half shaft and DMF design has been proceeded, both considering a given installation space. In the second part passenger specific operating conditions have been introduced and a 1D torsional MBS model has been created with characteristic properties of a hybrid vehicle. The model has been used to perform a modal and time domain analysis of pertinent operating conditions, the results have been compared and evaluated. Finally the engine of the hybrid vehicle has been modified and an optimization for this alternative has been made to improve the dynamic behavior.

## Key Words

Half shaft, dual-mass flywheel, hybrid vehicle, NVH, operating conditions, 1D MBS, modal analysis, time domain analysis, dual-mass flywheel optimization

## Table of contents

Abbreviations and Nomenclature .....	9
1. Introduction .....	11
2. Powertrains – state of the art.....	13
2.1. Hybrid vehicles .....	13
2.1.1. Definition and types of hybrid vehicles .....	14
Series Hybrid .....	15
Parallel hybrid .....	15
Strigear hybrid.....	16
Complex hybrid .....	16
Other classification .....	16
2.2. Half shaft and joint configurations.....	17
2.2.1. Shaft joints .....	18
Universal Joints .....	18
Constant Velocity (CV) Joints .....	19
2.2.2. Side shaft for steer drive axles.....	20
2.3. Dual-mass flywheel .....	20
2.3.1. Function and properties.....	20
2.3.2. Types of Flywheels .....	22
2.3.3. DMF components (12) .....	23
Primary flywheel disc.....	24
Secondary flywheel disc.....	24
Bearings.....	24
Flange.....	24
Arc springs.....	25
3. Component dimensioning.....	28
3.1. Half shaft design and dimensioning.....	28
3.1.1. Requirements.....	28
3.1.2. Stress analysis .....	29
3.1.3. Calculation.....	29
3.2. DMF Dimensioning .....	30

3.2.1.	Key Parameters .....	30
3.2.2.	Design conditions.....	32
3.2.3.	Dimensioning for a DMF with one outer and two inner springs .....	34
	Spring #1 .....	35
	Spring #2 .....	41
	Spring #3 .....	43
4.	NVH Aspect of hybrid vehicles.....	44
4.1.	Operating conditions and NVH effects (18) .....	46
4.1.1.	Idle operation.....	47
4.1.2.	Hybrid/conventional start/stop .....	47
	Conventional low engine speed start .....	47
	High engine speed/hybrid start .....	48
	Motor stop .....	49
4.1.3.	Cycling .....	49
4.1.4.	Run-up (full load/part load) .....	51
4.2.	Components affecting NVH in hybrid vehicles.....	51
4.2.1.	E-machine.....	51
4.2.2.	IC engine.....	52
4.2.3.	Clutch .....	52
4.2.4.	Transmission (21).....	52
	Low rotational frequency harmonics of shafts.....	53
	Gear whine.....	53
	Gear rattle.....	53
	Shift noise.....	53
4.2.5.	The wheels .....	53
4.2.6.	Dual mass flywheel .....	53
5.	NVH Evaluation .....	54
5.1.	Introduction into 1D MBS .....	54
5.2.	Creation of hybrid powertrain 1D torsional MBS model .....	55
5.2.1.	Idle.....	61
5.2.2.	Hybrid start/tow launch.....	63
5.2.3.	Cycling .....	64

5.2.4.	Run-uppart-load/full-load .....	64
5.3.	Modal analysis of hybrid powertrain .....	65
5.4.	Time domain analysis in hybrid specific operating conditions .....	71
5.4.1.	Idle - rattle.....	71
5.4.2.	Hybrid start/tow launch.....	72
5.4.3.	Cycling .....	75
	Second gear.....	76
	Fifth gear .....	77
5.4.4.	Run-up.....	78
	Fourth gear.....	78
	Fifth gear .....	81
5.4.5.	Run-up – Rattle .....	84
	Second gear.....	84
	Fourth gear.....	85
	Comparison .....	86
5.5.	Chapter Conclusions.....	86
6.	DMF optimization .....	88
6.1.	Comparison 2-cylinder- and 4-cylinder activated IC engine .....	89
6.2.	Adjustment for 2-cylinder activation .....	93
6.3.	Adjustment for 4-cylinder activation .....	95
6.4.	Adjustment for 2- and 4-cylinder activation, variable displacement .....	97
	2-cylinder activation result comparison .....	101
	4-cylinder activation result comparison .....	102
6.5.	Chapter Conclusions.....	103
7.	Conclusions .....	105
	Bibliography.....	108
	List of tables .....	110
	List of figures .....	111
	List of appendices.....	114

# Abbreviations and Nomenclature

---

Abbreviation	Unit	Description
$A$	[ ]	<i>Amplitude</i>
$AWD$		<i>All-wheel drive</i>
$b$	[mm]	<i>Width</i>
$b_{sy}$	[mm]	<i>Synchronization ring backlash</i>
$c$	[–]	<i>Spring index</i>
$CAE$		<i>Computer Aided Engineering</i>
$d, D$	[m]	<i>diameter</i>
$D_e/R_e$	[m]	<i>External diameter/Radius</i>
$D_i/R_i$	[m]	<i>Internal diameter/Radius</i>
$DCT$		<i>Dual-clutch transmission</i>
$DMF$		<i>Dual mass flywheel</i>
$EM$		<i>Electric motor</i>
$f$	[Hz]	<i>Frequency</i>
$F_i$	[N]	<i>Force acting on spring</i>
$F_{Ni}$	[N]	<i>Normal force</i>
$FWD$		<i>Front-wheel drive</i>
$G$	[Nmm <sup>-2</sup> ]	<i>Shear modulus</i>
$h_{sy}$	[mm]	<i>Synchronization ring gap height</i>
$HEV$		<i>Hybrid electric vehicle</i>
$ICE$		<i>Internal combustion engine</i>
$\theta$	kgm <sup>2</sup> ]	<i>Frahm's value</i>
$j$	[–]	<i>Engine order</i>
$J_i$	kgm <sup>2</sup> ]	<i>Inertia</i>
$k$	[Nmrad <sup>-1</sup> ]	<i>Torsional stiffness</i>
$L_{0i}$	[m]	<i>Nominal spring length</i>
$L_{ci}$	[m]	<i>Solid spring length</i>
$L_{ni}$	[m]	<i>Installation space length</i>

$l_s$	[m]	<i>shaft length</i>
$m$	[kg]	<i>mass</i>
$m_a$	[kg]	<i>Vehicle mass on axle</i>
$M_{BS}$	[Nm]	<i>torque transmitted by the bow spring</i>
$MBS$		<i>Multibody simulation</i>
$n$	[–]	<i>Number of active coils</i>
$n_t$	[–]	<i>Number of coils</i>
$NVH$		<i>Noise Vibration Harshness</i>
$P2$		<i>Parallel hybrid arrangement with clutch between crankshaft and electric motor</i>
$PHEV$		<i>Plug-in hybrid electric vehicle</i>
$r, R$	[m]	<i>radius</i>
$r_a$	[mm]	<i>Gear tip radius</i>
$RWD$		<i>Rear wheel drive</i>
$S_y$	[Nm <sup>-2</sup> ]	<i>shear stress</i>
$T$	[Nm]	<i>Torsional moment</i>
$\tau_t$	[Nm <sup>-2</sup> ]	<i>Torsional stress</i>
$\varphi$	[rad]	<i>Rotation angle</i>
$\varphi_{ci}$	[rad]	<i>Solid spring angle</i>
$\varphi_{ni}$	[rad]	<i>Installation space angle</i>
$\Delta\varphi$	[rad]	<i>Rotational difference</i>
$\omega$	[rads <sup>-1</sup> ]	<i>Angular velocity</i>
$W_t$	[mm <sup>3</sup> ]	<i>Torsional section modulus</i>

# 1. Introduction

---

Vehicles and passenger cars are widely used all over the world and the amount of cars is rising rapidly each year. Because of that currently a high effort is being made to make vehicles in all branches of the industry more ecological. Demands on lower emissions but also customer demands on the vehicle power and behavior are rising rapidly. This of course affects also the automotive industry and passenger cars. The main targets are lower fuel consumption, maintenance cost, but higher power and efficiency. At the same time, customers are searching for vehicles with low noise and comfortable riding ability making the task even more difficult.

The current approach of many automotive companies is either electrification or the use of new technologies like for example fuel cells. With both technologies still some issues are connected. In case of electric vehicles it is mostly the distance which can be reached using energy from batteries only and the huge impact of temperature on it which still seems to be for most of the users insufficient. These are the main reasons why hybrid vehicles represent a common compromise between driving more ecologically while keeping the possibility to overcome long distance journeys. On the other hand it also means a new call for powertrain optimization. By adding more and more components necessary for electric driving, the NVH behavior of the powertrain and therefore of the whole vehicle changes too. The new mass distribution has to be taken into account to achieve optimal results regarding vibrations and noises of the vehicle body and chassis. Another consequence is the change of the available installation space and magnitude of stresses caused by the higher weight and component characteristics. All these parameters go hand by hand since due to higher stresses and NVH behavior some of the carrying components need to get stiffer, more loadable and durable, that being mainly accomplished by bigger size. Consequently the ideal ratio between size and durability is being searched to find an optimal solution for all parameters mentioned above and more.

The aim of the present thesis is to create a calculation algorithm for half shafts and dual-mass flywheels under consideration of the available construction space, stress and NVH requirements and its usage in a final DMF optimization for an engine with variable displacement.

A research about half shafts and dual mass flywheels (DMF) will be made to show the current state of art and give some insight into the topic, to understand important parameters defining them. For the half shaft, the necessary basic equations for constructing its dimensions will be stated. Same will be made for a dual mass flywheel with respect to a given installation space whereby parameters of the later in the work presented vehicle will be used. DMFS are an important component used for optimizing NVH and are nowadays present in almost every passenger car. Comparison of the dynamic behavior with and without dual mass flywheel has been already made several times before which is why in this

thesis only the setting of the dual mass flywheel will be analyzed and its suitability evaluated. The modal behavior is a complex issue which can influence the vehicle in many ways and for that a compromise is searched to get the optimum in most of the operational states like start, idle drive, or part/full load drive. For both the side shaft and the DMS an algorithm will be compiled to make the dimensioning process faster and to get a quick overview on how the change of their parameters affect the whole system.

A MBS model of a by the company IAV specified P2 plug-in hybrid powertrain with front wheel drive will be created and its modal analysis performed in SimulationX, which is a CAE-Software for the simulation of physical-technical systems created on the basis of a discrete network approach. Based on this model, time domain analysis and the effect of powertrain components in comparison to operating conditions specific targets will be revealed. In the end of the work depending on the result, suggestions for optimization of the DMF for the same engine but with variable displacement will be made using the created DMF calculation file.

## 2. Powertrains – state of the art

---

### 2.1. Hybrid vehicles

Hybrid drives are more and more used due to some very easy facts: strict environmental regulations are being set in order to reduce harmful emissions and to keep the environment in future cleaner. Electric vehicles are still not at the right point to take over the market from regular internal combustion engine (ICE) vehicles. The main reason for it is the battery and its non-sufficiency for longer trips. Due to this many automotive companies started with the introduction of hybrid cars. While electric vehicles are limited in range because of the full battery drive, in hybrid vehicles with a second source in form e.g. of an internal combustion engine are the possibilities the same as in a conventional ICE vehicle. At the same time, less CO and CO<sub>2</sub> emissions are being produced while driving. Even though both conventional ICE and electrical vehicles have similar well-to-wheel efficiency, many more factors like the specific and relevant toxic gas production has to be considered. The source of electrical power for charging the battery in hybrid-electric cars represents an important parameter, since the production of the electrical power differs from country to country. However some studies show, that the emissions of battery electric vehicles and hybrid vehicles in general have lower emissions than ICE vehicles even for countries with a large amount of coal based electricity production (1). This could be due to the better filtering possibilities of stationary coal power plants, where the final amount of pollutants in the waste gas is lower than from vehicles.

For passenger cars emission restrictions are being made, in particular for bigger cities, where cars have to fulfill a certain emission limit to be able to enter the city or pass through it. This is made possible with hybrid electric, battery electric or fuel cell electric vehicles.

To understand how energy can be saved in hybrid-electric vehicle (HEV), all the factors which have to be overcome at the wheels have to be kept in mind, but also inertia, power for accessories etc. play an important role. Most of the produced energy is lost through cylinder wall heat losses, exhaust gas losses or non-ideal burning of fuel. Today's automobiles have a peak thermal efficiency around 35-45% depending whether it's a diesel or gasoline engine (2). In normal operation the engine doesn't stay in its ideal operating range and the average efficiency during driving is even lower, about 20-25% (3). In case of urban driving, losses due to braking and idling gain in importance.

Besides the possibility of zero emission driving another advantage of HEVs is regenerative braking. Regenerative braking is basically the conversion of kinetic energy via a generator into electric energy, which is afterward stored into the battery.

Drive cycles in conventional vehicles use many different torque-speed combinations, i.e. operating points whereas in hybrid vehicles the traction system is being controlled and optimum operating points are being chosen to lead to high efficiency and lower emissions.

The basic idea is to operate the ICE more efficiently including reduction of idle which can be achieved by the start/stop system used in many current vehicles. By using the electric drive of the HEV some losses can be reduced or avoided completely by using the battery to absorb some of the power of the ICE or replace it. This way the engine can be used only for operating points when it is most efficient. When comparing both based on a demanding driving cycle the main differences can be made visible. With HEV low efficiency points for the combustion engine can be avoided completely.

In HEV part of the load can be taken up by the battery and the combustion engine can be downsized. In conventional vehicles, even though the engine does not always operate at peak load, it has to be dimensioned for worst case operating points. When using the battery the engine can be only build for continuous load making it smaller in size and weight. This likewise enables the possibility to operate the engine at higher fuel efficiency during most of the driving.

One contra factor is the potential for higher weight. Although the fuel power-path components will be smaller in size, the total weight is often higher than when using only ICE because of the storage device, motors and other components. Electric devices tend to be efficient but often just for one-way energy flows. In many hybrids energy flows in both directions (from motor to wheels and opposite) leading to more noticeable losses. All components have to be picked carefully to retain the theoretical efficiency advantage often linked to electric vehicles.

Nowadays many different types of hybrid vehicles have been presented, a view of them will be mentioned below.

### 2.1.1. Definition and types of hybrid vehicles

One of many versions of the definition of a hybrid vehicle is:

“A hybrid vehicle is a vehicle with more than one power source” (4).

Power sources can be electric machines, fuel cells, capacitors, flywheels or ICE. In a technical way generally the hybrid vehicle is a technology which indulges both mechanical and electric drive train. The mechanical drive contains a fuel tank, an ICE, gear box and transmission to the wheels. Similarly the electric drive consists of a battery, an electric motor and components for converting and adjusting the electrical power as well as power electronics for its control. In this thesis a hybrid with an ICE is being considered.

Many different topologies of HEV are available, each with different fuel consumption, emission or performance characteristics. Hybrid vehicles can be classified as followed:

## Series Hybrid

This type of hybrid has no mechanical connection between the internal combustion engine and wheels, the engine serves as a propeller for the generator. Its principle is in Figure 2.1.1.

The electricity produced from the generator can be then stored into the battery or directly used for driving the electric motor. An advantage of this arrangement is the fact that the engine can be operated with maximum efficiency, speed and torque can be chosen at any time. The battery can be charged independently on whether the car is driving or not. The ICE can be turned off when needed. On the other hand, energy produced by the ICE is being converted multiple times before driving the wheels. This results in a higher loss in system efficiency and higher cost. The motor has to be able to transmit peak power and the generator engine power. Both can be installed separately allowing a better weight distribution in vehicles. This is favorable in low floor buses.

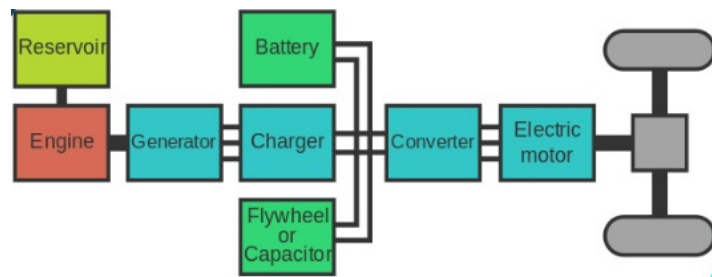


Figure 2.1.1- Series hybrid transmission scheme

The battery can be charged independently on whether the car is driving or not. The ICE can be turned off when needed. On the other hand, energy produced by the ICE is being converted multiple times before driving the wheels. This results in a higher loss in system efficiency and higher cost. The motor has to be able to transmit peak power and the generator engine power. Both can be installed separately allowing a better weight distribution in vehicles. This is favorable in low floor buses.

## Parallel hybrid

The main difference of the parallel hybrid compared to the serial hybrid is the possibility to drive the vehicle by using the internal combustion engine only (Figure 2.1.2). Wheels and ICE are connected mechanically. Thus some of the components needed in the serial hybrid are not necessary, resulting in an easier and cheaper system. Dimensioning of the drive components can be made more efficient, since the ICE can be constructed e.g. according to necessary maximum speed and the electric motor for city driving. It has a higher potential for achieving lower fuel consumption. The vehicle can be driven electrically while the ICE can charge the battery or is turned off; only by the internal combustion engine or both at the same time when peak power is being required. In some cases the electric motor is just used

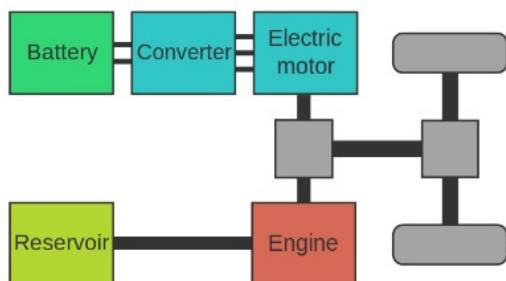


Figure 2.1.2 - Parallel hybrid transmission scheme

as a boost for driving. Different types of coupling between the motor and engine exist. Often used are planetary gears which can unite three power sources and hooks the engine and electric motor together and allows them to operate independently. Another possibility are in-wheel-electric motors. In this configuration electric motors are installed close to the driving wheels and are moving them through small drive shafts. The result is a very good responsiveness to accelerating demands and a better behavior during steering achieved by independent control of each driving wheel.

### Strigear hybrid

In the strigear hybrid are the two layouts just merged together by adding a clutch between two electric machines, therefore advantages from both arrangements are being exploited. In operation the onboard system compares the losses from both concepts and the better solution is chosen. This however results in a bigger complexity of the whole system. Strigear is a shortcut of “sequentially run, triple gearbox connected engine/motor hybrid” and is sometimes referred to as combined hybrid. (5)

### Complex hybrid

Complex hybrids cannot be classified into the above kinds because of its complex configuration. Two separate mechanical drives with a light transmission system are used. The generator and motor are both electric machines making it similar to the series-parallel hybrid. However the power flow is bi-directional in the motor unlike the unidirectional flow of the generator in series-parallel hybrids. The front wheels and back wheels can be powered by hybrid or electrical propulsion separately meaning high power flux flexibility.

### Other classification

Another classification of hybrid vehicles is depending on the relevance of the power source:

- Mild hybrid. Motors build in micro hybrids are usually not dimensioned for fully electric driving but for improving the power and efficiency of the engine when needed in certain drive situations. When braking or lowering the gear the battery is charged through the energy generated due to regenerative braking.
- Full hybrid. If the power supplied from the motor is higher and fully electric driving is possible then is the speech of full hybrids. The size/performance of the motor is sufficient for propelling the vehicle by itself and thus all driving modes, i.e. electric, mechanic or the combination of both is possible.
- Plug in hybrids (PHEV). Their difference from full hybrids is the possibility to charge the battery via the plug present in all typical households. They represent an intermediate between hybrids and electric vehicles.

And in parallel hybrid a nomenclature specified by Daimler AG depending on the electric motor position (according to Figure 2.1.3) in the powertrain has settled (6):

- P1. Powertrain with direct connection between crankshaft and electric-motor. Decoupling in electric driving modes is not possible and the engine is being dragged during all operating modes. The efficiency during electric driving is finite which is why this arrangement is used only in powertrains with low electric driving performance.
- P2. A clutch between engine and electric motor is present. The engine can be decoupled during operation increasing the electric drive and recuperation efficiency.
- P3. The electric motor is positioned at the output of the gearbox. The performance during electric driving and recuperation doesn't have to be conducted through the transmission enabling a wider rotational speed range.

- P4. Engine and electric motor drive different axes. Since the driving forces are reunited through the road, the arrangement is also considered as parallel with the possibility of switching to 4-wheel drive being its main advantage.

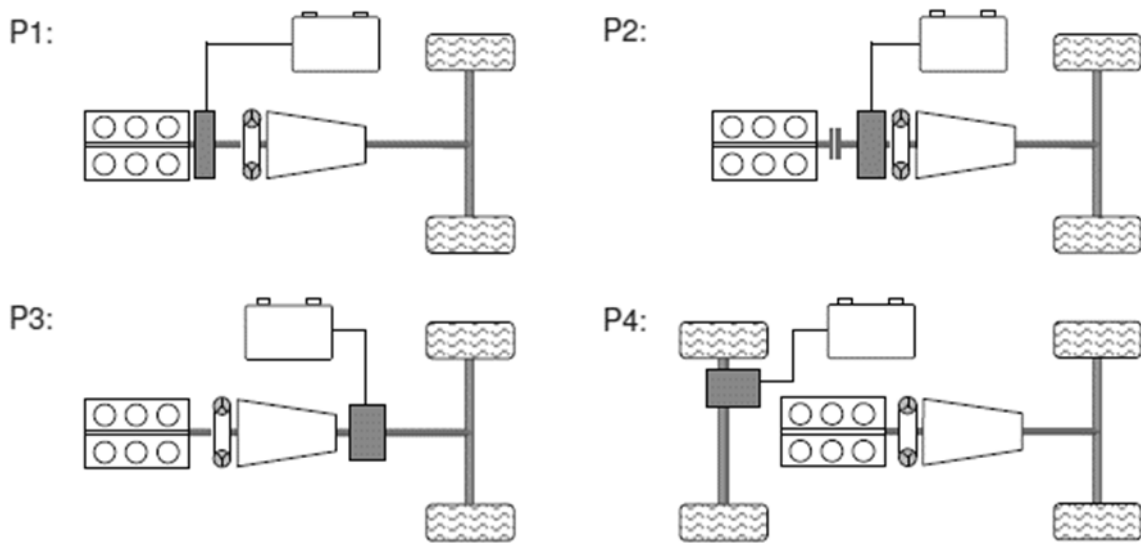


Figure 2.1.3 - Parallel hybrid powertrain distinction depending on the EM position (6)

## 2.2. Half shaft and joint configurations

In the previous sections the powertrain of a hybrid vehicle has been introduced. The arrangement of the powertrain depends on the gearbox position and a basic division is as followed:

- Front-wheel drive (FWD)
- Rear-wheel drive (RWD)
- All-wheel drive (AWD)

Depending on the placement of the gearbox and the driven axle, shafts with different types of joint are used to accomplish an optimal movement and torque transmission to the output shaft. Three types of drive shafts can be distinguished:

- Hooke's jointed (Figure 2.2.1)
- Ball jointed
- Poda jointed

The gearbox can be positioned either in the front or in the back of the vehicle. In case of an opposed position, e.g. gearbox in the front and rear-wheel drive, a propeller shaft is needed to transmit the torque from the engine to the differential. They have to be strong and resist the twisting action of the driving torque. It must be also resilient to absorb torsional shocks and resist the tendency to sag by reason of its own weight for vibration occurs when the axis of the shaft does not coincide with the center of gravity. Since the axes of the rigid rods are usually inclined to each other, a need for joints has emerged. In propeller shafts universal joints are used for the transmission.

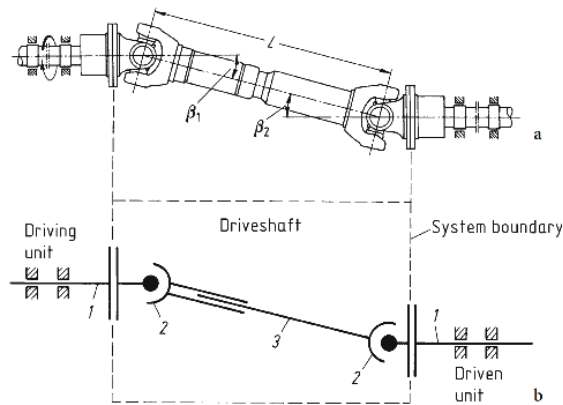


Figure 2.2.1 - Hooke's jointed shaft in a Z-configuration and diagrammatic representation of the system elements

The shafts mentioned in the next sections are side shafts or also called half shafts used for transmitting the torque from the differential to the wheels and thus differ from the propeller shaft by the used joint. Large wheel movement due to suspension deflection and short distance between the road wheel and final drive housing cause big drive angles of the joints and variation of length of the shaft. Also vibrations have to be isolated. Each side shaft has two constant velocity joints. In case of rear-wheel drive is the shaft in the back connected to the fixed-final drive assembly and having independent rear suspension. The individual parts of the driveshaft system are shown in (7).

### 2.2.1. Shaft joints

Angular agility is necessary in powertrains. In case of drive shafts, e.g. for vehicle suspension, non-coaxial positioning of the differential input and gearbox output or vibrational deformation of the vehicle body have to be enabled. Joint types can be distinguished by their flexibility:

- Torsionally elastic or rigid
- Longitudinal displaceability or longitudinal rigidity
- Uniform or non-uniform

The basic joint types are listed below.

#### Universal Joints

Universal joints are flexible couplings between two shafts permitting an angle between them. They belong to the family of spherical crank mechanisms (8). The simplest and most common type is the Cardan joint (also named Hooke joint), which consists of two yokes connected by a cross shaped member called spider (Figure 2.2.2). A basic characteristic of the Cardan joint is the non-uniform motion transmission varying the angular-velocity ratio between input and output shaft cyclically. It can be eliminated by using two appropriately phased joints in series; however the angular velocity fluctuation of the intermediate shaft cannot be avoided. (9) The driving shaft and driven shaft have to have equal angles with

respect to the intermediate shaft. Double Cardan shafts are used in rear-wheel drive vehicles as a propeller shaft.

Another option is also the Double Cardan's joint (Figure 2.2.2 – right) where two universal joints are mounted back to back with a center yoke which replaces the intermediate shaft and are depending on the configuration quasi-homokinetic or strictly homokinetic. Both are very complicated, thus many attempts to simplify the system have been made resulting in a variety of modifications, where the three most common types are the cross and roller, ball and trunnion joint.

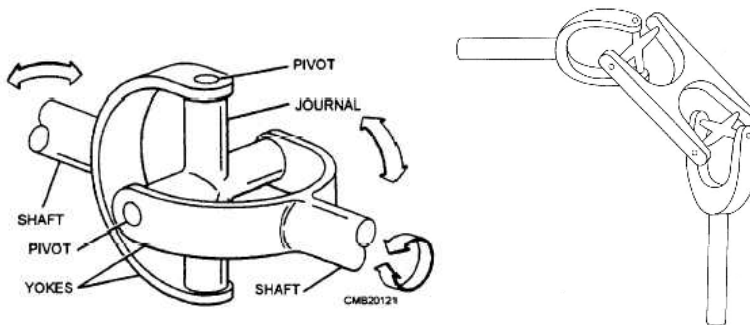


Figure 2.2.2—simple universal joint (left) and the double Cardan's joint concept (right)

### Constant Velocity (CV) Joints

Constant-velocity joints (also homokinetic or CV joints) allow power transmission through a variable angle at constant rotational speed and without a significant increase in friction or clearance. Their main usage is in front wheel drive-vehicles but also in modern rear-wheel drive vehicles with independent rear suspension.

Speed fluctuations caused by conventional u-joints are not a problem for rear-wheel drive shafts where they have to drive through small angles only. Much bigger angles have to be achieved in front-wheel drives due to steering and present velocity fluctuations can be a serious problem. The usage of u-joints would cause slippage, tire wear and hard steering. Constant velocity joints are designed to be used to connect the front axle shaft to the driving wheels.

The main functions of the side shaft have been stated before and to meet the requirements is the basic operation of a CV joint as followed:

- The outer joint is fixed and transfers rotating power from axle shaft to the hub assembly.
- The inner joint is in most applications a plunge joint allowing the effective length of the side shaft to change due to suspension with as little friction as possible

Examples for CV joints are:

- Tracta Joint
- Weiss Joint
- Rzeppa CV Joint

- Tripod Joint
- Thompson Coupling

### 2.2.2. Side shaft for steer drive axles

Side shafts for front-wheel drive axles are designed to transmit torque from the differential to the driven wheels of the front- and/or rear axle and enable movement of the suspensions and steering. To accomplish this it is built from three main components: CV joint on gearbox side, a connecting shaft and a joint on wheel side (7). The inner one as explained before is usually a plunged joint enabling the side shaft to follow the movement of the suspension. At the wheels are fixed ones.

Their function can be divided (8):

- Uniform transmission of torque and rotation
- Ability to alter distance between driven unit and driving unit
- Ability to alter angle between driven unit and driving unit

To optimize vehicle behavior and emissions, today's tendency in passenger cars is to downsize vehicle components and use lightweight construction and maintaining or increasing their performance. Even side shafts are affected and to minimize their weight, different construction types can be used. The shaft can be solid or hollow and even the hub-connection can be modified.

## 2.3. Dual-mass flywheel

Vibrations are often the result of ignition induced rotational irregularities. As the engine reciprocates, different forces and torques are being exerted at each stage of the engine cycle. The highest torque amount occurs during the power stroke when the piston is pushed downwards by the expanding gas causing the crankshaft to rotate rapidly. Another inconvenience regarding the comfort are load change reactions provoked by fast acceleration and deceleration causing the powertrain to wind up itself and oscillate while damping slowly. Dual-mass flywheels (DMF) are used to minimize these phenomena in vehicles and are positively influencing the behavior of the entire powertrain (7). They consist of a primary side which is connected to the crankshaft of the engine and a secondary side, which forms the friction surface of the clutch. Attachment is ensured via a set of springs with a progressive stiffness meaning a soft behavior at smaller deflections and harder behavior at bigger deflections. It is operated overcritical and isolates the secondary side from the high-frequency oscillations from the crankshaft (10).

### 2.3.1. Function and properties

Different configurations of DMF have been constructed to isolate the engine crankshaft from the gearbox. At engine idle and low engine speeds it helps reducing rattling sensitivity allowing driving also at low engine revolutions, whilst at cruising and starting/stopping it protects the gearbox from torsional shocks transmitted through the crankshaft from the

engine (7). With the DMF torsional oscillations can be almost completely isolated (11). Figure 2.3.1 shows the angular velocity at the engine outcome and gearbox entry for a conventional system with torsional damper in the clutch disk (on the left) compared to a system with DMF (on the right). By selection of an appropriate damping, resonance can be avoided.

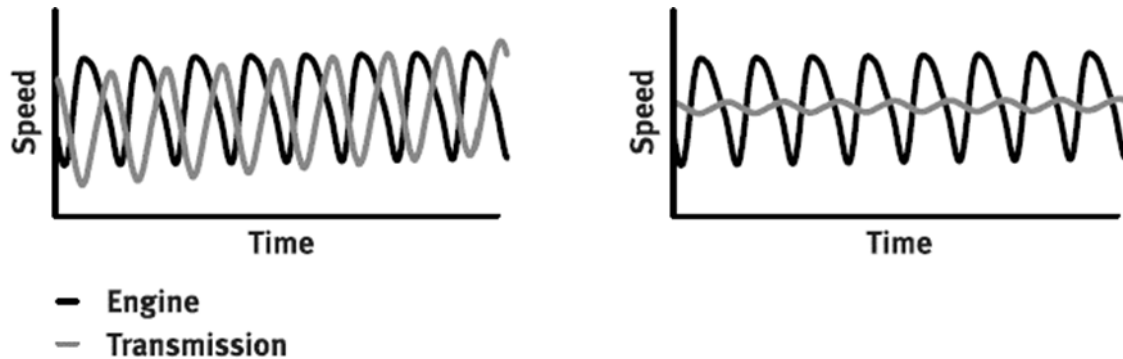


Figure 2.3.1 – Effect of the DMF (12)

This means also relieve for the transmission and crankshaft. The DMF eliminates almost completely high frequency oscillations resulting in the possibility to transmit a higher static torque for diesel engines. In conventional systems decrease of vibration is achieved by a heavy flywheel acting with its high moment of inertia against the vibrational and uneven movement of the crankshaft which can depending on its mass retard the engine's response to transient requirements. It is placed between the engine and transmission.

When using a system with a DMF, the mass of the conventional flywheel is separated into two flywheel masses. The secondary mass concerning its influence on the reaction force can be neglected due to its loose connection via torsion damper and roller bearings to the primary mass. Also the primary mass is significantly lighter than a conventional flywheel reducing crankshaft stress.

Driving in a wider speed range is one of the most important properties of passenger vehicles. Because of it, the importance of modal analysis is tremendous since natural frequencies and their natural modes have to be taken into account. When reaching a natural frequency during a driving cycle great damage can be caused. Usage of DMF generally moves the natural frequency of the system to a lower engine revolution range where the vehicle is not operated and the given frequencies are reached only during start up.

The dimensioning of the DMF always depends on the requirements of every individual vehicle and can only represent a compromise due to the variety of operating conditions and comfort specifications. The relevant operating points considered and drivetrain problems caused by it are:

- Idle (gear rattle)
- Drive/coast (gear rattle, boom)
- Engine stop (gear rattle, clatter)
- Tip-in and back-out (load changes, surging)

- Vehicle launch (judder, rattle, surging)
- Engine start (durability, comfort)
- Sub-idle speed resonance drive (durability)

Usually the operating condition with the highest probability of occurrence is dispositive and the optimization of the DMF parameters have to be considered already during the concept phase. Simulation of the powertrain system is one of the important keys in the design process and many additional requirements have to be achieved in order to reach the already mentioned targets.

### 2.3.2. Types of Flywheels

The most basic division of flywheels can be done in the following manner:

- Standard Flywheel
- Dual Mass flywheel

A standard flywheel is the type of system mentioned in the previous section. It consists only of one heavy disk connected to the end of the crankshaft or engine. Besides providing weight for smoothing out the 'pulses' created by the pistons it generally has a gear around its circumference on which the starter motor operates and is a convenient way of attaching the clutch.

All the rest description and main subject is the dual-mass flywheel. These can be further divided into:

- Conventional Dual Mass Flywheel
- Planetary Dual Mass Flywheel

The conventional DMF consists of the primary and secondary flywheel as well as a series of torsion springs and cushions. A friction ring is located between the inner and outer flywheel allowing them to slip. It alleviates damage to the transmission when torque loads exceed the vehicle rating of the transmission. It includes the clutch with pressure plate and friction disk.

Planetary DMFs are designed for engines with stronger vibrations in the lower speed range and have an integrated planetary gear. The result is greater driving, shifting comfort and reduced fuel consumption because of the possibility of lower idling speed. For this purpose the flywheel masses are linked via gears. When high torsional spikes occur, the two elements move in relation to each other. This is limited by the compression springs on the circumference. Multi-stage characteristic can be achieved by usage off springs with different stiffness.



Figure 2.3.2 – Planetary DMF (12)

Besides the spring arrangement different spring types and construction variations are possible. Mostly used in DMFs are two main outer arc springs built in semicircular. However since new technologies for the reduction of friction forces acting on the guides in the spring channel appeared, also sliding shoes mounted between the coils have been added. Another possibility is the sequence of in parallel arranged multiple compression springs with a plastic element in between for keeping them apart. Extra improvement during acceleration is achieved thanks to inner springs which are in some cases of newer versions of the DMF being replaced by a rotational speed adaptive vibration absorber (centrifugal pendulum). The main subject of this thesis is the conventional Dual Mass Flywheel with arc springs. A description of the components will be made further.

### 2.3.3. DMF components (12)

Typical components of a standard DMF are visible in Figure 2.3.3:

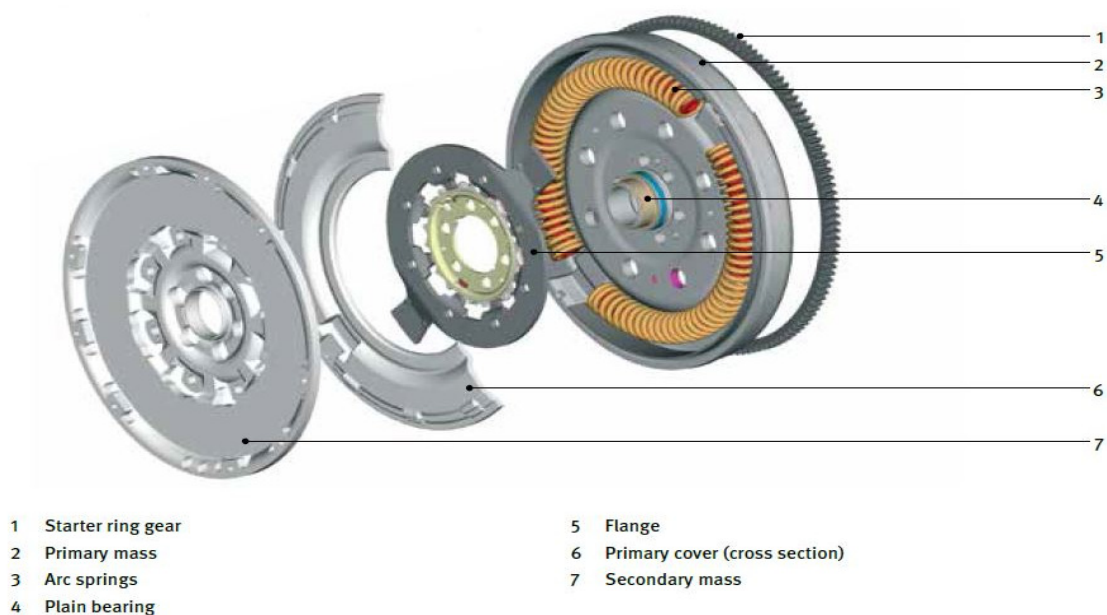


Figure 2.3.3- Components of a standard DMF

### Primary flywheel disc

The primary disc is connected to the crankshaft of the engine and creates with its mass a unit. It is lighter compared to conventional flywheels and reduces therefore the load acting on the crankshaft. A starter ring gear is positioned on it for engine starting. The primary mass with the primary cover form the arc spring channel and is generally split into two sections which are separated by the spring stops.

### Secondary flywheel disc

The secondary mass forms the connecting point to the transmission side of the powertrain. Transmission of torque between the primary and secondary flywheel disc is realized with a flange. When the primary disc is being moved, the springs inside are being compressed due to the spring stops between them. The flange also has two 'wings' positioned in between the springs and as a result being is moved by the springs. The primary and secondary mass can move independently relative to each other in tangential movements. Together with the clutch, modulated torque is transmitted where the clutch is the power output. A spring mechanism presses the clutch disk toward the friction surfaces of the secondary flywheel disc.

### Bearings

Bearings are a connection between two rotating masses. Their main task is usually the absorption of weight related radial and -axial forces generated by the release force when disengaging.

Either ball bearings or plain bearings can be used. Additional components are necessary because of the constantly rising demands on the rotary vibration damping increasing the construction space leading to a reduction of the bearing diameter. Plain bearings take less space and have a simpler design but have bigger demands on the oil supply.

### Flange

Torque transmission from the primary to the secondary flywheel is realized with the flange. It is tightly riveted with the secondary mass with its wings seated between the spring channels of the primary mass. The flange can be rigid as one piece or with an internal damper. As already mentioned centrifugal force acts on the arc spring at high engine speed pressing them against the guides and disabling the coils. Due to this the stiffness increases and spring action is lost.



*Figure 2.3.4- DMF with straight pressure springs on the outer (both) and inner radius (inner damper-right)*

To avoid this effect straight pressure springs are mounted within the flange and are subject to lower centrifugal force because of their smaller mass and mounting radius. Consequently lower friction and therefore independence on the engine speed is ensured. They help reducing vibration during acceleration and are visible in Figure 2.3.4 (right).

The flange can be also designed as a diaphragm spring and pre-tensioned by two retaining plates with a thin friction lining. Load on the flange wings occurring at sudden load changes can be with this construction minimized.

### **Arc springs**

An arc spring with a large number of coils is fitted in a semicircular position in the arc spring guides. In this guide friction is generated during operation causing damping. Varying the guides shape can reduce friction which led to the construction of several sliding shoe types. Either the standard arrangement with two semicircular bow springs can be used with sliding shoes between the windings in certain distances, or instead of a bow spring, multiple straight springs can be used with bigger sliding shoes keeping them apart from each other. For this case a combination of springs with different stiffness's can be mounted.

In case of using the bow (arc) spring various designs with different characteristics are available:

- Single-stage springs
- Two-stage springs – parallel or in-line arrangement
- Three-stage arc spring

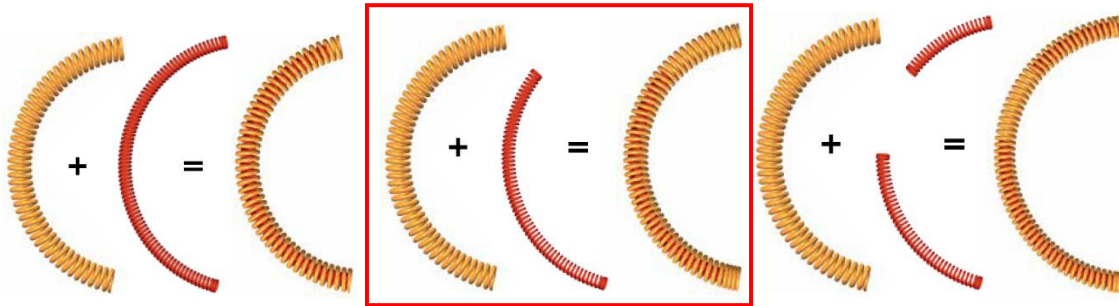


Figure 2.3.5 - From left: single-stage, two-stage and three-stage arc spring

Standard springs are called one-stage springs in parallel. The outer and inner spring are almost of the same length and connected in parallel according to Figure 2.3.5–left picture. Their individual characteristic curves are forming the characteristic curve of the spring pair. Similar is the two-stage spring in parallel type. In this case there are two springs, one inside the other (in the middle of Figure 2.3.5). The internal spring is shorter and therefore acts in cases of bigger deflection. The external spring is generally adjusted to the requirements at engine start-ups and has lower stiffness. When the applied torque rises, in ‘second stage’, the second internal spring is engaged and works together in parallel with the external spring. How the springs deflect for a two-stage DMF is presented Figure 2.3.6 and Figure 2.3.7. The two springs are drawn side by side for demonstration although in reality the 2<sup>nd</sup> spring (red) is placed inside of the 1<sup>st</sup> spring (yellow). In Figure 2.3.6 the DMF is in its initial position and no torque acts on spring 1 (yellow). When torque is applied spring 1 starts to deflect until stage 1 torque is reached. The stiffness for this deflection is only given by spring 1. In Figure 2.3.7 stage 1 torque is reached and spring 1 and 2 have the same length. After increasing the applied torque spring 2 starts to deflect too and due to the parallel arrangement, the final stiffness is:

$$k_2 = k_{spring1} + k_{spring2} \quad (1)$$

Where  $k_{spring1}$  is the stiffness of spring 1 and  $k_{spring2}$  the stiffness of spring 2.

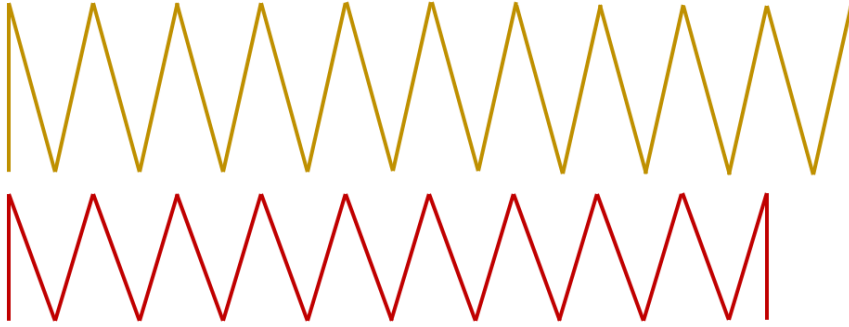


Figure 2.3.6 – Initial position - Torque starts to act on the DMF -> spring 1 (yellow) starts to deflect

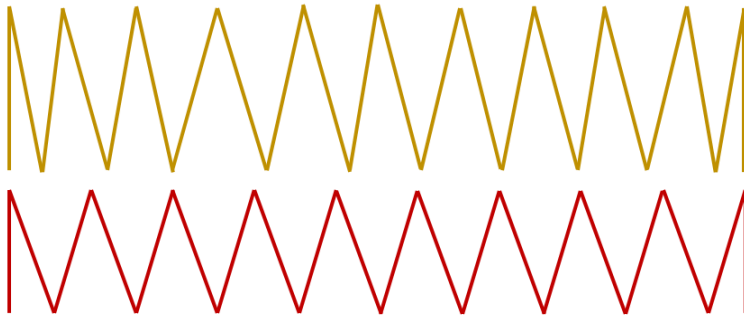


Figure 2.3.7 - Stage 1 torque reached -> spring 1 (yellow) has same length as spring 2 (red), when torque increases spring 1 and 2 start to deflect equally

The last type is the three-phase bent spring consisting of one outer and two inner springs, the inner ones connected in-line (Figure 2.3.5 - right). Springs with different stiffness' are utilized ensuring together with the parallel and series connection an optimal torsional compensation for each torque value. Its principal is similar as for the two stage spring. In stage 1 acts only spring 1. After reaching stage 1 torque, spring 2 and 3 start to deflect. With stage 2 torque, spring 2 reaches its solid length. Therefore, in stage 3, spring 1 and 3 act together till the end stop is reached (all springs reach their solid length).

# 3. Component dimensioning

---

The dimensioning conducted in this chapter is provisional to give an insight into the Excel calculation tools created by the author. For the half shafts only a gross concept for computation will be introduced since for half shafts and half shaft joints FEM analysis being based on the presumed cyclic load, which will be known after simulation, would be necessary. For the DMF, design values of the analyzed P2-hybrid vehicle will be used to show the calculation process and later in this work the file will be utilized again for optimization.

## 3.1. Half shaft design and dimensioning

### 3.1.1. Requirements

Half shafts are systems, which transmit torque from the differential to the wheels and at the same time mobility has to be ensured.

Basic requirements of side shafts are the transmission of the torque with a very high efficiency and constant gear ratio, long service life, operation with low or no maintenance and a low moment of inertia. On the front axle steering angles up to 52° have to be overcome leading to high stresses in normal operation. The working angles of the rear axis are usually smaller and limited by the self-steering angles of the suspension (7). To obtain a high lifespan, temperatures between -40° and 120°C have to be withstood. They can reach up to 2600 rpm. The joints are usually protected from impurities with an elastic plastic piece for covering them and also for keeping the grease inside the joint space. Dimensioning is made for permanent durability with consideration of peak loads.

Important parameters influencing the drive shaft design are:

- Length
- Outer diameter maximum
- Rotational speed maximum
- Ultimate strength requirements at different temperatures
- Desired torsional stiffness
- Fatigue/lifecycle requirements
- Attachment type front and rear, used joints
- NVH issues of the system – frequency problem concerns, sound or resonance vibration problems, etc.
- Torque spikes during use
- Environmental challenges

The final stiffness of the shaft also has to be mentioned. A shaft with very high torsional stiffness can apply shock loads back to the gearbox and engine. On the other hand low stiffness can cause the shafts natural frequency to lie in an improper speed range. Because of that it is important to keep the shaft diameter at reasonable values.

### 3.1.2. Stress analysis

Friction between road and tires, axial force due to cornering acting as pulling/pressure force and reaction force from the road act on the wheels. Besides them also shocks which are transmitted due to road surface irregularities have to be absorbed by the upright bearing and steering facilitated. (13)

The suspension used in vehicles eliminates this bending moment and tension/compression and only the torsional stress due to driving torque and has to be transmitted by the side shaft. (14)

### 3.1.3. Calculation

An easy example of side shaft designing will be inducted. The following simplified example calculation for a FWD shaft accounts only for stress caused by torsion which is also the main strain acting on the shaft. For solid shafts with a circular cross-section the torsional section modulus is:

$$W_t = \frac{\pi d^3}{16} \quad (3.1.1)$$

And the torsional stress:

$$\tau_t = \frac{T}{W_t} \leq \tau_{tall} \quad (3.1.2)$$

Where  $\tau_{tall}$  is the allowed torsional stress and  $T$  the on the shaft applied torque. For hollow shafts is the torsional resistance:

$$W_t = \frac{\pi(d_a^4 - d_i^4)}{16d_a} = \frac{\pi d_a^3(1 - k^4)}{16} \quad (3.1.3)$$

$k = \frac{d_i}{d_a}$  is the diameter ratio. The diameter can then be calculated for the solid shaft as:

$$d \geq \sqrt[3]{\frac{16 * T}{\pi * \tau_{tall}}} \quad (3.1.4)$$

The torsional moment  $T$  transmitted from the differential and acting on the side shaft can be calculated from the maximum torque given from the engine parameters. Because of the possibility of extreme situations a factor of safety is included in the formula:

$$T = \frac{1}{2} * T_{emax} * k_d * i_g * i_f * \eta_p \quad (3.1.5)$$

Where  $T_{emax}$  is the maximum engine torque,  $i_g$  the gearbox ratio and  $i_f$  the final drive ratio. Half of the engine torque is considered in equation (3.1.5) because of the symmetrical torque division at the differential.  $k_d$  is a dynamic factor used for accounting dynamic processes and depends on the DMF setting,  $\eta_p$  is the transmission efficiency.

When a change in stiffness is necessary and the diameter of the shaft has to be changed, the above mentioned equations can be used to check the shaft against failure.

## 3.2.DMF Dimensioning

### 3.2.1. Key Parameters

Rotational irregularities can be reduced with rising flywheel moment of inertia. The DMF makes it possible to obtain vibrational isolation while using lower mass. The two masses serially are linked with a spring-damper system with different characteristics. If the spring units are adjusted for a soft behavior, the resonance frequency can be lowered to a level beneath the idle speed.

The spring rate decreases with increasing spring diameter  $D_m$  and increasing amount of spring coils  $n$ .

$$k = \frac{G * d^4}{8 * D_m^3 * n} \quad (3.2.1)$$

To put this property into practice the spring has been moved more outward, i.e. on a bigger radius to ensure more installation space and the possibility to use bigger spring diameters. Effects of this action can be showed by the force resulting from the moment transmitted by the bow spring:

$$M_S = k_t * \Delta\varphi \quad (3.2.2)$$

$$F_{N1} = \frac{M_S}{r} \sin(\varphi_0 - \Delta\varphi) = \frac{k}{r} \Delta\varphi * \sin(\varphi_0 - \Delta\varphi) \quad (3.2.3)$$

Where  $M_S$  is the torque acting on the arc spring,  $k_t$  the torsional stiffness,  $F_N$  the related radial force (Figure 3.2.1 – right),  $\Delta\varphi$  the deflection angle and  $\varphi_0$  the initial spring angle. The characteristic damping behavior of the DMF is strongly influenced by Coulomb's friction. It has partly a revolution- and frequency dependent damping and on the other hand a constant damping evocating a basic hysteresis. The basic attrition is composed by seal-, bearing friction and friction of the integrated discs. Dominant friction forces are caused by the contact between the bow spring coils and the spring guides. The line of action of the spring forces are not identical due to the bow shape of the spring. Radial forces arise in every coil with which the bow spring leans on the guides. (15)

One part of the radial force is caused by the tangential spring force called redirection force and can be calculated according to equation (3.2.3). An example for its formation is visible in Figure 3.2.1 - left.

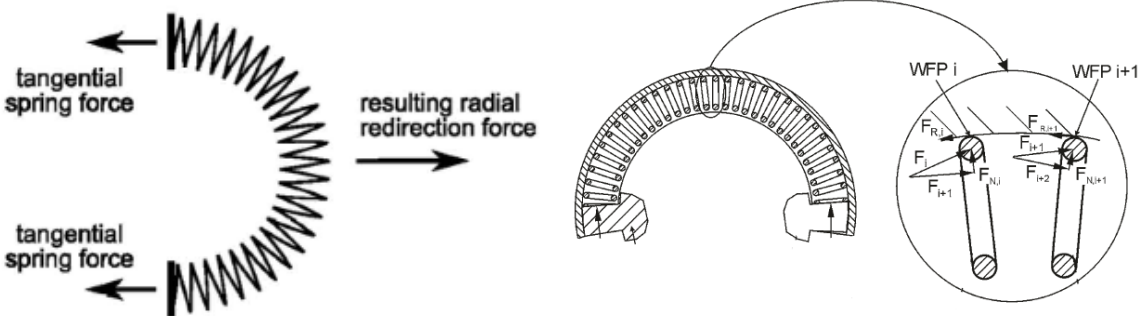


Figure 3.2.1 – Radial forces acting on the spring guides (left) (16) and forces acting on spring coils and absorption areas (WFP) (right)

The second part are the with rotational speed increasing centrifugal forces ( $F_{N2}$ ). As mentioned before they dominate the redirection force from a certain angular velocity:

$$F_{N2} = m * \omega^2 * r \tag{3.2.4}$$

Where  $m$  is the spring weight and  $\omega$  the DMF angular velocity. Both forces developing at loading and relief have a damping effect on the system and increase with higher twisting angles. Thanks to this damping effect, jerking oscillations during load changes can be filtered.

An increasing twist angle  $\Delta\varphi$  also means an increasing radial force, visible in

Figure 3.2.1 – Radial forces acting on the spring guides (left) due to deflection, but at the same time, the angle between the bow spring endings  $\varphi_0 - \Delta\varphi$  decreases. Increasing friction in turn results in a bigger hysteresis area. This effect is visible in Figure 3.2.2.

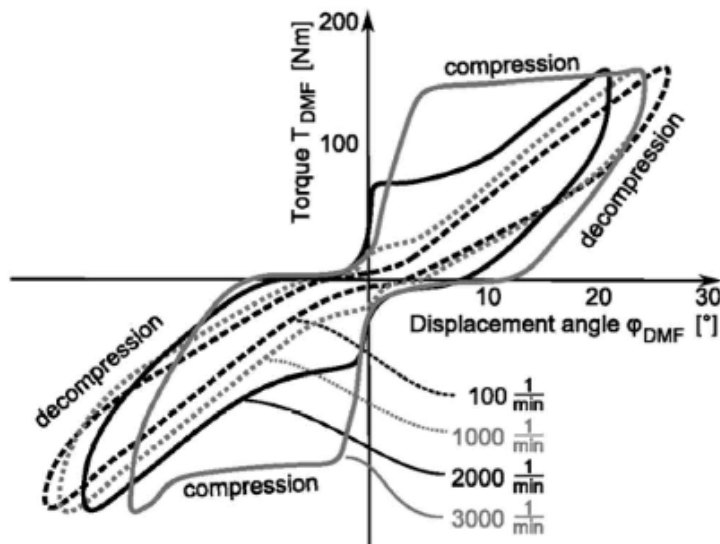


Figure 3.2.2 –Torsion at different engine speeds (16)

At low rotational speed friction is low, but with an increasing twist angle the hysteresis gets wider. At higher rotational speed a higher torque is necessary to move the spring in the guide and just a part of the windings will be moved. This is an explanation for the steepness of the curves representing the spring behavior at higher speed. In this case it is also not possible for the spring to unwind, thus the spring effect shows again after a certain twist angle when decompressing. The friction  $\mu$  can be influenced by using a lubricant or sliding shoes influencing the spring damper characteristics.

When searching the ideal combination between spring stiffness and damping behavior a few more factors have to be considered. Forces acting on the spring are also causing shear stresses in the wire which have to be calculated to ascertain, that the spring is able to transmit the load. The main parameter adding to the spring strength is the wire diameter. Besides adding strength it also influences together with the number of coils, spring length and material the final spring stiffness.

### 3.2.2. Design conditions

For this thesis, dimensioning of a dual-mass flywheel considering the construction space shall be performed. Important parameters and their calculation have been acknowledged. The operating modes of interest have also been mentioned earlier. For choosing the basic spring parameters, the torsion damper requirements have to be stated first. These are listed in Table 3.2-1.

Table 3.2-1 – Torsion damper requirements

Operating mode	Problem	Excitation Frequency	Vibration Angle	Spring rate	Damping
Idle, drive, coast	Noise	High	Low	Low	Low
Load cycle	Surging	Low	High	Medium	High
Resonance break-through	Noise, durability	Low	High	Low	High

Important for these operating modes is the individual frequency and vibration amplitude. The general excitation frequency for the first category (idle, drive, coast) is at ca. 20-400 Hz. In these operating modes mean torque is usually low and irregular engine torque has a very small influence even for diesel engines with their characteristically high torsional irregularities. The vibration angle isn't usually larger than  $\pm 2^\circ$ . A low spring rate and damping characteristics is necessary to achieve the best possible isolation. (17)

The resonance break-through is the designation for the action happening during engine start and stop, when the speed increases or is decreased to zero. During this phase the resonance frequency of the drive train is passed and low frequency vibrations at large vibration angles occur. Because of it, a low spring rate and high damping effect are required so the resonance will not be magnified during passing the resonance range.

The same accounts for load cycles. Sudden excitations caused by for example tip-in/back-out result in large vibrational angles combined with low frequency excitation (e.g. jerking – 3 Hz). The DMF operates in the same stage as for drive which is why high spring rates cannot be chosen and a medium spring rate has to be selected. To decrease the negative effect of the sudden torque change, high damping is necessary where part of the energy is dissipated to accomplish reduction of the vibration amplitudes.

All coils of the arc spring become active during large vibrational angles typical for resonance break-through and load cycling which results in a lower spring rate and higher damping. The spring rate and damping caused by friction is also dependent on the engine speed and vibration angle. Higher speed and lower vibration angle increase the spring rate because of coil deactivation as described before. At high engine speeds, centrifugal force acting on the coils increases causing higher friction force and resistance against the coil movement. In combination with small vibration angles when small spring forces act on the coils, movement is inhibited.

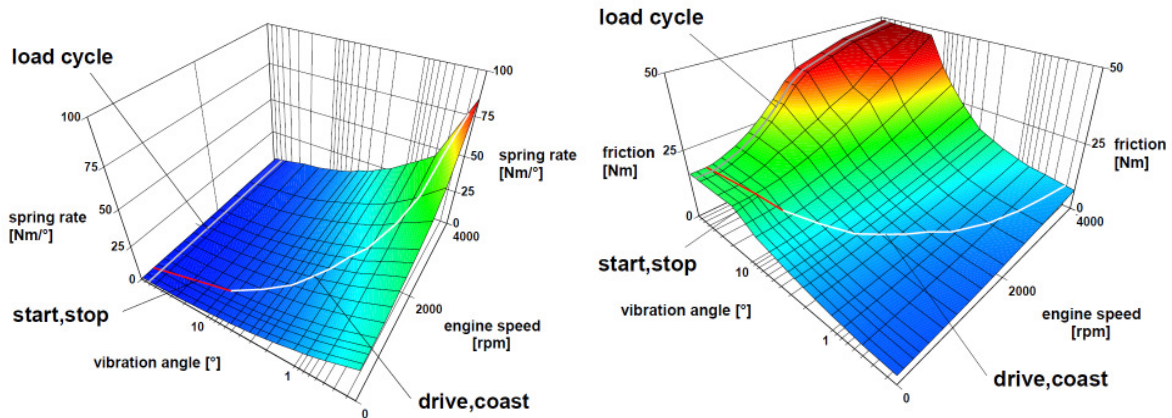


Figure 3.2.3 - Spring rate (left) and friction damping (right) as function of engine speed and vibration angle for a 2.5l diesel (17)

Dependence of the spring rate and friction damping on engine speed and vibration angle are visible in Figure 3.2.3.

For three-stage characteristics linear springs connected in series can be used. The arrangement in this example consists of one external and two internal springs, a usual arrangement produced by e.g. Schaeffler. The external spring has a low stiffness and provides enough damping for low engine speed where high vibrational angles occur. Two internal springs are arranged in-line thus both the advantage of parallel and in series arrangement can be accomplished. The highest stiffness in stage 3 is generally used for worst case situations when unexpected high dynamic torque arises. Its stiffness is being chosen in a manner to avoid achievement of the solid length for all three springs. When optimizing a DMF for 4-cylinder engines it has to be kept in mind that two cylinders fire at the first revolution of the engine crankshaft and the other two at the second causing two vibration cycles per revolution. The frequency transferred to the DMF is the second engine order of the engine revolution frequency.

### 3.2.3. Dimensioning for a DMF with one outer and two inner springs

In this chapter an example for the dimensioning of the DMF arc springs shall be performed. All initial parameters mentioned have been given by the company and belong to the P2-hybrid analysed later in this work. These are the DMF installation space, the applied torque, the individual torque stages and the corresponding stiffness's. Depending on them the number of coils, wire diameter, coil diameter and applied stress can be calculated. The known installation space dimensions are the maximum outer DMF radius ( $R_e = 135 \text{ mm}$ ) and the internal limitation for the arc spring ( $R_i = 100 \text{ mm}$ ). The maximum applied torque which is equal to the maximum engine torque is  $M_{eng} = 250 \text{ Nm}$  multiplied by a safety factor to cover the dynamic part. The vehicle analysed has a safety factor of 80%, which is quite high and in normal cases 40-50% are used. The maximum dynamic torque ( $M_{dyn} = 450 \text{ Nm}$ ) magnitude determines when the solid length, which is the length of a completely compressed spring, is being reached.

An excel file with all the specified equations has been created to ease the calculation process. In two tables it is either possible to dimension the spring with the knowledge of the load on each of them or with the knowledge of the desired stiffness for each stage. As mentioned, in this case the stiffness is known. Multiple coil and wire diameter variations are used in the file to find the optimal combination for the given parameter. The functioning of the file will be explained further although the calculation example will be made to determine one specific dimension possibility.

**Spring #1**

The DMF in the vehicle given and analysed later has a first stage stiffness of  $k_1 = 2.5 \frac{Nm}{deg}$  acting till  $M_1 = 14 Nm$  ( $k_1$  in Figure 3.2.5 and Figure 3.2.6). During engine start, when it’s rotational speed increases from zero and the critical frequency range is being passed, the biggest risk is the possibility that the DMF natural frequency is being excited causing the powertrain to get stuck at its value and to critically oscillate. This is why for the first stage the stiffness should be chosen as low as possible. In case of the usage of bow springs in the DMF, two sets of springs are inserted according to Figure 2.3.5 (right – three stage DMF). The stiffness and transmitted torque are combined values for both spring halves in the DMF. All known values are collected in Table 3.2-2:

*Table 3.2-2 – spring 1 calculation parameters*

Spring #1			
Measure	Magnitude	Unit	converted Unit
Installation Space - outer radius	135.00	mm	0.1350 m
Installation Space - inner radius	100.00	mm	0.1000 m
Torque applied	250		250000 Nmm
Torque factor	0.80		
Final torque	450.00	Nm	0.4500
Number of springs	2.00	-	
Free angle	1.00	°	0.0175 rad
Stopper width	5.00	°	0.0873 rad
Active inner spring	2 inner		
Transmitted torque	66.21	Nm	
Torque Stage 1	14.00	Nm	14000.0000 Nmm
Optimal spring stiffness	1.25	Nm/°	71.6197 Nm/rad
Wire diameter tolerance	0.045	mm	
Mean installation space radius	117.50	mm	0.115 m
Nominal spring length	356.83	mm	0.3568 m
Nominal spring angle	174.00	°	3.0369 rad
Twist angle till block	59.60	°	1.0401 rad
Solid spring angle	114.40	°	1.9967 rad
Tensile strength Rm	1900.00	N/mm <sup>2</sup>	1900000000.0000 N/m <sup>2</sup>
Stress correction factor	0.50		
Admissible shear stress	950.00	N/mm <sup>2</sup>	950000000.0000 N/m <sup>2</sup>
Shear modulus	79160.00	N/mm <sup>2</sup>	79160000000.0000 N/m <sup>2</sup>
Minimum spring index	3.99	-	
Minimum number of coils	36.00	-	

In further calculations only one of the two spring sets in the DMF will be used and thus the half stiffness and torque value. Normal engine operations should occur in the second stage

being an indicator for the torque range in which both the external and internal springs should be acting. Due to the dynamic behaviour of the power train the torque for the second stage was chosen to be higher than the maximum engine torque, resulting in  $M_2 = 326 \text{ Nm}$ . As mentioned before the external spring is arranged in parallel with the internal springs, the internal springs being in a mutual series arrangement. The stiffness of two springs in series is:

$$\frac{1}{k_{23}} = \frac{k_2 * k_3}{k_2 + k_3} \quad (3.2.5)$$

For  $k_2 = 6.4 \frac{\text{Nm}}{\text{deg}}$  and  $k_3 = 21.2 \frac{\text{Nm}}{\text{deg}}$  is  $k_{23} = 4.9 \frac{\text{Nm}}{\text{deg}}$ .

Before the dimensions can be defined, torque transmitted by every single spring has to be calculated, since they are a scale for determining the stress acting on them. Between each spring and stopper is a backlash present as visible in Figure 3.2.4.

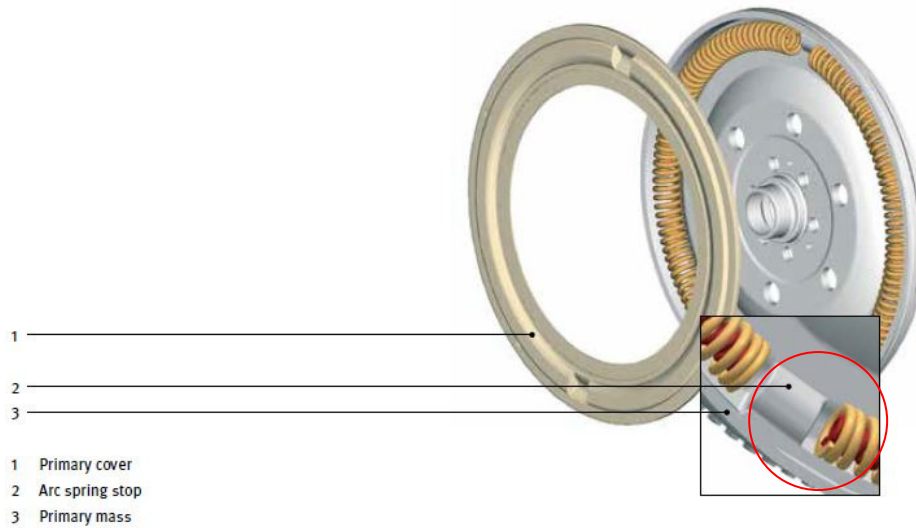


Figure 3.2.4 - DMF stopper and free angle (12)

Its influence on the system will be discussed later. For the DMF used in the vehicle is the given backlash  $\varphi_f = 1^\circ$ . The outer spring is larger in length and has to transmit the full magnitude of stage one (in this case  $M = \frac{M_1}{2} = 7 \text{ Nm}$ ). After reaching the first stage, the external and internal springs are of the same length and the torque with a higher magnitude than stage 1 torque will be divided between them till the last stage is reached. Spring 2 has a smaller stiffness than spring 3 and should reach its solid length with the second stage torque ( $M = \frac{M_2}{2} = 163 \text{ Nm}$ ). The solid length is the length of the spring when the coils are fully compressed. No further deflection of spring 2 is possible and has therefore no longer influence on the torsional stiffness. In stage 3 torque vibration decoupling is ensured just by the first and third spring which continue to deflect until the maximum torque  $M = \frac{M_3}{2} = 225 \text{ Nm}$ .

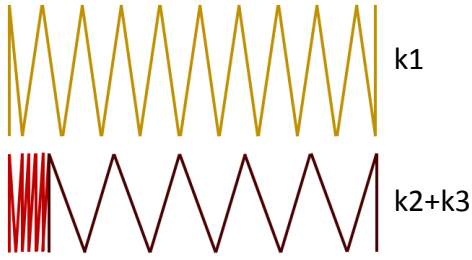


Figure 3.2.5 - Spring arrangement in stage 3

A bigger stiffness starts to act due to the remaining parallel arrangement of the outer and third inner spring (Figure 3.2.5). To be able to calculate the spring geometry, torque acting on each single spring in all for it relevant stages has to be calculated. The related equations express the torque acting on the respective spring (each term is divided by two to account just one of the two):

- Torque acting on spring 1 – deflecting in all three stages

$$M_{s1} = (M_1 + \frac{M_2 - M_1}{k_1 + k_{23}} * k_1 + \frac{M_{EST} - M_2}{k_1 + k_3} * k_1)/2 \quad (3.2.6)$$

$$= (14 + \frac{326 - 14}{2.5 + 4.9} * 2.5 + \frac{450 - 326}{2.5 + 21.2} * 2.5)/2 = 66.21 \text{ Nm}$$

- Torque acting on spring 2 - only in the second stage – in 3<sup>rd</sup> stage fully compressed (not deflecting anymore)

( $k_{23}$  is the combined stiffness of spring 2 and 3)

$$M_{s2} = (\frac{M_2 - M_1}{k_1 + k_{23}} * k_{23})/2 = (\frac{326 - 14}{2.5 + 4.9} * 4.9)/2 = 103.3 \text{ Nm} \quad (3.2.7)$$

- Torque acting on spring 3 - in the second and third stage

$$M_{s3} = (\frac{M_2 - M_1}{k_1 + k_{23}} * k_{23} + \frac{M_{EST} - M_2}{k_1 + k_3} * k_3)/2 \quad (3.2.8)$$

$$= (\frac{326 - 14}{2.5 + 4.9} * 4.9 + \frac{450 - 326}{2.5 + 21.2} * 21.2)/2 = 158.7 \text{ Nm}$$

The deflection difference angle of each spring can be expressed:

$$\Delta\varphi_{s1} = \frac{M_{s1}}{k_{1/2}} = \frac{66.21}{1.25} = 52.97^\circ \quad (3.2.9)$$

$$\Delta\varphi_{s2} = \frac{M_{s2}}{k_{2/2}} = \frac{103.3}{3.2} = 32.28^\circ \quad (3.2.10)$$

$$\Delta\varphi_{s3} = \frac{M_{s3}}{k_{3/2}} = \frac{158.7}{10.6} = 14.97^\circ \quad (3.2.11)$$

This means if a torque with the magnitude of 66.21 Nm will be applied on spring 1 it deflects or shortens by 52.97°. For spring 2 and 3 it is not possible to reach bigger deflection angles together as they are smaller and their maximum length is given by spring 1. Both together

cannot be longer than spring 1 after reaching stage 1 torque. The DMF characteristic curve and representation of the torque stages and springs acting during them are in Figure 3.2.6. The springs are represented in a non-deflected state.

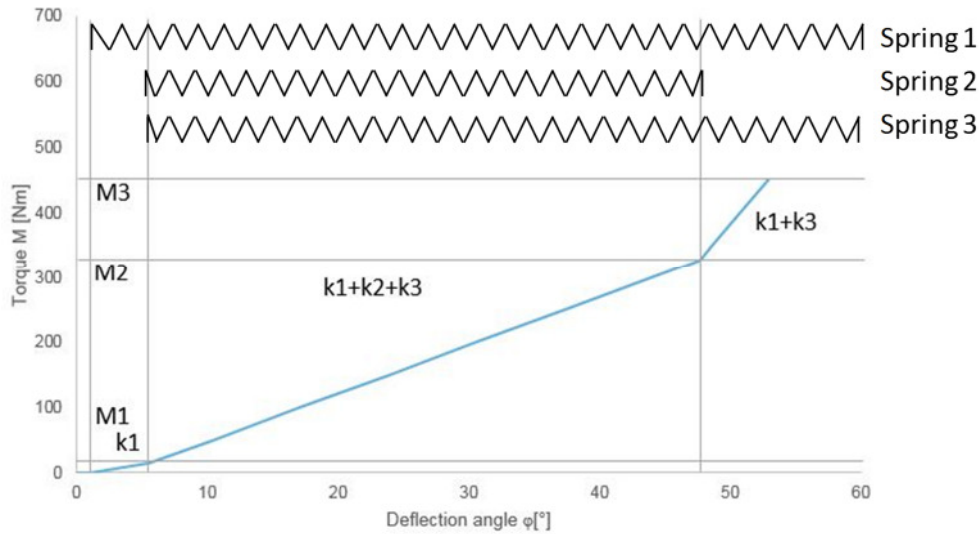


Figure 3.2.6 - DMF characteristic curve

By means of these equations (based on the equations given in (18)) it is now possible to determine the dimensions of all springs. Spring 1 is limited by the available constructing space thus the outer spring diameter can be calculated from the dimension limitations:

$$D_1 = R_e - R_i = 135 - 100 = 35 \text{ mm} \quad (3.2.12)$$

$D_1$  is the coil diameter,  $R_e$  the external installation space radius and  $R_i$  the inner installation space radius.

Since the stiffness's mentioned before are torsional, they have to be recalculated to the linear form and  $k_{1/2}$  in  $Nm/rad$  has to be used:

$$k_{lin1} = \frac{k_{1/2}}{R_m^2} = \frac{1,25 * \frac{180}{\pi} * 1000}{117,5^2} = 5.19 \text{ N/mm} \quad (3.2.13)$$

$R_m$  is the mean radius between  $R_e$  and  $R_i$ .

The force  $F$  applied on the spring is:

$$F_1 = \frac{M_{s1}}{R_m} = \frac{66.21}{0,118} = 561.10 \text{ N} \quad (3.2.14)$$

With the outer spring diameter also the wire diameter can be calculated.  $k$  is an empirical constant used for first spring dimensioning and depends on the used manufacturing technology, wire material and diameter. Assumed is a wire diameter less or equal 5mm,  $k$  is then 0.15 (according to (18)):

$$d_1 \approx k * \sqrt[3]{F * D_1} = 0,15 * \sqrt[3]{561.10 * 35} = 4,05 \text{ mm} \rightarrow d_1 = 5 \text{ mm (DIN 2076)} \quad (3.2.15)$$

The wire diameter was chosen higher because of the dependency of the number of coils on it. A higher amount of coils are necessary for bigger wire diameters according to equation (3.2.18). In (18) are further restrictions given by the spring production procedures for cold drawn wires:  $d \leq 17 \text{ mm}$ ,  $l_0 \leq 600$ ,  $n \geq 2$ ,  $c = 4 \div 20$ , where the spring index  $c$ :

$$c_1 = \frac{D_{m1}}{d_1} = \frac{(35 - 5)}{5} = 6 \quad (3.2.16)$$

$D_{m1}$  is the mean coil diameter. The applied force acts as a torsional stress on the spring and a stress analysis has to be performed to check if the selected diameter withstands the load. The wire is assumed to be made of a steel wire according to EN 10270-2, a SiCr-alloyed spring steel with a tensile strength of  $UTS = 1900 \text{ MPa}$ . For dynamic loaded springs corresponding fatigue stress diagrams exist. As a starting value the stress utilization factor is used (50%) thus the resulting admissible shear stress is  $\tau_{adm} = 950 \text{ MPa}$ . The stress increases on the inside of the spring and must be reflected upon when fatigue is being considered. To account for shear stress resulting from spring curvature several empirical factors have been set. Here calculation according to Bergstrasser (18) is shown:

$$\tau_1 = \frac{8 * D_m * F}{\pi * d^3} * \frac{c + 0,5}{c - 0,75} = \frac{8 * (35 - 5) * 561.10}{\pi * 5^3} * \frac{6 + 0,5}{6 - 0,75} = 424.566 \text{ MPa} \quad (3.2.17)$$

$$\leq 855 \text{ MPa}$$

The wire and coil diameter fulfil the strength and spring index criteria and the number of active coils can be determined:

$$n_1 = \frac{G * d^4}{8 * D_m^3 * k_{target1}} = \frac{79160 * 5^4}{8 * (35 - 5)^3 * 5.19} = 44.13 \quad (3.2.18)$$

Results from this equation don't have to be necessarily reasonable values and may have to be adjusted. Because of the limited space a maximum number of coils has to be determined according to which the final number of coils can be selected. The maximum available length can be calculated from the radius and amount of degrees available for the spring. Each spring would have in an ideal case a  $180^\circ$  space. The stoppers between the two springs (Figure 3.2.4) take usually around  $5-10^\circ$ . For this example  $\alpha_{stopper} = 5^\circ$  stoppers have been picked. In case of the arc spring DMF some backlash is left between the spring and stopper ( $\alpha_{backlash} = 1^\circ$ , Figure 3.2.4). Due to this small torque oscillation are not being transmitted. When considering the length differences on the inner and outer side of the spring it is reasonable to use the inner installation space radius to add some safety to the calculation. The resulting available installation space expressed in degrees  $\varphi_{n1}$  and millimetres  $L_{n1}$  is then:

$$\varphi_{n1} = \frac{360}{2} - \alpha_{stopper} - \alpha_{backlash} = 180 - 5 - 1 = 174^\circ \quad (3.2.19)$$

$$L_{n1} = \varphi_{n1} * \frac{\pi}{180} * R_m = 174 * \frac{\pi}{180} * 117.5 = 356.83 \text{ mm} \quad (3.2.20)$$

The nominal spring length  $L_{01}$  in unloaded condition has to be smaller than the available installation space length:

$$L_{01} < L_{n1} = L_1 + L_{c1} = \left( \frac{F_1}{k_1} + (n_1 + 2) * d_{max1} \right) \quad (3.2.21)$$

Where  $L_1$  is the deflection length meaning the value by which the spring is shortened if deflected:

$$L_1 = \frac{F_1}{k_{1/2}} \quad (3.2.22)$$

And the solid spring length:

$$L_{c1} = (n_1 + 2) * d_{max1} \quad (3.2.23)$$

Since the goal is to use the available space efficiently, the non-deflected spring length should be equal to the available space.  $d_{max}$  is the sum of the wire diameter and its upper permissible deviation  $es$  which can be found in (18) table TB 10-2a. When expressing  $k_1$  from equation (3.2.18) and inserting into equation (3.2.22), equation (3.2.21) can be transformed and accordingly the maximum number of active coils  $n_1$  is:

$$n_1 \leq \frac{L_{n1} - 2d_{max1}}{\frac{F_1 * 8 * D_m^3}{G * d_1^4} + d_{max1}} = \frac{356.83 - 2 * (5 + 0,045)}{\frac{561.10 * 8 * 30^3}{79160 * 5^4} + (5 + 0,045)} = 46.26 \quad (3.2.24)$$

The number of coils calculated in equation (3.2.18) meets the condition of (3.2.24) and can be used for further computation. After choosing a meaningful value for the number of active coils, the real stiffness can be calculated:

$$k_{real} = \frac{G * d^4}{8 * D_m^3 * n} \quad (3.2.25)$$

For this case the number of active coils is fitting and will be only rounded to a value of 46.5, which shouldn't have a big impact on the final stiffness. The total number of coils  $n_t$  for cold drawn wires is:

$$n_t = n + 2 \quad (3.2.26)$$

And the solid length which is the blocking length of the spring, if sanded:

$$L_{c1} \leq (n_1 + 2) * d_{max1} = (46.5 + 2) * (5 + 0.045) = 244.68 \text{ mm} \quad (3.2.27)$$

All linear measures have to be converted into angular dimensions using the installations space radius. The resulting solid spring angle  $\varphi_{c1}$  is:

$$\varphi_{c1} = \frac{L_{c1}}{R_m} * \frac{180}{\pi} = \frac{244.68}{117.5} * \frac{180}{\pi} = 119.31^\circ \quad (3.2.28)$$

The minimum nominal angle of the unloaded spring is the sum of the spring deflection  $\Delta\varphi_{s1}$  during maximum torque and its solid length  $\varphi_{c1}$ :

$$\varphi_{c1} + \Delta\varphi_{s1} = 119.31 + 52.97 = 172.28^\circ < 174^\circ \quad (3.2.29)$$

All conditions necessary to obtain the requested parameters have been verified and the dimension for the outer spring set.

In case of the excel file the installation space, stress utilization, spring index, minimum wire diameter and maximal number of coils have been used, for the inner springs also the winding diameter has been adjusted to meet the stiffness requirement. If it is not possible to find any value fulfilling the demands, the following parameters have to be modified: it is feasible to either lower the number of coils or to increase the wire diameter resulting in a higher stiffness and the possibility to transmit higher torque; to lower the torque which gives the possibility to use a smaller wire diameter or if possible the coil diameter can be increased, both lowering the resulting stiffness. If none of these changes are appropriate, only increase of the stiffness is possible.

### Spring #2

When using the combination of an external and internal spring it is favourable to use the biggest diameter possible for the external spring to facilitate a bigger space and more diameter options for the internal spring, especially when higher torque has to be transmitted in the second stage.

Table 3.2-3 - spring 2 calculation parameters

Number of springs	2.00	-	
Transmitted torque	103.33	Nm	
Torque Stage 1	326.00	Nm	326000.0000 Nmm
Optimal spring stiffness	3.19	Nm/°	182.7735 Nm/rad
Wire diameter tolerance	0.045	mm	
Nominal spring length	341.25	mm	0.1482 m
Nominal spring angle	72.25	°	1.2610 rad
Twist angle till block	32.39	°	0.5653 rad
Solid spring angle	39.86	°	0.6957 rad
Tensile strength Rm	1900.00	N/mm <sup>2</sup>	1900000000.0000 N/m <sup>2</sup>
Stress correction factor	0.50		
Admissible shear stress	950.00	N/mm <sup>2</sup>	950000000.0000 N/m <sup>2</sup>
Shear modulus	79160.00	N/mm <sup>2</sup>	79160000000.0000 N/m <sup>2</sup>
Minimum spring index	3.99	-	
Minimum number of coils	6.00	-	

The coil diameter of spring 2  $D_2$  is the inner coil diameter of spring 1  $D_1$ :

$$D_2 = D_1 - 2d_{max1} = 35 - 2 * (5 + 0,045) = 24,91 \text{ mm} \rightarrow 24 \text{ mm} \quad (3.2.30)$$

The torque transmitted by spring 2 is defined by equation (3.2.7) and using equation (3.2.9) the deflection difference angle can be specified. When using equation (3.2.14) in equation (3.2.15) the wire diameter  $d_2$  is:

$$d_2 \approx k * \sqrt[3]{F_2 * D_2} = k * \sqrt[3]{\frac{M_{s2}}{R_m} * D_2} = 0,15 * \sqrt[3]{875.42 * 24} = 4.1 \text{ mm} \rightarrow d$$

$$= 3.8 \text{ mm}$$
(3.2.31)

For the stress analysis and spring index the value  $\tau = 820.65 \text{ MPa}$  and  $c = 5.32$  were obtained and are sufficient.

The length of both internal springs cannot exceed the rest length of the external spring after reaching stage one torque. Again for both enough space has to be facilitated to ensure the needed deflection length for the given parameters. When determining the installation space and deflection angle of the springs, the blocking length and thus the number of coils can be calculated. For this all the equations from the sections before can be used. If just one internal spring is used, all of the left space after the external spring reaches stage 1 is left for spring 2. After the external spring reaches its solid length no more deflection is possible, which is why the solid length for the second and third spring together should be chosen to be the same as the external spring 1 length. When considering two internal springs in serial arrangement the situation is somehow different. The goal is to reach a higher stiffness in the last stage when the highest torque is applied. The two springs arranged in serial have a lower final stiffness than each of them alone, so to ensure a high stiffness in stage 3, one of the two internal springs has to reach their blocking length in stage two. It is clear that the one with lower stiffness will reach its blocking length earlier. The second spring has to reach its solid length with stage 2 torque and should be as small as possible to provide more space for the third spring. First we consider all the space available after stage 2 has been attained:

$$\varphi_{n2} = \varphi_{n1} - \frac{M_1}{k_1} = 174 - 5.6 = 168.4^\circ$$
(3.2.32)

$$L_{n2} = \varphi_{n2} * \frac{\pi}{180} * R_m = 168.4 * \frac{\pi}{180} * 117.5 = 345.35 \text{ mm}$$
(3.2.33)

And with the available installation space is the maximum number of coils (equation (3.2.24)):  $n \leq 46.45$ .

To obtain the desired stiffness ( $k_2 = 3.19 \frac{Nm}{deg}$ ) the number of active coils has to be according to equation (3.2.18)  $n = 18.9$ , which is in the desired range. When using a higher number of coils the stiffness will get lower, so to maintain the same stiffness value the wire diameter would have to be raised, too. On the other hand if the space for the second spring is too low the only other possibility would be to lower both the wire diameter and number of active coils. For  $n = 18.9$  is the solid length  $L_{c3} = 80.36 \text{ mm}$  (equation (3.2.27)). The nominal length of spring 2 in unloaded condition is then:

$$L_{02} = L_{c2} + \frac{M_{s2}}{k_2} = 80.36 + 32.38 = 112.74 \text{ mm} \rightarrow \varphi_{02} = L_{02} * \frac{180}{\pi * R_m}$$

$$= 112.74 * \frac{180}{\pi * 117.5} = 54.98^\circ$$
(3.2.34)

### Spring #3

Table 3.2-4 - spring 3 calculation parameters

Number of springs	2.00	-	
Transmitted torque	158.79	Nm	
Torque Stage 1	450.00	Nm	450000.0000 Nmm
Optimal spring stiffness	10.60	Nm/°	607.3353 Nm/rad
Combined stiffness spring 2+3	2.45		
Wire diameter tolerance	0.045	mm	
Nominal spring length	197.18	mm	0.1972 m
Nominal spring angle	96.15	°	1.6782 rad
Twist angle till block	21.61	°	0.3771 rad
Solid spring angle	74.55	°	1.3011 rad
Tensile strength Rm	1900.00	N/mm <sup>2</sup>	1900000000.0000 N/m <sup>2</sup>
Stress correction factor	0.50		
Admissible shear stress	950.00	N/mm <sup>2</sup>	950000000.0000 N/m <sup>2</sup>
Shear modulus	79160.00	N/mm <sup>2</sup>	79160000000.0000 N/m <sup>2</sup>
Minimum spring index	3.99	-	
Minimum number of coils	10.00	-	

The remaining space for spring 3:

$$\varphi_{n3} = \varphi_{n1} - \varphi_{02} = 174 - 54.98 = 119.02^\circ \quad (3.2.35)$$

Since it's favourable to attain with the addition of spring 2 and 3 the same solid length as spring 1, the solid length of spring 3 is already given:

$$\varphi_{c3} = \varphi_{c1} - \varphi_{c2} = 119.31 - 39.19 = 80.12^\circ \quad (3.2.36)$$

The final check is if the remaining space is enough to ensure the deflection angle of spring 3 necessary for stage 2 and 3. For  $M_{s3} = 158.7 \text{ Nm}$  is  $\varphi_{s3} = 14.97^\circ$  and meets therefore the requirements. After this check the rest of the parameters can be calculated.  $D_3$  is the same as  $D_2$ , the wire diameter of spring 3 is  $d_3 = 4,78 \text{ mm}$ . A slightly smaller size from TB 10-2a in (18)  $d_3 = 4,75 \text{ mm}$  was chosen, the shear stress for this value is  $\tau_3 = 848.17 \text{ MPa}$  and the spring index  $c_3 = 4,05$ . For this wire diameter and the chosen stiffness is the number of coils  $n = 16.05$ . The final solid length  $\varphi_{c3} = 42.21^\circ$ , which is smaller than the value computed before and means that with this coil and wire diameter chosen spring 3 would not reach its solid length after maximum deflection of the outer spring. The difference to the requisite value of  $\varphi_{c3} = 75.2^\circ$  is  $32.99^\circ$ . An option to find a value better fitting into the given space limitations, the spring coil or wire diameter and number of coils would have to be modified.

## 4. NVH Aspect of hybrid vehicles

---

NVH is a shortcut for Noise-Vibration-Harshness. It's a summarizing topic concerning hearable and perceptible vibrations (frequency range: 20 - 100 Hz) in vehicles which are directly affecting the drivers driving experience. Mechanical oscillations appear in the automotive technologies in various ways and are mainly unwanted even though in particular cases these vibration phenomena are used to emphasize the vehicles character. Low frequency oscillations are perceived by car occupants as vibration, whereas higher frequencies up to 1 kHz are of importance as structure-borne noise. The latter will only be perceived by the car occupant if airborne sound arises thus resulting in a for the human ear hearable sound. Frequencies of a certain range (20 – 100 Hz) are perceptible as well as hearable and are therefore termed as harshness. The combinations of acoustic- and vibrational effects are still a hardly explored field. Important parameters for expressing oscillation are distances, angles, angular velocity and acceleration, forces, torques and so on. Oscillations can be divided into free, where the observed system will be oscillating with its natural frequency, forced oscillations, which are induced by an outer energy source, self-excited and parameter-excited oscillations. Latter are the most complex since one or more not constant periodically changing coefficients can appear. All of these categories are for passenger cars relevant.

Three main sources for the oscillations are known: road-excited, wheel-excited and engine-excited oscillations. The former is caused by irregularities on the road. Wheel-excited oscillations arise due to un-uniformities of the wheel resulting in fluctuating wheel load. These are at higher velocities mainly perceived at the steering wheel and seat. The latter as the name suggests are excitations induced by the engine. These arise from the forces acting on the crankshaft. The dominant periodic tangential and radial forces acting on the crankshaft are resulting from the combustion process inside of the cylinders. Energy produced during the combustion process is transformed into a piston stroke, which is converted by the crankshaft into torque available at the flywheel. For 4-cylinder engines combustion occurs twice every engine revolution leading to acceleration and deceleration of the reciprocating power-transfer components generating inertia forces. As mentioned before, in case of the 4-cylinder engine analyzed in this thesis, forces and torques of the 2<sup>nd</sup> order (often referred to as main harmonics) originate. Except of the forces originating in the combustion process, the inertia forces caused due to motion of the reciprocating masses act on the crankshaft. These inertia forces combined with operating gas and gravity forces act on the crank mechanism and are the primary source of engine vibrations (19). In case of the cylinder forces it is usual to talk about average peak cylinder pressure since a deviation of the maximum pressure occurs. They are split into the ones acting on the rod and the other sideway on the cylinder wall resulting in the crankshaft output torque. Excitation forces due to the rotating parts like centrifugal force or torque from unbalances are a secondary source.

Engine noise is mostly radiated from larger and flexible surfaces, e.g. sumps, timing case covers and induction manifolds. These should be therefore isolated. Ideal gear pairs should be running at constant speed with smooth power transmission. However in reality tooth errors and in some cases shaft eccentricities exist and can become a fundamental component of vibration. Gear teeth are elastic and bend slightly when operating under load. When contact between the teeth of the driving and driven wheels is made, abrupt transfer of load causes torsional vibration and noise in the transmission. Teeth oscillation can be recognized by a characteristic whining or whistle noise. Oscillation of loose components are named rattle. Also noise when changing the gear or from the bearings are possible.

Frequently encountered are torsional and bending vibrations of the crankshaft and valves-camshaft. Those can lead to fracture of the shaft or bearing damage. To external vibrations of the entire engine as a block is referred to as external vibrations and is usually integrated with the transmission case. These are caused by unbalanced, inertial moment or variable-output torque.

Engine oscillations are e.g. Start-Stop oscillations as well as powertrain oscillations and load cycling and friction oscillations at clutch slipping. Resonance occurs when an excitation torque is applied which coincides with the natural frequency of any powertrain component and if severe can end up in overall failure.

At the wheels a transformation of the rotational movement into translational occurs and torsional torque oscillations are being transformed into oscillations in the vehicles longitudinal direction. Very important is load cycling usually caused by the driver (tip-in, back-out). Low frequency excitations are known as jerking (closed clutch) and picking (slipping clutch), high frequency load shocks or clicking. The mass forces of the crank mechanisms and balance shaft act as reaction forces in the bearings. Engine torque must be supported via a contra-torque in the engine bearings.

Since the structure of hybrid vehicles is of bigger complexity than conventional vehicles, NVH challenges have to be adapted and are the following:

- Increased system complexity and inertia due to the electric motor rotor– more potential noise sources and shifting of the system natural frequencies
- No masking by IC-engine in full electric mode – NVH effects shifted to higher frequencies
- NVH from transient operating conditions – change of torque flow and activation/deactivation of components during:
  - Start/Stop
  - ICE Engagement
  - Transition between operating conditions
- E-machine, inverter and relay noise

Consequently are control strategies more complex and lead to more NVH critical operating conditions.

Only vibration arising in the powertrain are going to be analyzed in this thesis, the main focus being set on their source and importance during hybrid specific operating conditions.

### 4.1. Operating conditions and NVH effects (20)

The goal of this thesis is to simulate individual operating conditions of a P2 hybrid vehicle and to evaluate NVH in the drive train depending on different DMF settings. During normal operation, hybrid vehicles pass several operation states. In these states the rotational speed and torque process can be according to Figure 4.1.1:

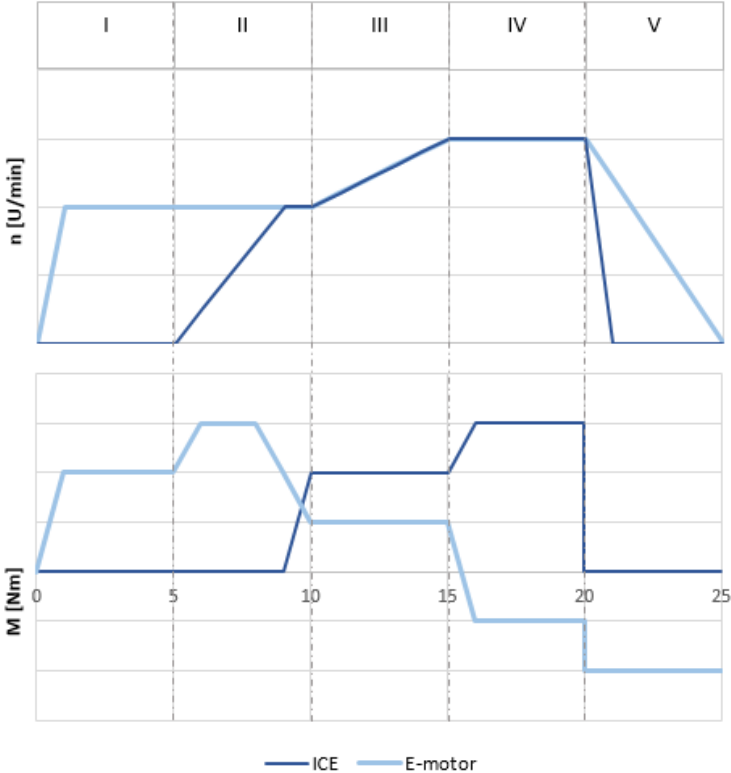


Figure 4.1.1 - Rotational speed and torque in hybrid specific operating conditions

The operation states presented are:

- I. Electric motor start and operation
- II. Internal combustion engine start
- III. Hybrid operation – electric motor and ICE
- IV. Load-raise – engine operated at higher load to charge battery
- V. Breaking – recuperation, battery charging

Operating conditions which are part of the above mentioned and which will be analyzed within this thesis are:

- Idle drive
- Run-up
- Start/stop process
- Cycling

These and usual NVH effects will be further described in the next chapter.

#### 4.1.1. Idle operation

Idle drive is the condition when no torque is transmitted by the engine and energy from the fuel is only used to overcome friction and other losses in the cylinder. The usual idle drive rotational speed is around 600-1000 rpm. Oscillations arise through cyclic and stochastic excitation from the engine. Different oscillation modes can be excited:

For lengthwise installed engines the most typical are:

- Aggregate waving in the engine bearings
- Opposite aggregate/vehicle-lateral oscillations
- Vehicle rolling on wheel spring

All these conditions appear at different frequencies. If one of them is being reached through the dominant engine order, critical vibration occur. For a 4-cylinder engine the second order is from importance and the vehicle has to be adjusted to it.

To avoid the excitation of vehicle natural frequencies through the engine order, torsional and bending frequencies have to be between 27 and 33 Hz with at least 3 Hz spacing (20). Most typical for idle speed operation is gear rattle induced by the teeth on the loose gear-wheel hitting the pinion gear. The components of engine vibration at idling are multiples of engine speed. The primary bending mode of cars can be less than 20 Hz. It's easy to excite body resonance at idle if the engine is not isolated well.

To control NVH appearance during idle some natural frequencies of the vehicle have to be taken into consideration. For this reason their value has to be determined and further vehicle design adapted.

#### 4.1.2. Hybrid/conventional start/stop

Vibro-acoustic effects of relevance appear when the ICE is being started or stopped. With the start-stop system, vibrations occurring at idle loose of importance since they are in less situations relevant. The oscillations originating should be kept bellow perceptibility especially when they are initiated automatically. When starting a vehicles IC-engine, first the starter has to overcome the breakaway torque of the engine and increase its speed. Everything after depends on the moments of inertia of the crank train, the gas forces of all cylinders and on the friction torque. Three start processes can be distinguished depending on the engine speed when first combustion occurs:

##### Conventional low engine speed start

To increase engine speed from zero electric starter motor starts the turning. A pinion gear is located on its shaft and engages with a larger gear ring around the rim of the engine flywheel. Electric current is drawn from the battery to initiate rotation. The pinion is not fixed to the shaft and threaded on to it, so when rotation speed increases, the pinion gear shifts along the thread until a stop is reached and afterwards it starts to turn with the shaft

and engages with the gear ring on the flywheel. When the engine picks up speed and the pinion gear starts to turn faster than its shaft, it disengages again to avoid damage of the starter motor.

At low engine speed start, first combustion occurs at 250-300 1/min. Important is the fast haul up of the engine via a sufficiently designed starter motor. Especially in powertrains with a DMF it is necessary to ensure a fast run-up from zero to avoid excitation of the DMF natural frequency, which usually lies below idle speed. Very often synchronous machines with belt drive are used as starter and generator since they offer more starting comfort than pinion gears. Even better in performance are starting-generators.

High rotational speed-fluctuations occur during start up and are caused by unstable combustion forces, which arise when the resonance frequency of the engine mounting is being reached. These fluctuations are perceptible as shaking.

Critical are slightly decreasing starter-speed and premature disengagement of the starter.

Some P2 hybrids use a starter to launch the vehicle instead of a hybrid start so the ICE can be started independently of the EM and the EM is only used to ensure traction during IC-engine start.

#### High engine speed/hybrid start

In vehicles, where purely electrical driving is possible and an additional clutch is present, start processes are very often used and can be initiated depending on the driving situation independently of the driver. High demands are being set to make the engine start as seamless as possible. This is possible by means of high engine speed start-ups, occurring at 600-750 1/min. Electro motors with more power have to be employed to drag the engine to its initial speed in a short time making this technology ideal for full hybrids or plug in hybrids, where electro motors of sufficient size are already present.

The launch-up is ensured in the following steps:

- The electric motor transmits a torque value depending on the gas pedal position
- After clutch-closure initiation this torque is being raised by a value necessary for the IC-engine tow
- The linearly increasing torque is being transmitted during the clutch-closing process to the ICE; the electric motors and IC-engines' relative speed start to balance
- When the ICE reaches its target value, firing is being started causing the IC-engine torque to rise and the EM torque to lower down again to the gas-pedal position value

Natural frequencies, which are in the start-up speed range, are being passed through during engine start and cannot be avoided. To lower these, small cylinder fillings are advantageous. The throttle valve should be almost closed. Another option is optimization with the help of the DMF via e.g. damping modification (usage of inner damper).

A compromise between the tolerated resonance amplitude and oscillation isolation has to be found. When increasing the DMF's damping value, isolation in overcritical areas is

worsened since isolation effects decrease with rising frequency ratio according to Figure 4.1.2 (20).

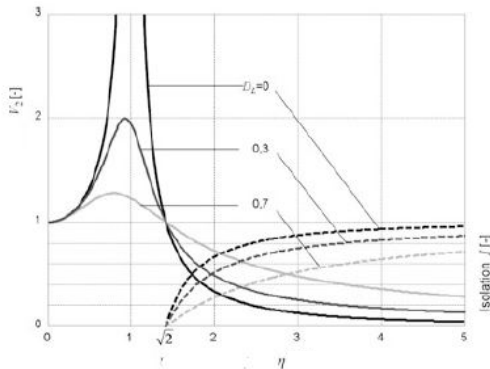


Figure 4.1.2 - Ideal isolation for different damping values  
( $V_2$ =amplification function,  $\eta$ =frequency ratio)

Where  $\eta$ :

$$\eta = \frac{\Omega - \text{excitation frequency}}{\omega - \text{natural frequency}} \quad (4.1.1)$$

### Motor stop

Motor stop occurs when the engine is being shut down. In hybrid vehicles this is induced by the start-stop system during idle or standing phases. Similarly to the engine start, also during engine stop the resonance frequency is being passed through.

An important parameter during engine stop is again cylinder filling, since it directly affects the magnitude of the gas torque. The filling inside the cylinder acts as a spring and its stiffness depends on the filling amount. The gas-exchange torque dominates the moment of inertia and friction torque and the gas torque in the at last compressed cylinder to a value which causes a change of direction. The filling is being again compressed until the engine stops. Higher bearing forces appear and are transmitted to the car body. If the throttle valve is closed, peak pressure is being reduced and the stopping process takes place in an even manner.

### 4.1.3. Cycling

Standard passenger vehicle powertrains with DMF are usually designed torsionally flexible. When maximum torque is applied, twisting angles up to 90° from the crankshaft to the wheel can occur. Due to this torsional oscillation are excited during cycling and can be perceived as longitude-low-frequency oscillation (jerking) or higher frequency acoustic phenomena (load change reaction, clonk). At low frequency oscillations two types of jerking appear: picking with closed clutch or shudder, when the clutch is slipping. Both have a strongly negative effect on the driving comfort.

Jerking oscillation appear in a for humans very sensitive frequency range from 2-8 Hz, depending on the activated gear. This excitation is not caused by the engine orders but by

sudden torque changes occurring when suddenly accelerating (Tip-In) or decelerating, i.e. quick foot removal from the gas pedal (Tip-Out). The system reacts to this impulse and starts to oscillate with a frequency in accordance with some of the natural frequencies. This appears often in vehicles with a manual transmission at low engine speed and low gears.

Load shocks appear at higher frequencies and gears than jerking. Similarly as before is the cause sudden torque change induced by quick gas pedal movements. The vehicle makes an abrupt translator movement in the driving direction causing the transmission to oscillate against the engine and vehicle followed by a hollow beat noise. The noise results from the bearings and loose transmission components reaching their end stop position or just moving between their end stop positions, dependent on the magnitude of the load change. This is perceptible as a higher metallic sound often called clicking and clatter.

Picking arises due to periodically alternating torque originating when the clutch is not fully engaged and slipping. If the alternating torque lies in between some of the natural frequencies of the through the clutch uncoupled part of the power train, longitude movements appear. When the clutch is closed, the same natural frequencies lie above and have typical values around 8-12 Hz.

Two types of picking exist:

- Self-excited picking occurs when the clutch friction coefficient is between the stick-and slip value. Firstly the output side is being dragged due to static friction and twisted. After a certain deflection the torque is higher than the static friction causing both sides to rotate relatively to each other until sticking occurs again and the procedure repeats, the power train oscillates.
- Forced excitation is the result of a periodically varying normal force on the friction partners. Also in this case the clutch disc starts to oscillate. Causal are geometrical deviations in the clutch system effecting fluctuations of the normal force. To obtain better power train efficiencies, friction reduction in the drive train are being researched having a bad impact on the picking tendency.

Gear changing is another cause of oscillations considering it as a fast change of output torque. The easiest way to control these effects is to implement some kind of regulation into the engine control system and prevent the engine from getting commands directly from the pedal position by filtering and adjusting the signal. The torque rise is more controlled and limited by the load shock damping, anti-jerking functions modify the ignition angle and cause additional damping of the drive train. Further improvements can be made with slip-controlled clutches or by specific adjusting of the power train components stiffness. The usage of dual mass flywheels has a perceptible impact and is likewise often used in modern vehicles.

#### 4.1.4. Run-up (full load/part load)

The biggest issue regarding NVH in hybrid vehicles appearing during run-up is connected to the change of torque flow caused by activation or deactivation of the electric motor or combustion engine. Depending on the driving mode and activated component, during accelerating often both electric motor and engine are used to provide a sufficient boost. The results are similar to the ones described in section 4.1.3.

### 4.2. Components affecting NVH in hybrid vehicles

A driveline usually consists of the engine flywheel (single- or twin mass), clutch, manual or other transmission system including all shafts, the differential with the side shafts, wheel and tires (21). An example of drive components of a passenger car with the possibly occurring corresponding NVH phenomena are in Figure 4.2. Some of the most important will be described further.

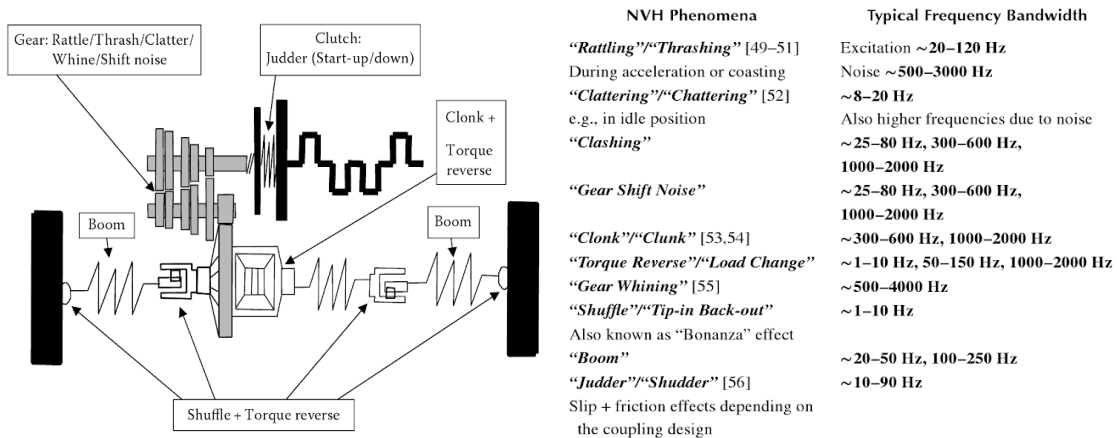


Figure 4.2 - NVH phenomena in a passenger car powertrain (FWD-left) and their characteristic frequencies (right) (21)

#### 4.2.1. E-machine

Often used in HEV systems are asynchronous-motors and permanent magnetic synchronous-motors. These are contributors to the interior noise.

The electric motor can cause NVH related problems, mainly of acoustic nature. Saturation or ripple torque effects of motors are not big enough to be noticed from the driver. The noise level emitted by the electromotor is very low compared to the ICE, but has different frequency content due to its high frequency level and appears to be more annoying. The IC-engine noise is in many cases even a requirement from the driver, since it enhances the sporty drive feeling. With electric motors there is no dependency of the interior noise on the load which is compared to the ICE to the drivers perceived as a shortage.

Electric motor noises are most significant during generator operation. In most HEVs the electric motor is being converted into a generator whenever the vehicle is braking and produces variable frequency noise depending on the generator speed. The generators noise

amplitude increases with decreasing vehicle speed (22). In these conditions motor noises get also more apparent since the overall background noise levels decrease.

#### 4.2.2. IC engine

Noise intensity of combustion engines is proportional to the square of the pressure rise rate and the sound pressure level of noise to the logarithm of heat generation or release rate in each cylinder (23). The pressure rise rate is defined by the ignition delay, speed and torque load and can therefore influence noise intensity. Mechanical sources are mainly the piston slap, friction, gear and tooth belt meshing, belt slippage, bearings and the timing, accessory and pump system. These are proportional to engine speed. As mentioned before noise radiation from the engine surface as the engine block surface, oil pan and cylinder head and cover are another relevant source. Fan, intake and exhaust noise are aerodynamic sources and are determined by their dimensions, e.g. in case of the fan by its blades and also number of blades and in case of intake and exhaust the pressure pulse, flow friction and turbulence.

Contribution of ICEs to the vehicles NVH characteristic is different for various operational conditions and dependent on the engine type. Former and latter differ for hybrid vehicles. Transient operating conditions appear which have to be analyzed. Due to the present electric motor, engines in hybrid vehicles are even more downsized changing the vehicles NVH significantly. An example for the operating condition dependent noise is the missing correlation between engine speed and vehicles speed in hybrid driving modes. The engine does not necessarily increase its speed when moving the gas pedal and increasing the speed requirement. This is due to the demand for lower fuel consumptions. A control unit monitors the drivers demand and calculates the best engine operating point. Extra torque needed to increase vehicle speed is provided by the electrical motor.

#### 4.2.3. Clutch

The clutch has an important effect on torsional vibrations. These are either dry friction damping or torsion spring effects. Clutch activation happens in two steps: first the transition period and second the traction period. Dry friction damping influences the vibrational behavior only during the transition period, when power is slowly passed from the engine to the gearbox, or in case of too high torque transmission, when the clutch starts to slip. Both are also influenced by the spring stiffness of the damping springs included in the clutch. In case of this work torsion springs are included in the DMF, the clutch being directly a part of it. NVH behavior can be modified with the used friction material and transition time.

#### 4.2.4. Transmission (23)

Many of the driveline noises can be connected with its gear box. Most problems are connected with manual transmission and have been partly resolved with the entry of new transmission systems like the dual clutch transmission or automatic transmission. Different types of gear box noise are:

- Low rotational frequency harmonics (~1-400Hz)

- Gear whine (~500-4000 Hz)
- Gear rattle (~20-120 Hz)
- Shift noise (~25-80 Hz)

In this thesis the occurrence of transmission rattle is going to be inspected.

#### Low rotational frequency harmonics of shafts

Low rotational frequency harmonics are caused by imbalances, layer offset and curvature of the drive shaft and have impact in low frequency spectra. Primary affected are components which drive the gear behind the clutch.

#### Gear whine

Whining is caused by the torque transmitting tooth pairs in gearboxes and their relative movement. Its main cause variable is the number of tooth pairs in mesh, further geometry errors or the shaft bending stiffness (20). With a higher number of teeth in mesh, the final force which has to be transmitted by each tooth is decreasing causing subsequently a lower tooth deformation and hence lowering also the resulting noise.

#### Gear rattle

Rattle is a typical result of unengaged gear pair or other loose components moving freely within their backlash and generating contact force impacts. The movement itself is caused by torsional excitation at the transmission input. Rattle noise occurring during traction at low load or low velocity and speed ranges are also called creeping. Rattle appears mainly at spur gear manual and dual clutch transmissions. It is perceived as especially annoying because of its broken-like noise.

#### Shift noise

Shift noise occur at synchronization malfunction caused by scratching of gear switching teeth, or are cycling conditioned due to transient excitement also called clonk. The same noise can likewise arise during fast clutch engagement or disengagement.

### 4.2.5. The wheels

The wheels consist of rim, rigid rotating components and the tire. When simulating wheels, interactions with the road have to be taken into account. It is assumed that deformation takes place on the tire surface and that the tire material has viscous-elastic properties. Due to this, deformation and self-damping effects are assumed to be a combination of elasticity and damping.

### 4.2.6. Dual mass flywheel

Facts about the DMF and how it influences the vehicles NVH has already been described in detail in section 2.3.

# 5. NVH Evaluation

---

## 5.1. Introduction into 1D MBS

Multibody systems are technical systems consisting of different rigid or flexible bodies which are connected. Connections can be created with classical force laws (mass less springs and dampers, actuators, contact) or by kinematical constraints (e.g. joints).

Multibody simulation (MBS) is a branch of mechanics dealing with movement behavior of mechanical systems. The bodies themselves are represented by their inertia. All bodies have 6 degrees of freedom when spatial movement is considered, 3 translational and 3 rotational. These can be defined by boundary conditions and with addition of initial conditions the transient motion of these systems and the forces and moments acting in the connection points can be analyzed through simulation. Typical examples are moving gears in vehicles, robotics, etc.

MBS plays a considerable role in the automotive industry where the gain is to simulate movements of all parts of the designed vehicle. This is very important to recognize undesired behavior already in the designing phase. Important parameters are:

- Comfort/NVH
- Performance
- Durability
- Costs
- Installation space/mass
- efficiency

Thanks to the usage of CAE software, development time can be significantly shortened; the production performance increased and costs of production lowered since no prototype is necessary.

In case of drive technologies following characteristics and tasks have to be written:

- Investigation of dynamic behavior of complex drive systems
- Comparison of natural frequencies and excitation frequencies especially in drives with variable rotational speed and broad excitation spectra's to determine possible resonance occurring during operation

In this thesis the CAE software Simulation X from ESI ITI, version 3.9 was used. It is an interdisciplinary software for modeling, simulating and analyzing multi physics systems on the basis of Modelica. Included is a library with system components which ease the modeling process. Both one-dimensional and three-dimensional systems can be simulated.

1D MBS will be used to perform a modal and time domain analysis of a passenger vehicle P2 hybrid. Through modal analysis the systems natural frequencies can be obtained and used for comparison when evaluating the time domain analysis. In the time domain analysis the

behavior for hybrid vehicles typical operating modes will be specified via simulation and the critical natural frequencies visualized. The source of excitement can be determined and the system optimized by modification of the sources properties. For this thesis models for hybrid specific operating conditions have been constructed to simulate the behavior of a P2 hybrid powertrain. They differ not only in construction but also their boundary conditions and starting values are different for every mode. Because of this, individual models for each mode have been prepared. Their structure and the used values will be explained in the next chapter.

### 5.2.Creation of hybrid powertrain 1D torsional MBS model

One topic of this master thesis is the creation of a hybrid powertrain as 1D torsional MBS model with characteristic properties to simulate its dynamic behaviour in hybrid specific operating conditions. The basic model for this master thesis has been entirely created in SimulationX by the author according to the P2 hybrid arrangement of the given vehicle and will be now introduced more in detail in this section.

To create a simulation model first the basic structure of the P2 hybrid powertrain has to be determined. All important sections have to be considered and divided into elementary parts to ensure as realistic results as possible. The basic structure is visible in Figure 5.2.1:

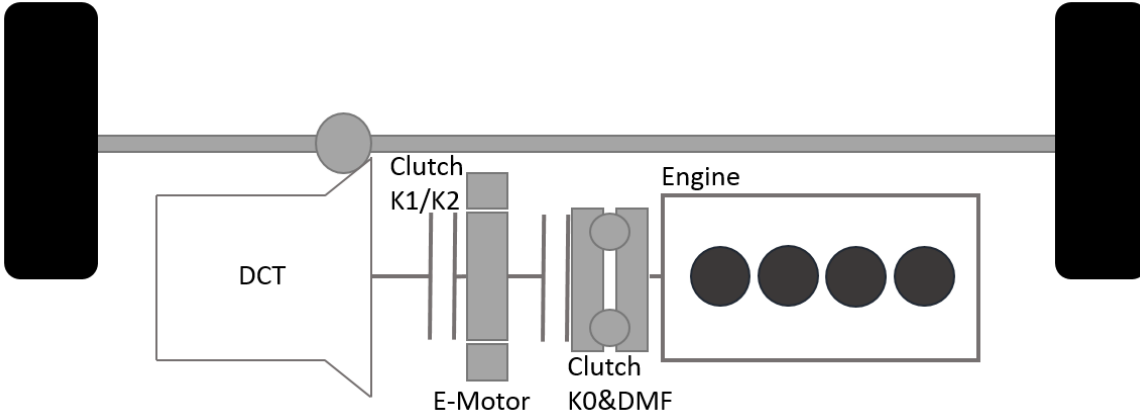


Figure 5.2.1 - P2 hybrid arrangement

Subject of analysis in this section is a passenger vehicle P2 hybrid with 4-cylinder engine, DMF and Dual-Clutch-Transmission (DCT) connected via differential to the side shafts. All basic vehicle parameters from importance for the simulation model are in Table 5.2-1:

Table 5.2-1 - parameters of the analysed vehicle

Vehicle type	P2 - hybrid passenger vehicle
Coupe type	Hatchback
Electric motor Torque	330 Nm (short time)
ICE Torque	250 Nm/1600-3500 rpm

Number of cylinders	4
Position of cylinders	Inline
Fuel type	Hybrid – petrol/electricity
Transmission type	Dual-Clutch Transmission
Number of gears	6

In Figure 5.2.3 is the MBS model showing the motor side of the hybrid powertrain. On the engine side of the P2-hybrid is the internal combustion engine with the crankshaft broken down into several rotational inertias and spring and damping units. Their values have been obtained from a test bench. The engine itself is divided into 4 individual cylinders, their pistons driven by a force calculated from a pressure characteristic. The engine has a maximum performance of 110 kW and torque of 250 Nm. The crankshaft is divided into several inertias representing the mass of the Damper, Pulley, Journals etc. Due to its asymmetric shape, the rotating mass has to be reduced to a representative value (*Frahm1-4*). This value is delivered by Frahm's formula:

$$\theta_{red} = r^2(m_{rot} + \frac{1}{2}m_{osc}) \quad (5.2.1)$$

Where  $r$  is the cranking radius,  $m_{rot}$  the rotating mass and  $m_{osc}$  the oscillating mass.

Directly connected to the crankshaft is the primary part of the DMF consisting of several external straight compression springs and two internal springs. Its characteristic is divided into 3 stages with the stiffness and parameters used in section 3.2.3. The DMF setting in the SimulationX program environment is in Figure 5.2.2.

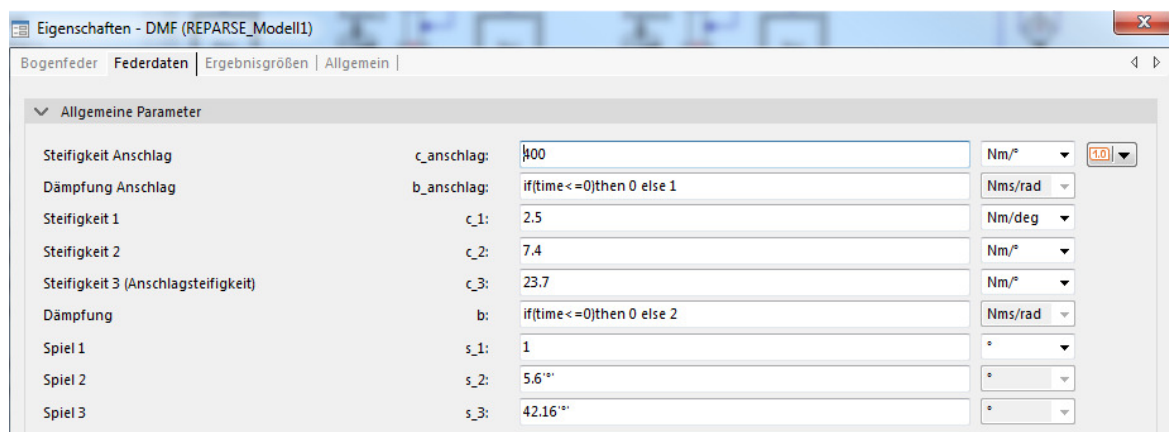


Figure 5.2.2 - DMF settings in SimulationX

Attached to the secondary DMF side is the main clutch K0, ensuring the connection between the electric motor and internal combustion engine. K0 is visible in Figure 5.2.4 (*J\_K0\_EM*).

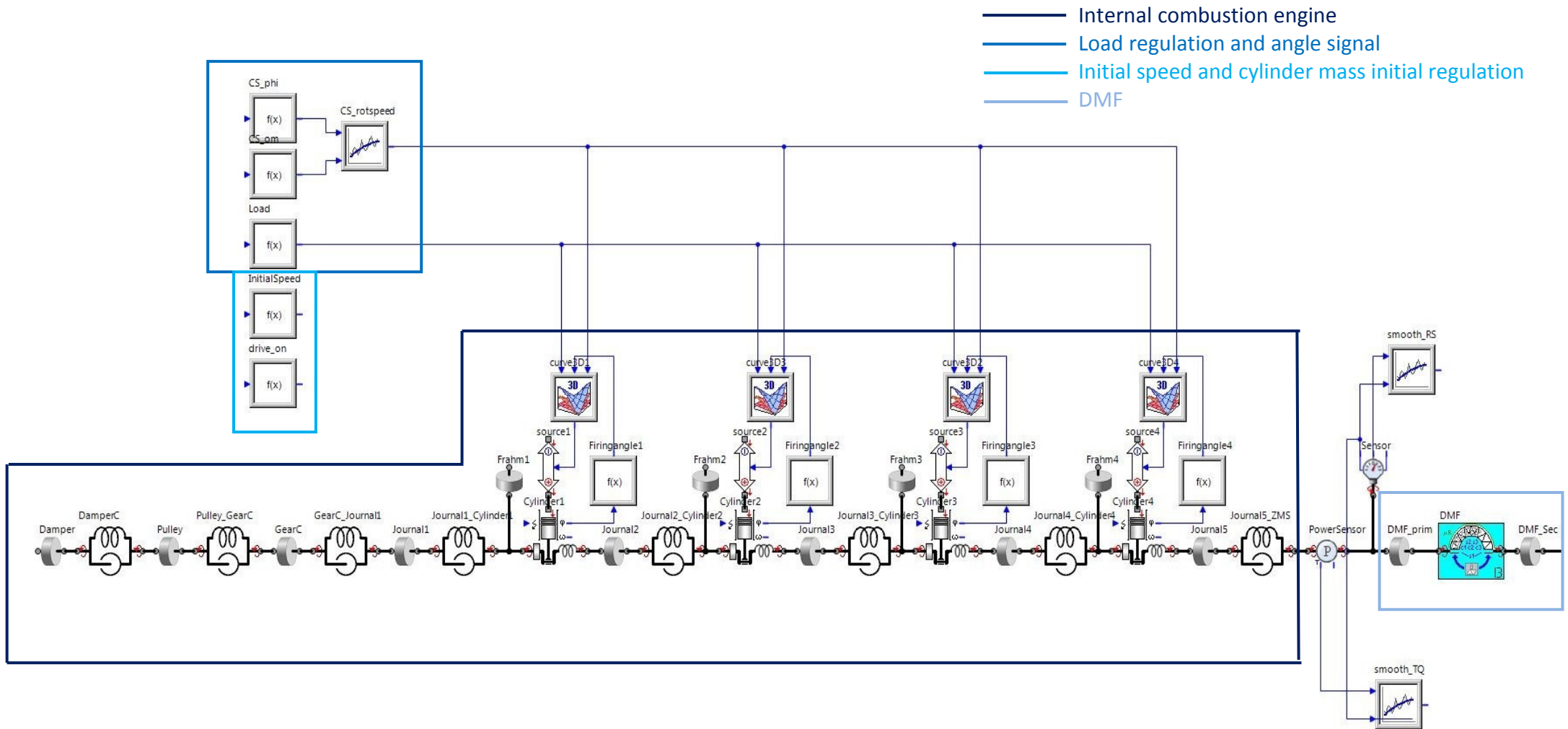


Figure 5.2.3 - MBS simulation model - engine side

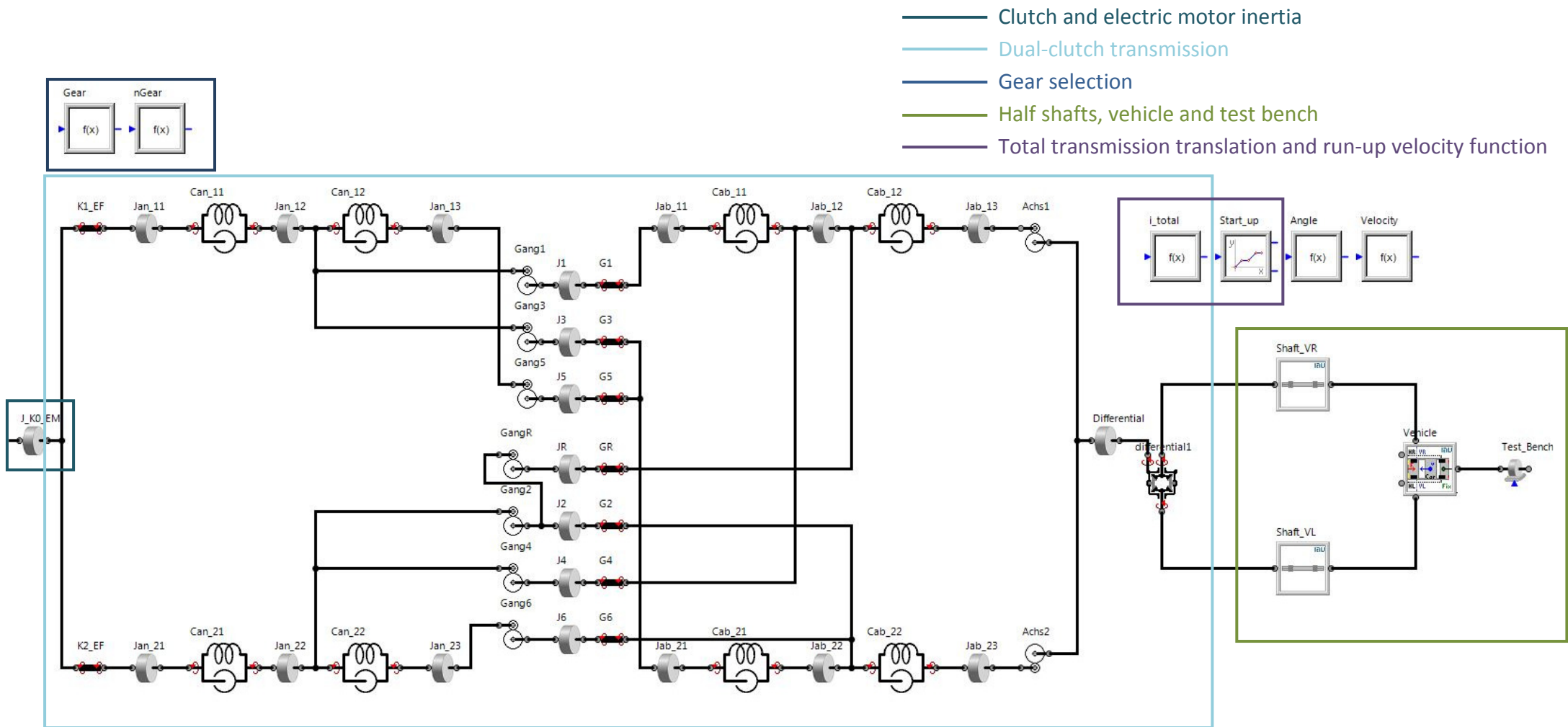


Figure 5.2.4 - MBS simulation model - transmission side

Through this clutch the switching between the individual operating modes and the hybrid start of the IC-engine is enabled. The electric motor is placed on the gearbox input shaft and directly coupled with the primary K1 and secondary K2 clutch of the 6 gears dual-clutch transmission. For the simulation only the inertia of the EM has been considered since for the analysis performed in this thesis, the difference caused by the extra weight of it is from biggest importance and has been added to the K0 inertia. Its maximum performance is 75 kW and torque 350 Nm (short time). These clutches are controlled by an electro-hydraulic control unit comparable to automatic transmissions. Clutch K1 controls the odd and K2 the even gears. Thanks to this, gears can be changed without interruption of the power flow shortening the shift times, ensuring better fuel economy and ease of operation.

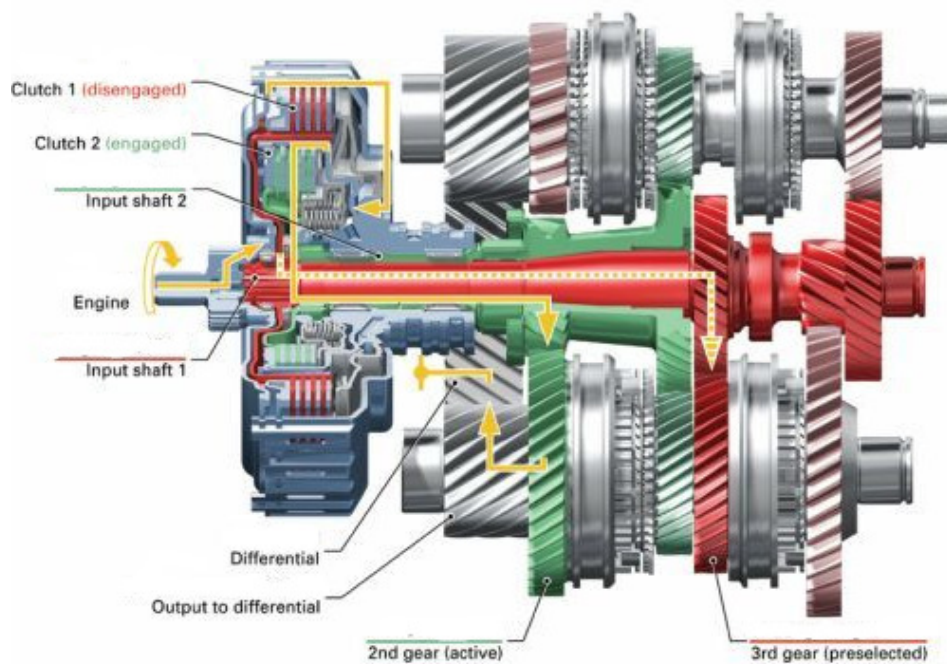


Figure 5.2.5 - dual-clutch transmission with selected 2nd gear (27)

The shaft to clutch K1 is inserted into the clutch K2 shaft according to Figure 5.2.5. Each shaft is divided into three inertias to increase the accuracy of the simulation model and each inertia represents the weight of a part of the shaft and pinion gear (viz. Figure 5.2.4, the full shaft is divided into *Jan\_11*, *Jan\_12* and *Jan\_13* and the hollow shaft *Jan\_21*, *Jan\_22* and *Jan\_23*). Between them are spring-damper modules ensuring the stiffness and damping properties of the shaft (*Can\_XX*). The loose (freely rotating) gears are represented by an individual inertia (*J1-6*, *JR*). Also the output shafts (*Jab\_11-13*, *Jab\_21-23*) and differential are included in the gear box. The differential is represented as one separate inertia and rigid connection between the output shafts and side shafts. The side shafts are similarly divided like the gearbox shafts. The right side shaft is assembled from an additional intermediate shaft since the gearbox is not centred. Penultimate part is the vehicle mass. It is a complete model of the vehicle mass, tires and rims. It includes the tire stiffness and damping properties as well as the torsional stiffness between tire and rim. Besides defining the

vehicles basic characteristics, all parameters necessary for calculation of the driving resistances acting against the vehicle movement have to be input. The last point is the test bench, where the vehicle velocity is being preset.

All elements in the simulation model are shortly explained in Table 5.2-2.

*Table 5.2-2 - elements included in the simulation model*

Element	Input parameters
Damper	Crankshaft damper (inertia, stiffness and damping)
Pulley	Crankshaft pulley for the drive belt (inertia, stiffness and damping)
GearC	Crankshaft gear for timing chain (inertia, stiffness and damping)
Journal 1-5	Journals between rods for each cylinder (inertia, stiffness and damping)
Frahm 1-4	Reduced rotating inertia of the crankshaft
Cylinder 1-4	Specification of the cylinder geometry, initial conditions, mass division
Curve 1-4	Engine pressure characteristic
Source 1-4	Conversion of engine pressure to force acting on piston
Firing angle 1-4	Specification of the firing angle for each cylinder
DMF_prim	DMF primary side inertia
DMF	Specification of the spring masses, stiffness, damping, deflection angles
DMF_sec	DMF secondary side inertia
J_K0_EM	Clutch K0 and electric motor inertia
K1_EF	Clutch K1 switching element
K2_EF	Clutch K2 switching element
Jan_1x	Full shaft (input shaft 1) inertia
Can_1x	Full shaft (input shaft 1) stiffness and damping
Jan_2x	Hollow shaft (input shaft 2) inertia
Can_2x	Hollow shaft (input shaft 1) stiffness and damping
Jab_1x	Output shaft 1 inertia
Cab_1x	Output shaft 1 stiffness and damping
Jab_2x	Output shaft 2 inertia
Cab_2x	Output shaft 2 stiffness and damping
Gear1-6,R	Transmission translation

J1-6, R	Loose gears inertia
G1-6, R	Gear switching element
Axis 1-2	Differential translation for output shaft 1 and 2
Differential1	Differential rigid connection joint
Shaft_VR/VL	Right/left half shaft inertia, stiffness and damping specification
Vehicle	Vehicle specification (mass, values for resistance calculation, wheel stiffness, damping, radius, inertia etc., tyre slip, initial conditions)
Test_Bench	Powertrain velocity specification

The basic simulation settings are obtained in Table 5.2-3. CVODE is a solver for ordinary differential equations (C-language Ordinary Differential Equation solver). Since the results will be analysed in MATLAB, equidistant result recording was chosen to ensure a constant time step.

*Table 5.2-3- Simulation settings*

Starting time	0 [s]
Stopping time	10 [s]
Solver	CVODE
Minimal calculation step	1e-08 [s]
Maximal calculation step	1e-4 [s]
Result recording	equidistant
Maximum output step	0.0001 [s]

Further on each simulation model for hybrid specific operating conditions will be displayed and explained more in detail.

### 5.2.1. Idle

The MBS model created to simulate the phenomena rattle during idle is in Appendix 2 and 3. The rotational speed during idle is being kept at a constant value with the help of an idle-regulator and torque-to-load converter. In this case the rotational speed is 1000 rpm. The idle regulator keeps the engines rotational speed at a given value if the clutch is opened and a driving desire missing (Appendix 2 – idle speed regulation). In this case clutch K0 and K1 is closed but no gear synchronized. Input values are the actual engine rotational speed, which is measured at the DMF primary side and adjusted by a mean value filter, and the target rotational speed. A PI-regulator calculates the corresponding engine torque which is required to reach the target value. To ensure good control behaviour, the desired value is in case of abrupt changes modified by a PT1-filter (control technology transmission element).

The cylinder pressure is regulated via a load specification. To convert the output torque from the idle regulator a torque-to-load converter is included after. The result is a load value between 0 and 1, where 0 stands for zero load (overrun conditions) and 1 for full load.

Depending on the load value, rotational engine speed and engine angle, a linearly interpolated pressure value results from the 3D zero-load and full-load engine characteristics.

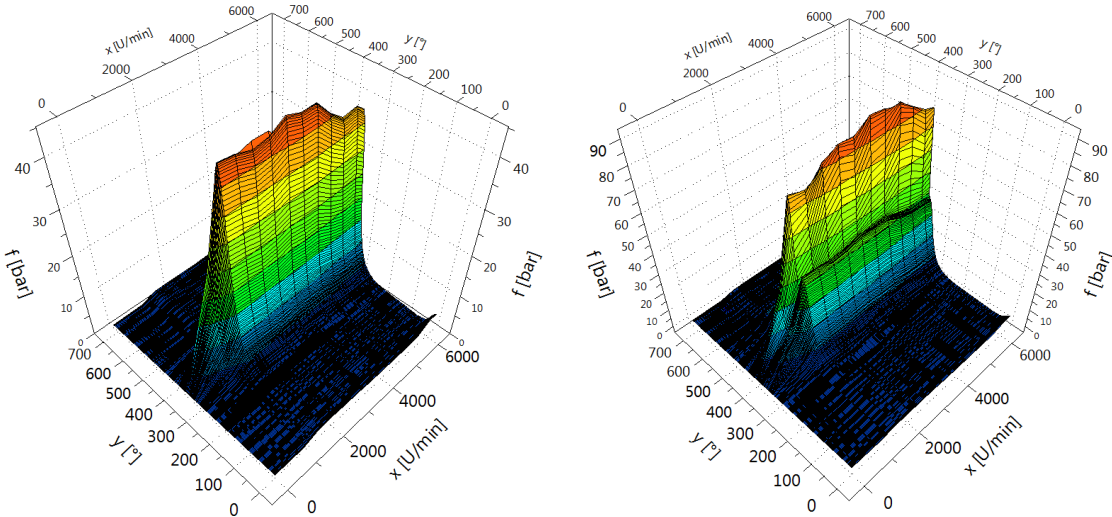


Figure 5.2.6 - Engine pressure characteristic – zero load (left), full load (right)

The simulation model will be used to analyse gear rattle in the powertrain. To obtain a more realistic model, resistances occurring at the loose gears have been included (Appendix 3 – drag torque definition). These involve:

- Splashing drag torque
- Bearing drag torque
- Synchronizer drag torque

Splashing is the resistance caused by the presence of oil which is braking the individual gear. It depends on the immersion depth into the transmission oil sump (gear tip radius  $r_a$ ), gear width  $b$ , oil density  $\rho$ , the absolute loose gear rotatory speed  $\omega$  and a factor  $K_1$  which has to be determined via correlation with measurements:

$$T_{Sp} = K_1 * \rho * \omega^2 * r_a^4 * b \tag{5.2.2}$$

Bearing drag torque has its origin in the moving bearing under the loose gears. These have a load dependent and independent proportion. Loose gears do not transmit any torque which is why the load independent parts are being taken into account. The gears and shafts have a different velocity causing movement of the bearings resulting in small resistance which is depending on the bearing type. Bearing drag torque depends on the kinematic oil viscosity  $\nu$ , on the absolute relative speed between the loose gear and the shaft  $\Delta n$ , the average

diameter of the bearing  $d_m^3$  and as before on a factor  $K_2$  that has to be determined via correlation with measurements:

$$T_{BT} = K_2 * 10^{-7} * (v * \Delta n)^{\frac{2}{3}} * d_m^3 \quad (5.2.3)$$

Last type included in this work is the synchronizer drag torque. The synchronizer cones fixed to the loose gears and the cones fixed to the synchro hub rotate with different speeds. Between the cones is a gap generally filled with oil. Due to the speed difference a shear force acts between the opposing cone areas. The drag torque caused by this shear stress depends on the axial backlash  $b_{Sy}$ , the gap height  $h_{Sy}$ , the average diameter  $D_m$ , and relative speed between loose gear and blocker-ring  $\Delta\omega$ .

$$T_{Sy} = \frac{1}{4} * \pi * D_m^3 * \Delta\omega_{cones} * v * \rho * \frac{b_{Sy}}{h_{Sy}} \quad (5.2.4)$$

### 5.2.2. Hybrid start/tow launch

The hybrid start has been described in section 4.1.2 – high engine speed/hybrid start. To simulate the effects on the DMF during hybrid launch an initial speed of  $n_0=1600$  rpm has been set and the clutch starts to close after 2 seconds. The electric motor has a short time maximum torque of 330 Nm. For simulation a torque of 300 Nm was set as an initial condition. The simulation model arrangement is in Appendix 4.

The effect of three parameters on the dynamic behaviour is going to be analysed. One of them is the electric motor torque raise. After the clutch starts to close the torque available for driving decreases by the value necessary for the engine tow. To maintain a constant acceleration it is necessary to increase the electric motor torque, in this case 15 Nm. Initiation has been set to the same time the clutch starts to close (Figure 5.2.7- right). The clutch closing process and torque raise were chosen to be defined by a cosines function of identical shape to ensure even transition of the control signal and thus even clutch closing and simultaneous transmission.

The second parameter is the transition time which is the duration of the clutch transition from opened to engaged state. The third parameter is the clutch torque, which defines how much torque can be transmitted by the clutch.

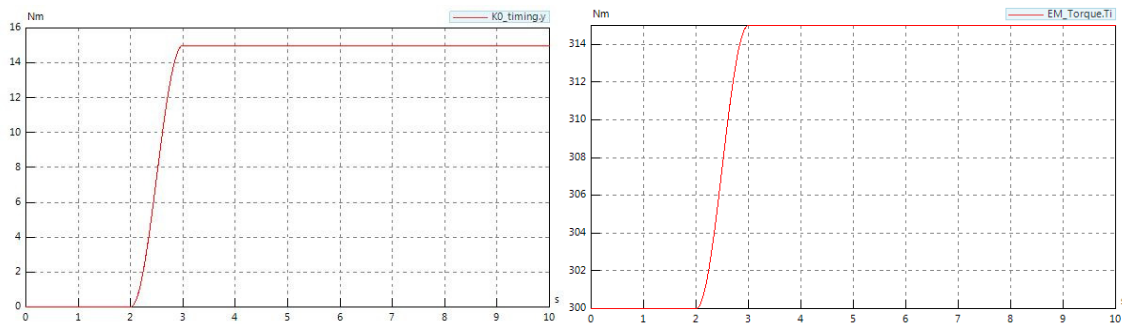


Figure 5.2.7 - Clutch torque (left) and electric motor torque (right) timing

In Figure 5.2.7 a transition time of 1 second is set. It can be assumed, that by shortening the transition time a bigger excitation appears at the DMF during the clutch closing process. Its influence on the DMF response will be analysed in section 5.4.2.

### 5.2.3. Cycling

Cycling occurs during abrupt load change when the gas pedal position is changed by the driver due to sudden change of mind. As already mentioned during cycling the first natural mode is exited and a vibration node between vehicle and transmission arises.

In the simulation model a constant engine speed of 2000 rpm will be considered, since in the range between 2000-3000 rpm maximum torque is applied. A situation like this can be only achieved on a test bench, since in normal operation the vehicle velocity slows down if the vehicle is moving on a straight road and the foot is moved from the gas pedal. Nevertheless, the excitation itself is independent of these circumstances and therefore simulation according to test bench conditions can be performed.

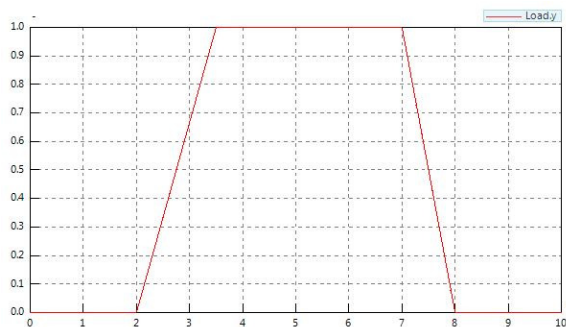


Figure 5.2.8 - Load change curve

Figure 5.2.8 is the engine load curve simulating cycling. As already mentioned before, the value 1 stands for 100% load and 0 for 0% load. In the first 2 seconds the engine load is being kept at a constant value of 0 load, after being slowly raised for 1.5 seconds to 1. This time delay has been selected to simulate realistic drive behaviour. In cars when the driver suddenly decides to accelerate, the signal is being adjusted before reaching the fuel throttle actuator to lower the gradient. Same applies for tip-out from the 7<sup>th</sup> second, where for the load decrease a transitional period of 1 second was chosen, a realistic value taken over from vehicle measurements. After the vehicle is being towed again.

### 5.2.4. Run-up part-load/full-load

The simulation model in Figure 5.2.3 and Figure 5.2.4 is used to simulate the operating mode run-up with part-load or full load. The clutch KO dividing the electric motor from the engine crankshaft is engaged during the entire run-up process and the car is being driven by the internal combustion engine starting at a value of  $n_0=800$  rpm. The rotational speed is being increased from 800 rpm to 1000 rpm during the first 2 seconds to ensure a sufficient settling time and to avoid transient oscillation.

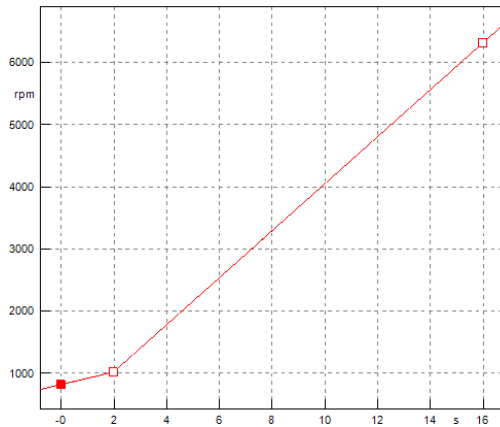


Figure 5.2.9 - Run-up - Time settings

For further analysis only the start-up from 1000 rpm to 6300 rpm, the idle speed and a maximum revolution value given by the vehicle manufacturer, has been considered. Depending on the drive torque, part-load (50%) and full-load (100%) can be distinguished. As described in the section before, 1 stands for full load and 0 for motoring mode. Depending on the load value, rotational engine speed and engine angle, a linearly interpolated pressure value results from the 3D zero-load and full-load 3D engine map (Figure 5.2.6).

### 5.3. Modal analysis of hybrid powertrain

Modal analysis is an important field in NVH and serves to analyse oscillating systems. These appear in many areas of everyday life, e.g. in cars, domestic appliances etc. Crucial is the systems stability in normal operation towards oscillation. It is necessary to investigate these to minimize their effect and to find possible causes for undesired behaviour.

It is recommended to start the dynamic analysis of an assembly with a modal analysis in which besides natural frequencies likewise natural modes are identified. Knowledge about the natural frequencies and modes of a system are from great importance when evaluating the dynamic behaviour.

If a prototype is available, it is usually recommended to perform also an experimental analysis.

Natural frequencies influence the system behaviour more or less depending on the systems damping factor. To every natural frequency belongs a certain oscillation pattern. When forced excitation acts on the system and corresponds to one of the natural frequencies, high amplitudes occur.

When a linear system is excited by some kind of force in one point it starts to oscillate and responds to the excitement with particular vibration behaviour. Its response in another point depends on the system properties. They influence the transmission behaviour between these two points. These are the three variables necessary for its description.

As mentioned before an oscillating system can be described by the combination of mass (or inertia), springs and dampers. By connecting these, more complex systems with many

degrees of freedom can be described. Such kinds of models are expressed by differential equations of motion, boundary and initial conditions which describe the systems behaviour and displacement, velocity and acceleration can be calculated. With these it is possible to calculate the transfer function and the systems dynamic behaviour. The basic matrix entry of these equations is:

$$M\ddot{\varphi} + B\dot{\varphi} + K\varphi = Q(t) \tag{5.3.1}$$

Where  $M$  is the matrix of mass,  $B$  the damping matrix and  $K$  the stiffness matrix.  $Q(t)$  is the time dependent excitement.

In this master thesis the modal analysis for the 2<sup>nd</sup>, 4<sup>th</sup> and 5<sup>th</sup> gear has been performed to analyse the behaviour for a gear from both full and hollow shaft and with higher and lower gear ratio. In 4-cylinder engines is the 2<sup>nd</sup> order from biggest relevance and related frequency range can be calculated according to the engine speed range (max. 6300 rpm):

$$f = j \frac{\omega}{2\pi} = j \frac{n}{60} = 2 * \frac{6300}{60} = 210 \text{ Hz} \tag{5.3.2}$$

Where  $f$  is the frequency, and  $j$  the relevant engine order. Multiples of the 2<sup>nd</sup> order can appear and a slightly higher frequency (250 Hz) has been chosen to include them. The whole powertrain modal analysis can be directly performed in SimulationX, where besides the natural frequency values also the deflection, kinetic, potential energy can be analysed. The kinetic energy indicates which inertia in the powertrain is influenced most whereas the potential energy specifies the source. Latter is an important indicator to point out which stiffness has the biggest impact on the related natural frequency:

$$E_{pot} = \frac{1}{2} * k * x^2 \tag{5.3.3}$$

All system natural frequencies of relevance are listed in Table 5.3-1. The potential energy from importance for the belonging natural frequency will be mentioned in the text below.

Table 5.3-1 - natural frequencies (P2 hybrid)

	2 <sup>nd</sup> gear [Hz]	4 <sup>th</sup> gear [Hz]	5 <sup>th</sup> gear [Hz]
f1	3.547	6.45	7.45
f2	13.65	13.75	13.81
f3	16.81	16.81	16.81
f6	22.09	23.21	23.65
f7	51.99	51.99	51.99
f10	55.81	55.93	55.58
f11	225.28	188.33	87.34
f12	230.67	230.68	230.70

The natural frequencies  $f_2$ - $f_{10}$  and  $f_{12}$  differ only slightly and show independency on the shifted gear. This means that the reason and stiffness having effect on them is a component besides the gear box. Their source are according to the modal analysis of the powertrain mainly the DMF, the tires and wheel-road contact. The natural frequency increases with decreasing gear ratio due to the increasing inertia of the transmission output side during low translations. In the following figures are the natural modes of the powertrain for the natural frequencies in Table 5.3-1. On the y-axis is the relative comparison of the amplitude of all mass points in the powertrain and 1 is the highest value. After the gear pairs the deflection direction changes due to translation. All figures illustrating the inertia deflection have been therefore modified to compensate this effect.

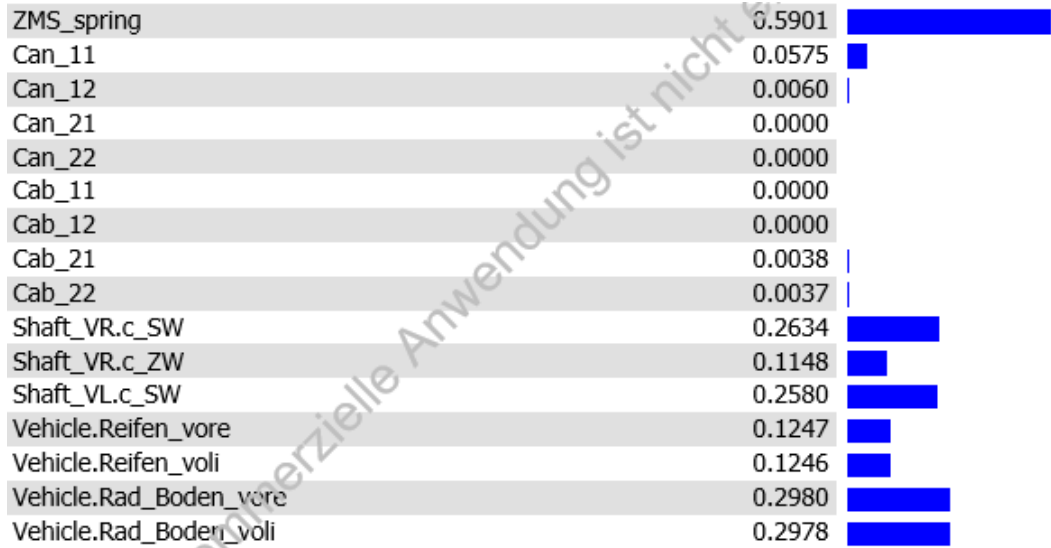
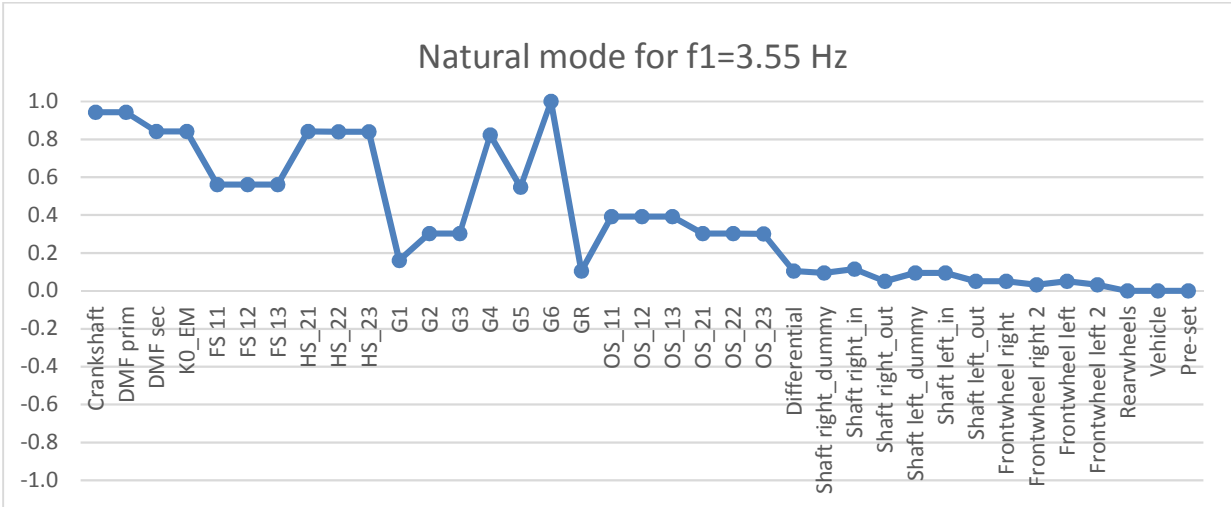


Figure 5.3.1 -  $f_1$  - for the 2<sup>nd</sup> gear – jerking natural mode (top), potential energy (bottom)

In Figure 5.3.1 is the 1<sup>st</sup> powertrain natural mode for the 2<sup>nd</sup> gear shifted and potential energy for each stiffness.

The shape for all 1<sup>st</sup> natural frequencies have the same deflection and only their value differs slightly. In the modal analysis has been found out that its main source are the side shafts and wheels. Due to its low value, which is in the ‘vibration range’, it will be perceived as jerking

and excitation appears predominantly during cycling or is road initiated. Excitation through engine rotational irregularities is excluded.

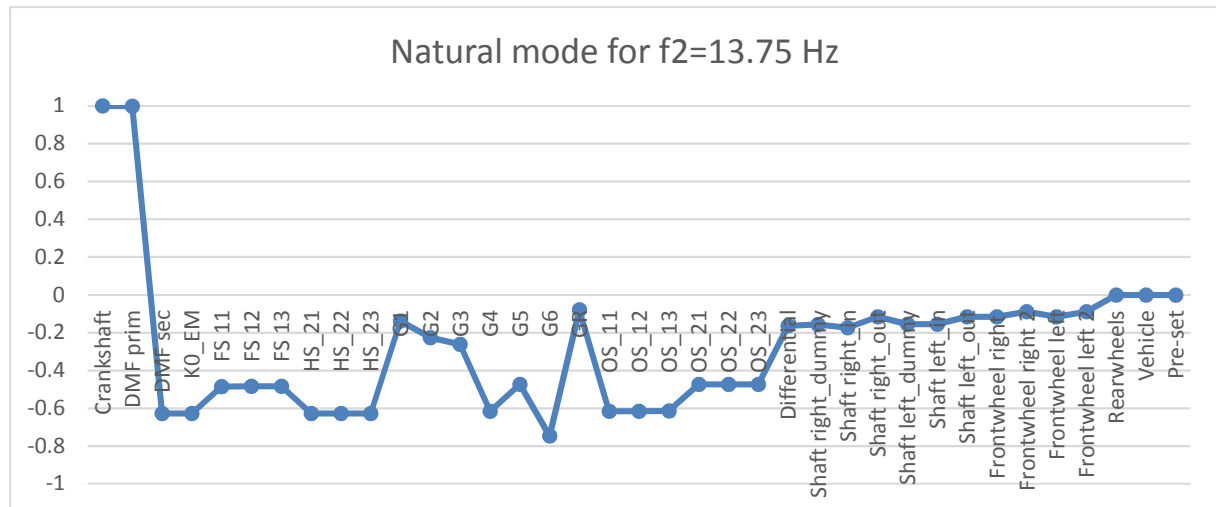


Figure 5.3.2 -  $f_2$  - DMF natural mode (top), potential energy (bottom)

$f_2$  represents the DMF natural frequency (Figure 5.3.2). It is called DMF natural frequency due to the deflection node between the DMF primary and secondary mass. Mostly affected is the primary side of the DMF. This frequency is from high importance during idle and run-up. For the 4-cylinder engine it will be passed only during start-up, since the relevant engine rotational speed  $n$  is 412.44 rpm, which is below the operating range.

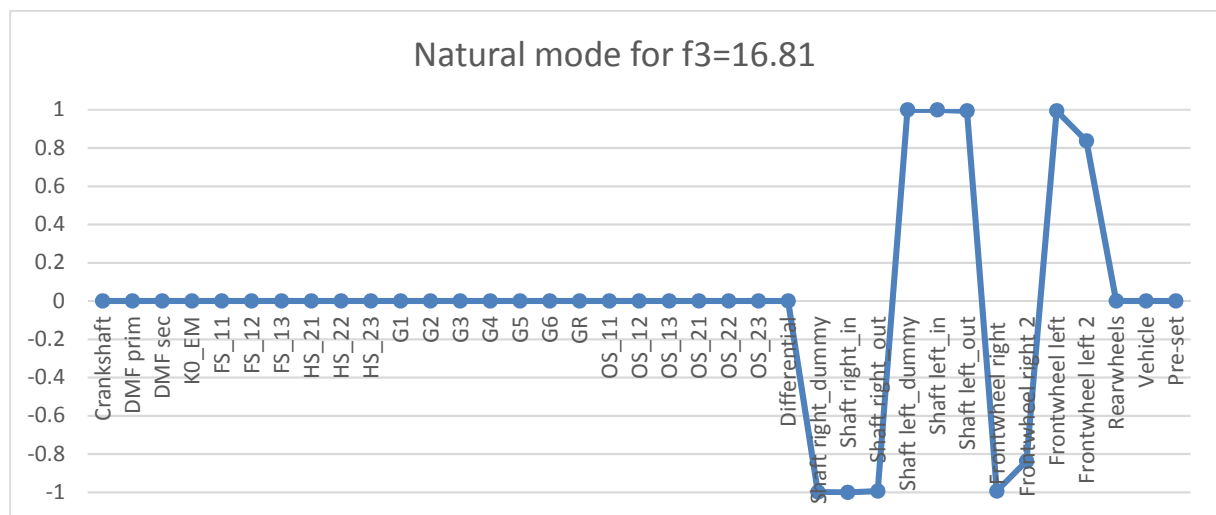


Figure 5.3.3 -  $f_3$  – side shafts and wheels twist against each other (top), potential energy (bottom)

$f_3$  (Figure 5.3.3) has the same value for all gears and is already in the speed range from importance for 2-cylinder engines (1008.6 rpm). Excitation of this frequency causes the right

and left side shaft and wheels to oscillate against each other. Mainly affected are the vehicle wheels and the source is the wheel-floor contact stiffness due to the potential energy (Figure 5.3.3 – bottom – Vehicle.Rad\_Borden\_vore/voli).

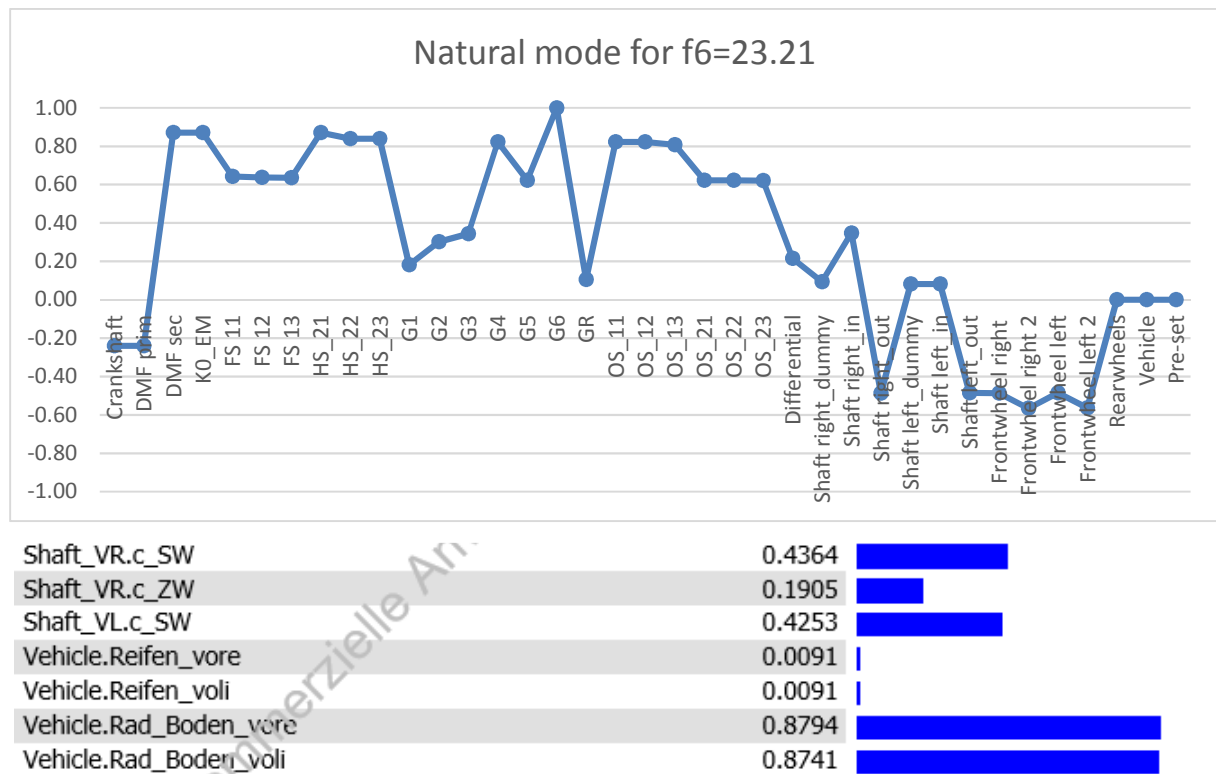
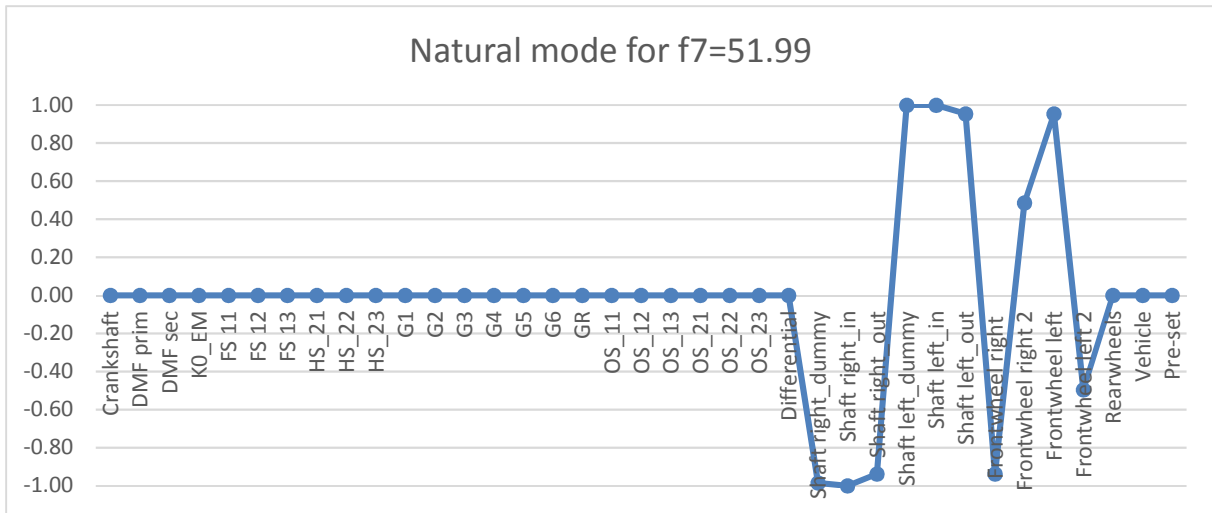


Figure 5.3.4 –  $f_6$  - Wheels oscillate against transmission (top), potential energy (bottom)

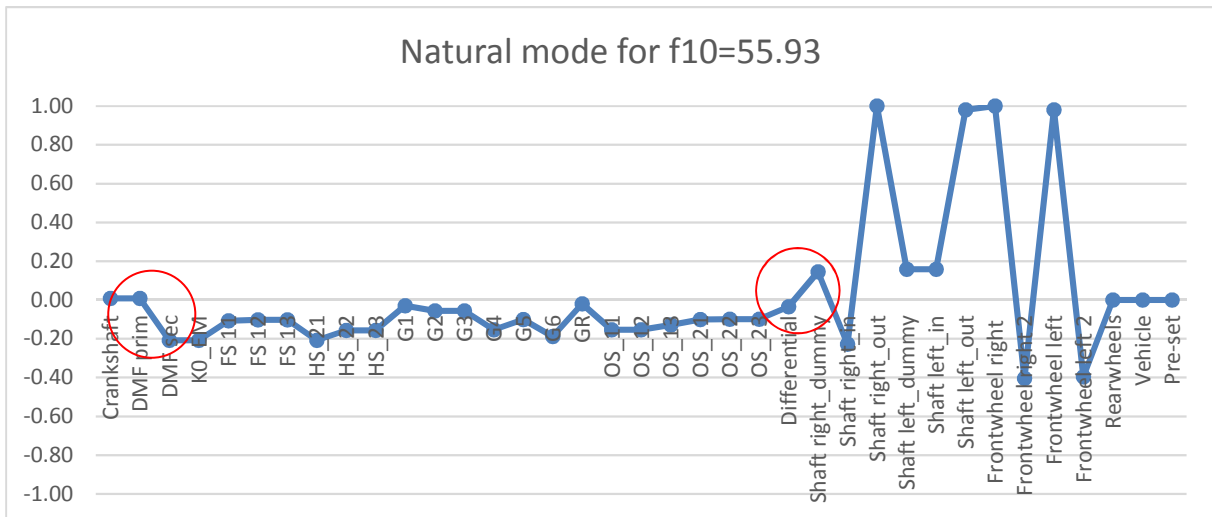
In SimulationX has been found out that  $f_6$  has mainly impact on the electric motor and wheels. The side shafts and wheel-floor contact have the most significant potential energy (Shaft\_X, Vehicle.Rad\_Boden\_X). Through variation of the side shaft stiffness the natural frequency  $f_6$  can be shifted if needed. For the second engine order this frequency value still lies beneath the usual engine speed operation range (for the 4-cylinder engine) and has therefore no impact during normal operation.



Vehicle.Reifen_vore	0.9673	█
Vehicle.Reifen_voli	1.0000	█
Vehicle.Rad_Boden_vore	0.0624	█
Vehicle.Rad_Boden_voli	0.0645	█

Figure 5.3.5 –  $f_7$  - Right and left side shaft and wheels twist against each other (top), potential energy (bottom)

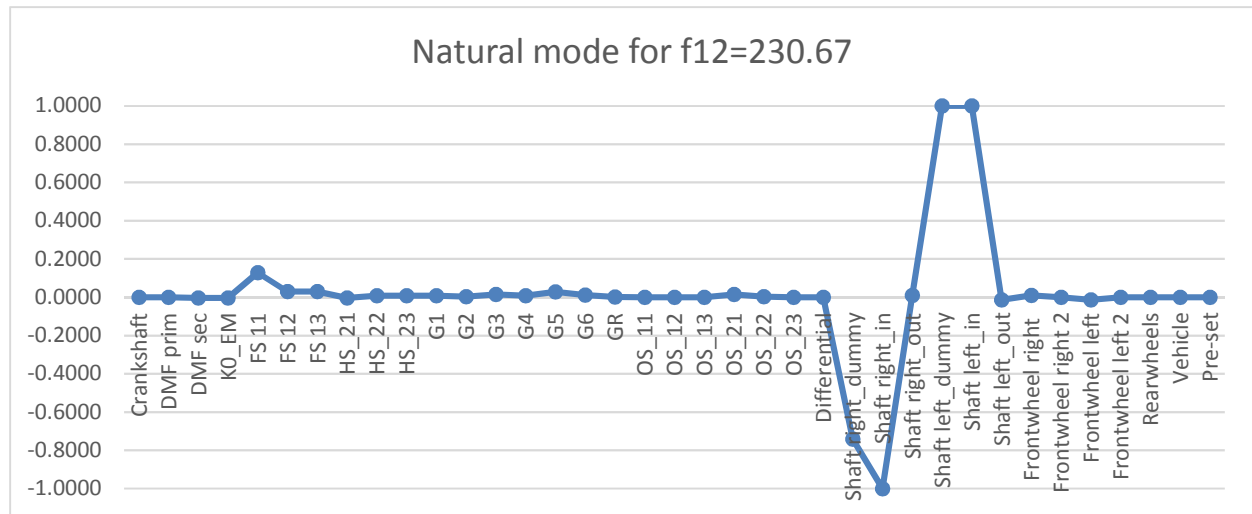
Similarly to  $f_3$  when excitement of  $f_7$  occurs (Figure 5.3.5), oscillation between the right and left side shaft and wheels arise with its most significant source of potential energy in the wheel stiffness (Vehicle\_Reifen\_X).  $f_7$  is the first natural frequency having relevance during normal operation for a 4-cylinder engine (for 51.99 Hz -> 1559.7 rpm).



Shaft_VR.c_SW	0.1171	█
Shaft_VR.c_ZW	0.0514	█
Shaft_VL.c_SW	0.1105	█
Vehicle.Reifen_vore	1.0000	█
Vehicle.Reifen_voli	0.9629	█
Vehicle.Rad_Boden_vore	0.0471	█
Vehicle.Rad_Boden_voli	0.0454	█

Figure 5.3.6 –  $f_{10}$  - Lower differential natural mode (top), potential energy (bottom)

For  $f_{10}$  (Figure 5.3.6) a twist of the transmission against the DMF, side shafts and wheels is visible. This state is referred to as differential natural frequency.



Shaft_VR.c_SW	0.5332	<div style="width: 53.32%;"></div>
Shaft_VR.c_ZW	0.1454	<div style="width: 14.54%;"></div>
Shaft_VL.c_SW	1.0000	<div style="width: 100%;"></div>
Vehicle.Reifen_vore	0.0003	<div style="width: 0.03%;"></div>
Vehicle.Reifen_voli	0.0005	<div style="width: 0.05%;"></div>
Vehicle.Rad_Boden_vore	0.0000	<div style="width: 0%;"></div>
Vehicle.Rad_Boden_voli	0.0000	<div style="width: 0%;"></div>

Figure 5.3.7 –  $f_{12}$  - Side shaft swing against each other (top), potential energy (bottom)

$f_{12}$  (Figure 5.3.7) has similarly as  $f_3$  and  $f_7$  effect on the side shafts and is caused by the side shaft stiffness, mainly due to the left side shaft stiffness (Shaft\_VL.c\_SW).

$f_{11}$  is also gear dependent and caused by the input shaft stiffness. Due to this fact can be assumed that it will be from highest importance during time domain analysis. This presumption will be confirmed and described more in detail in section 5.4.4.

## 5.4. Time domain analysis in hybrid specific operating conditions

### 5.4.1. Idle - rattle

The phenomena rattle often occurring during idle has been analysed. Whether rattle appears in the transmission or not can be found out when analysing the normal force on both tooth flanks. When the gear set is engaged, the force acts only on one of the tooth flank, depending on the drive source. In our case the drive source is either the 4-cylinder engine or the test bench, which is keeping the simulation model at a desired constant velocity.

In Figure 5.4.1 are the difference in position (top) and forces (bottom) acting on the left and right tooth flank. The difference in the position difference between the left and right tooth flank has the magnitude of the backlash between them ( $80 \mu\text{m}$ ). In case of rattle the position

difference would have to reach this value and interference of the two plotted parameters would be visible in Figure 5.4.1. Same accounts for the force acting on each tooth flank.

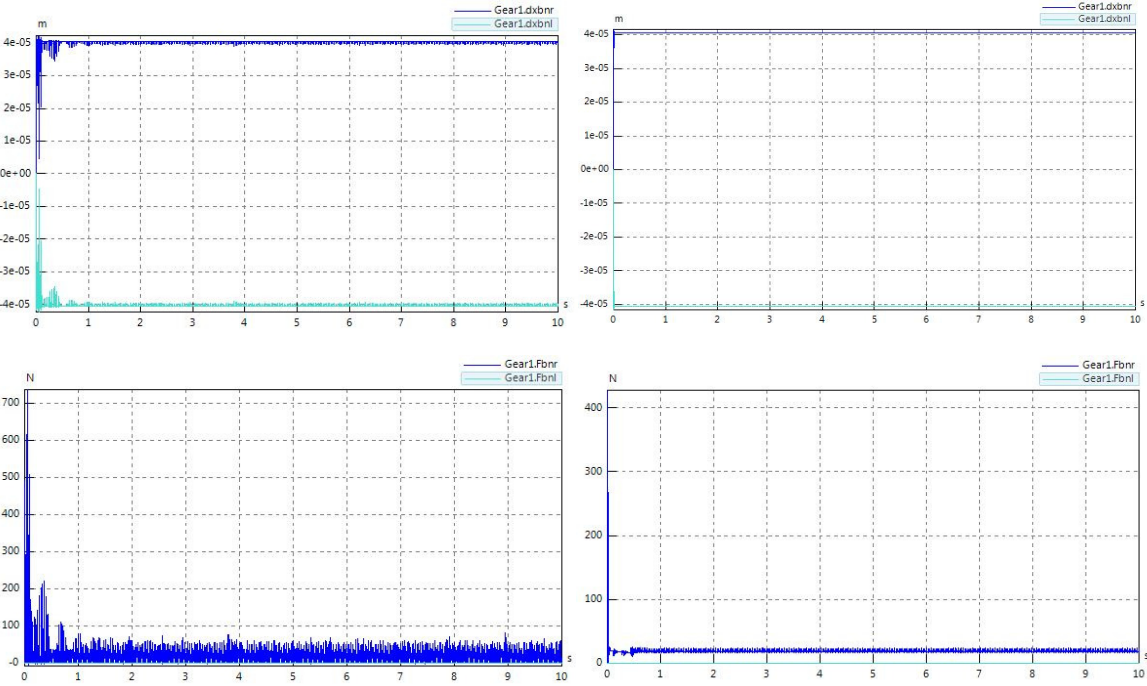


Figure 5.4.1 - Position difference and normal tooth flank force without DMF (left) and with DMF (right)

According to Figure 5.4.1 – bottom no force acts on the left tooth flank indicating that no contact between the left and right tooth flank occurs. Therefore can be deduced that for the analysed 4-cylinder P2 hybrid no rattle has been detected. To figure out how much of an impact on this result the DMF has, another simulation without has been conducted (Figure 5.4.1.-left). Also for a powertrain without DMF the same results were found. Although in both cases no rattle occurs, clear difference between the powertrain without and with DMF is apparent. Without the DMF, the normal force acting on the tooth flank has a significantly higher amplitude. Likewise a higher movement during idle is visible in the position difference diagram. From these two can be concluded that the DMF is already fulfilling its purpose in the powertrain.

### 5.4.2. Hybrid start/tow launch

The hybrid launch, when the crankshaft velocity is being raised from 0 to its firing velocity, has usually negative effect on the powertrain dynamics. To optimize the behaviour, various conditions for the hybrid launch have been tested. Three variables have been modified to analyse their effect on the system response. The clutch transition time, which defines the period in which the clutch is closing, second the clutch torque which defines how much torque can be transmitted by the clutch, and third the tow torque, which is the torque by which the electric motor torque will be raised during clutch closure.

First the influence of the clutch press torque will be investigated. For the transition time  $t_t=0.1$  seconds will be set and for the tow torque  $T_t=0$  Nm. The transmissible torque for the

clutch in conventional vehicles has usually a magnitude up to 90 Nm during start-up operations and is then being raised to a value depending on the maximum engine torque after the engine is ignited. To show why awareness of the chosen value is important and its impact on the dynamics, two simulation for 15 Nm and 80 Nm have been proceeded.

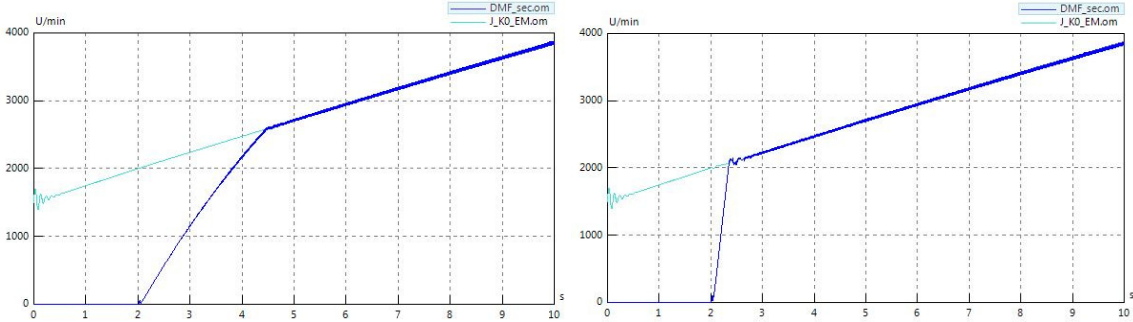


Figure 5.4.2 - Electric motor (light blue) and DMF secondary side (dark blue) angular velocity with 15 Nm (left) and 80 Nm (right) clutch torque

In Figure 5.4.2 influence of the clutch torque magnitude is visible. The short excitation after the 2<sup>nd</sup> second, when both masses reach the same velocity is caused by the torque difference between the torque provided by the clutch and needed by the engine. This effect is visible in Figure 5.4.3.

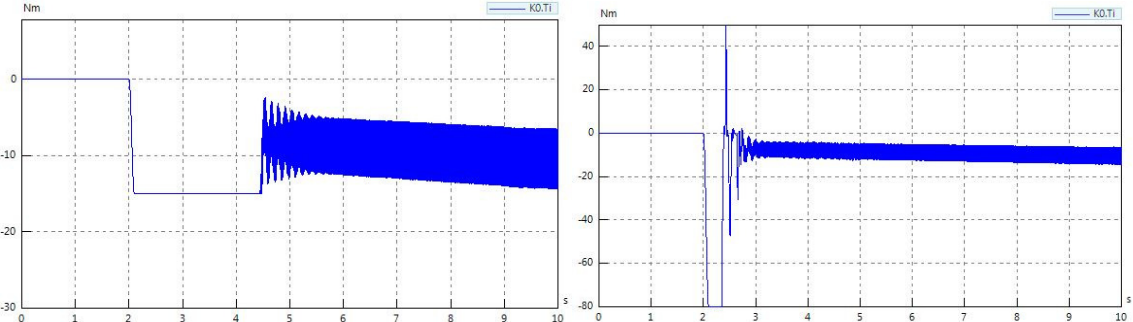


Figure 5.4.3 - Clutch torque withdrawal for 15 Nm (left) and 80 Nm (right)

After the DMF secondary side velocity balances, the torque withdrawal from the clutch decreases from 80 Nm to approximately 8-9 Nm according to Figure 5.4.3, increasing slowly again with increasing velocity. This torque difference causes oscillation at the clutch leading to the conclusion that higher clutch torque will lead to increased vibration. To completely avoid it, the clutch torque would have to be decreased again as soon as the secondary side reaches the same velocity as the electric motor and transmission side or the clutch torque would have to be decreased to an even lower value almost equal to the tow-torque according to Figure 5.4.3 (right). Latter has negative influence on the duration during which the electric motor and crankshaft velocities equalize, in this case ca. 2.5 seconds after clutch closure (for 15 Nm clutch torque) instead of 0.4 second (for 80 Nm clutch torque). The difference in time in which the crankshaft or DMF are being balanced and equalize to the EM velocity is according to the torque, which is being transmitted by the clutch, significantly shorter when 80 Nm are set (Figure 5.4.3).

When the clutch torque is being kept at 15 Nm,  $T_t=0$  and only the clutch closing transition time is being modified from 0.1 to 1 second, the velocity of the secondary side changes more smoothly in the beginning of the engagement process. Besides the prolonged speed balancing time, no further difference is visible (Figure 5.4.4)

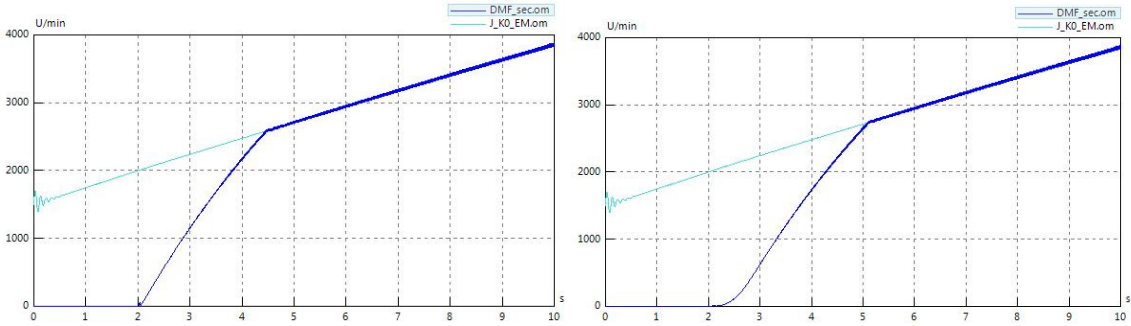


Figure 5.4.4 - Electric motor (light blue) and DMF secondary side (dark blue) angular velocity with 0.1 s (left) and 1 s (right) clutch closing time

What noticeably changes is the power loss process in the clutch according to Figure 5.4.5. The power loss is given by the relative velocity between the two shaft ends and the clutch torque, both in dependence on time. When the clutch is being closed quickly, the two clutch discs don't have enough time to even out their velocity causing a sudden transfer of the maximum clutch torque. In this moment although the two sides are still slipping causing torque to 'get lost' due to dissipation by friction. When providing enough time, torque transmission occurs in a more even manner. The overall energy loss is given by the area below the curves and seems to be similar for 0.1 second and 1 second clutch closing time. It is clear, that when raising the clutch torque, the power loss curve will have a steeper ascent but at the same time sharper decline resulting in a similar power loss as for 15 Nm clutch torque.

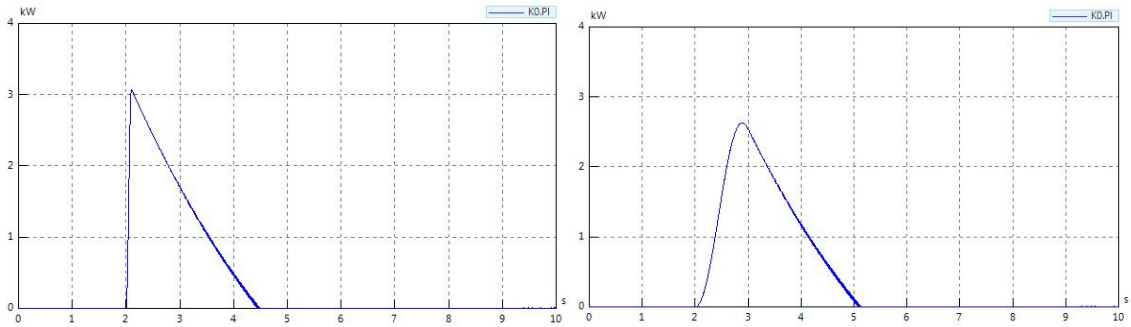


Figure 5.4.5 - Power loss for 0.1 s (left) and 1 s (right) clutch closing time

The last parameter modified is the tow torque. The tow torque mainly influences the acceleration, i.e. how fast the engine velocity increases. In powertrains where a higher tow-torque is needed for the engine to reach its firing velocity, the torque provided from the electric motor has to be increased to ensure enough torque for the driving desire and engine start up. If the electric motor torque is not being increased a sudden velocity decrease at the

time when the clutch starts to close would occur slowing further down the acceleration process.

The clutch torque will be kept at 80 Nm, the clutch closing transition time at 0.1 second. As already mentioned before and visualized in Figure 5.4.3 (left), in case of the 4-cylinder engine the tow torque has a very low mean value of approximately 8 Nm. For this reason no considerable velocity decrease is visible in neither Figure 5.4.2 nor Figure 5.4.4 and only a slight oscillation can be seen as an example of this impact in Figure 5.4.6. (left), after the 2<sup>nd</sup> second, when the clutch starts to close. A dotted straight line has been inserted to highlight the decrease in acceleration. In Figure 5.4.6 (right) the electric motor torque has been raised at the same time as the clutch starts to close. Slight improvement of the dynamic behaviour is visible with a red circle and a stable acceleration is visible.

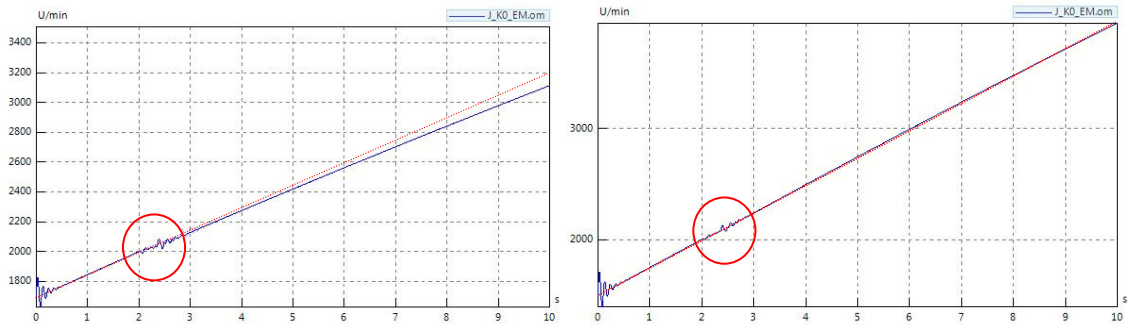


Figure 5.4.6 - Electric motor angular velocity for 0 Nm (left) and 15 Nm (right) torque increase during clutch closure

To avoid all three mentioned occurrences visible in Figure 5.4.3, Figure 5.4.4 and Figure 5.4.6 during clutch closure a special procedure has been developed. The clutch torque is during closure being slowly raised to avoid losses and to keep the advantage of a quicker velocity equalization after it is closed. Also the tow torque is being raised simultaneously to avoid a velocity drop at the wheels and keep the transmitted torque constant. After engine ignition the electric motor torque is being lowered to a value for keeping the driving desire.

### 5.4.3. Cycling

The results presented in this section corresponds the driving state cycling when sudden load changes are being made by the driver. So called tip-in, which is the sudden adding of engine speed by stepping on the gas pedal, and tip-out or sometimes also called back-out, which is the abrupt removal of the foot from the gas pedal. Change of mind situations like this occur on a regular basis during operation, e.g. when the traffic light turns from red to green, during heavy traffic or during overtaking.

For the analysis the 2<sup>nd</sup> gear and 5<sup>th</sup> gear have been chosen to understand how the transmitted output torque affects the system behaviour during cycling. Due to the higher translation in 2<sup>nd</sup> gear also the output torque is higher than for 5<sup>th</sup> gear. To include analysis of torque transmission through the full input shaft as well as through the hollow input shaft. The results are listed below.

## Second gear

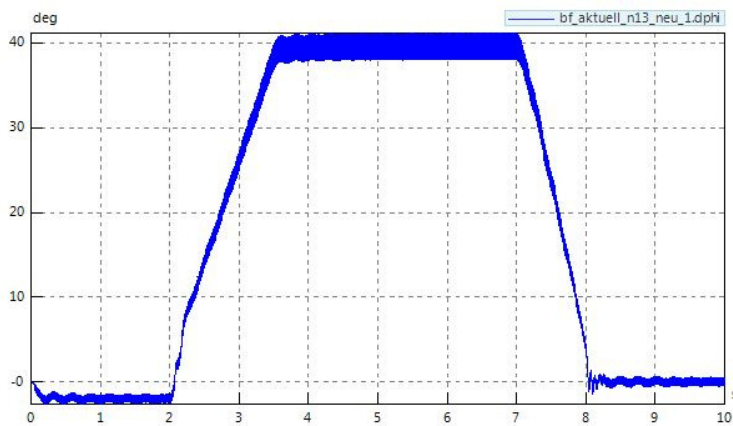


Figure 5.4.7 - Cycling - angle difference DMF arc spring – second gear

First, the arc spring is deflected in the opposite direction during zero load than during tip-in. This is given by the fact, that the system is first driven by the test bench visible in Figure 5.2.4. When load is being increased, the engine cylinder pressure starts to increase transmitting more torque to the powertrain and the engine takes over the propulsion of the system, which is why the DMF spring is being deflected in the opposite direction. After tip-out (zero load) from the 7<sup>th</sup> second the system is still driven by the engine and the spring stabilizes in a neutral position. These changes of load also have impact on the velocity development. Upswings with a frequency of ca. 3.5 Hz are visible when the load changes and stabilizes and indicates the occurrence of jerking (Figure 5.4.8).

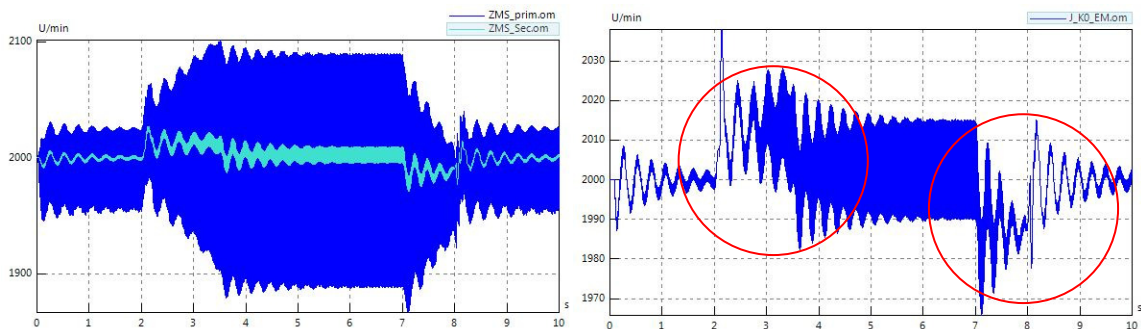


Figure 5.4.8 - Cycling 2<sup>nd</sup> gear - angular velocity at the DMF primary side and secondary side (left) and clutch (right)

All inertias in the powertrain have been checked for further excessive torsional oscillation or strain. None has been detected.

In Figure 5.4.9, the DMF inner torque and its characteristic curve is shown. During cycling in 2<sup>nd</sup> gear, the DMF operates in its second stage.

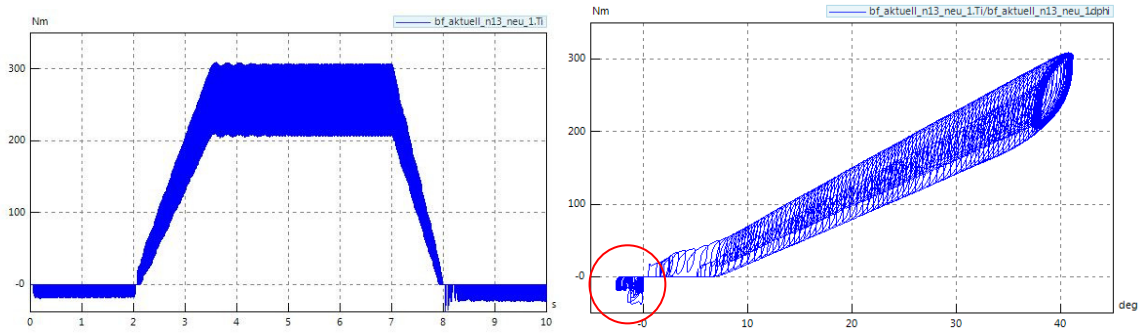


Figure 5.4.9 - Cycling 2<sup>nd</sup> gear - DMF torque (left) and DMF characteristic curve (right)

In the left corner of the DMF characteristic curve (Figure 5.4.9 - right) deflection in the opposite direction is visible (red circle) and verifies the test bench as a driving force in the first two seconds. The end stop is not being reached, the curve has a smooth course.

### Fifth gear

The angle difference for the DMF during 5<sup>th</sup> gear is the same as for 2<sup>nd</sup> gear in Figure 5.4.7.

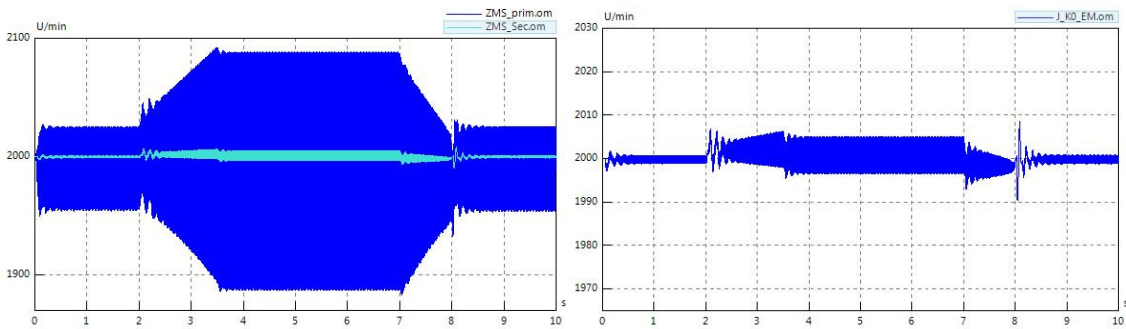


Figure 5.4.10 – Cycling 4<sup>th</sup> gear - angular velocity at the DMF primary side and secondary side (left) and clutch (right)

Compared to acceleration in 2<sup>nd</sup> gear, the amplitude at the DMF secondary side is significantly smaller; oscillation amplitude appears lower but at higher frequency. The difference is noticeable when studying the angular velocity of the clutch and electromotor. According to Figure 5.4.8 in 2<sup>nd</sup> gear an amplitude of almost 30 rpm is being reached whereas in 5<sup>th</sup> gear only 10 rpm (Figure 5.4.10). This can be explained by the fact that during 5<sup>th</sup> gear a torque of almost the same value as at the engine is being transmitted to the wheels resulting in lower load shocks during cycling. The system stabilizes faster.

To ensure lower oscillation during load change, a development with a lower gradient would have to be chosen to lower the load shock, in other words the load change would have to be prolonged and thus the reaction time of the vehicle slowed down.

Another possibility is to lower the spring stiffness of the DMF in second stage to lower the overall amplitude. A disadvantage would be slower settlement and a necessary redesign of the DMF since when lowering the second stage stiffness also the end stop would be reached earlier causing higher oscillation amplitudes. In Figure 5.4.11,  $k_2$  has been lowered from 7.4 Nm/deg to 3 Nm/deg. Due to this also the deflection angle had to be prolonged to ensure

operation in second stage. A slight decrease of the oscillation amplitude is apparent from the 2<sup>nd</sup> second to the 8<sup>th</sup> second (Figure 5.4.11 – left). However the jerking amplitude stays almost the same. Confirmation of main operation in the second stage is in Figure 5.4.11 – (right).

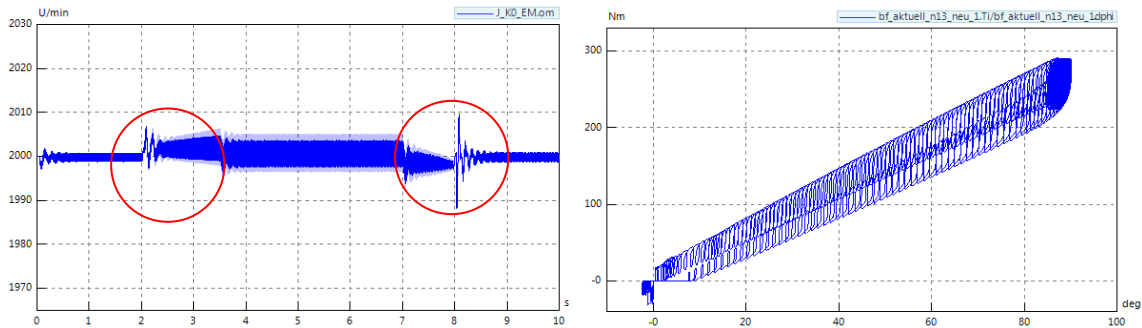


Figure 5.4.11 - Cycling 5th gear – clutch angular velocity (left) and DMF characteristic curve (right) with  $c_2=3\text{Nm/deg}$

#### 5.4.4. Run-up

Linear run-up from 1000 rpm to 6300 rpm has been performed under full and half load for the 4<sup>th</sup> and 5<sup>th</sup> gear. The analysed values are angle, angular velocity and acceleration in all shafts as well as the inner deflection torque acting on the shafts. Further are the results of the analysis.

#### Fourth gear

##### Full load

In fourth gear, the clutch K2 is engaged and torque is being transmitted via the hollow shaft to the 1. output shaft, see Figure 5.4.12 – blue path.

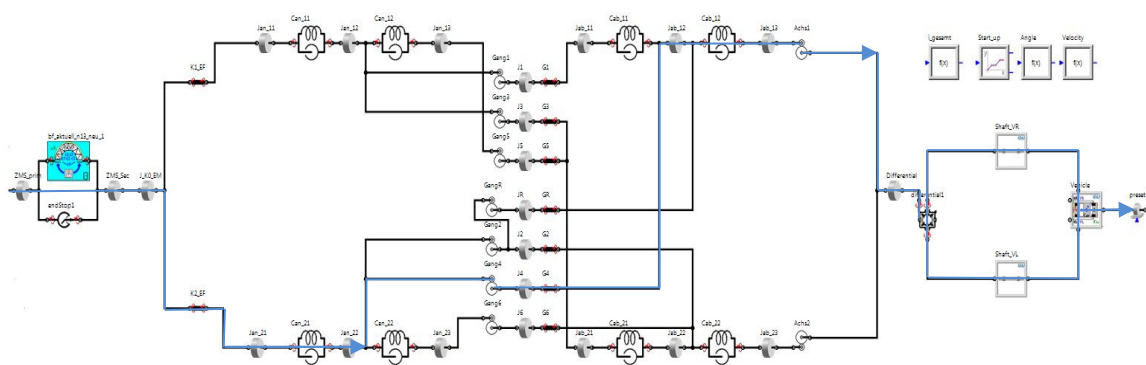
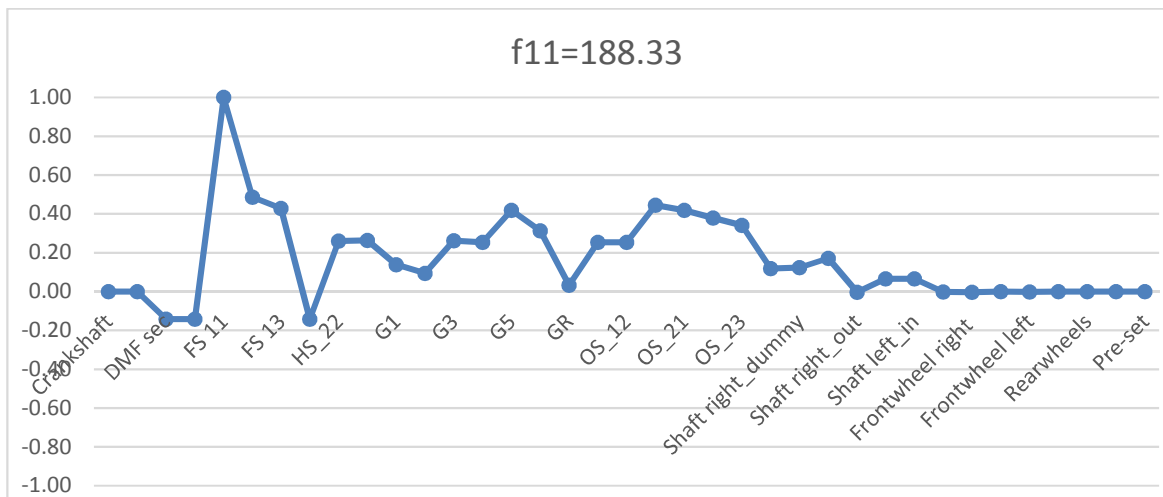


Figure 5.4.12 - Fourth gear power path

To determine which natural frequencies are being excited during run-up, the data obtained from the simulation in SimulationX have been analysed in Matlab and presented via order analysis, Campbell diagram and amplitude analysis. It has been found out that the crucial frequency for the fourth gear is 188 Hz. This value is consistent with the values determined in the modal analysis (viz. Table 5.3-1).



ZMS_spring	0.0007	
Can_11	0.3349	█
Can_12	0.0409	█
Can_21	1.0000	█
Can_22	0.0002	
Cab_11	0.0000	
Cab_12	0.4643	█
Cab_21	0.0310	█
Cab_22	0.0298	█
Shaft_VR.c_SW	0.0135	█
Shaft_VR.c_ZW	0.0044	█
Shaft_VL.c_SW	0.0038	█

The full input shaft which is connected to K1 is divided into three inertias and lies inside the hollow shaft connected to K2 (Figure 5.2.5). Their mass depends on the gear position. In this case the gears are positioned closer to the end of the shaft. Due to the small distance between gear 3 and 5 is the shaft stiffness between them higher than the stiffness between the clutch and gear 3. Similarly at the remaining shafts. As visible in Figure 5.4.13, the cause of the deflection in this frequency is partly the stiffness on the output shaft between the first and second inertia and partly the one on the input shaft between the first and second inertia, thus the smaller stiffness. This assumption was confirmed by examination of the angular velocity between the shaft endings. According to Figure 5.4.13 and this context also the amplitude at the full shaft (input shaft) should be of highest value. This conjecture can be inspected via the Campbell diagram.

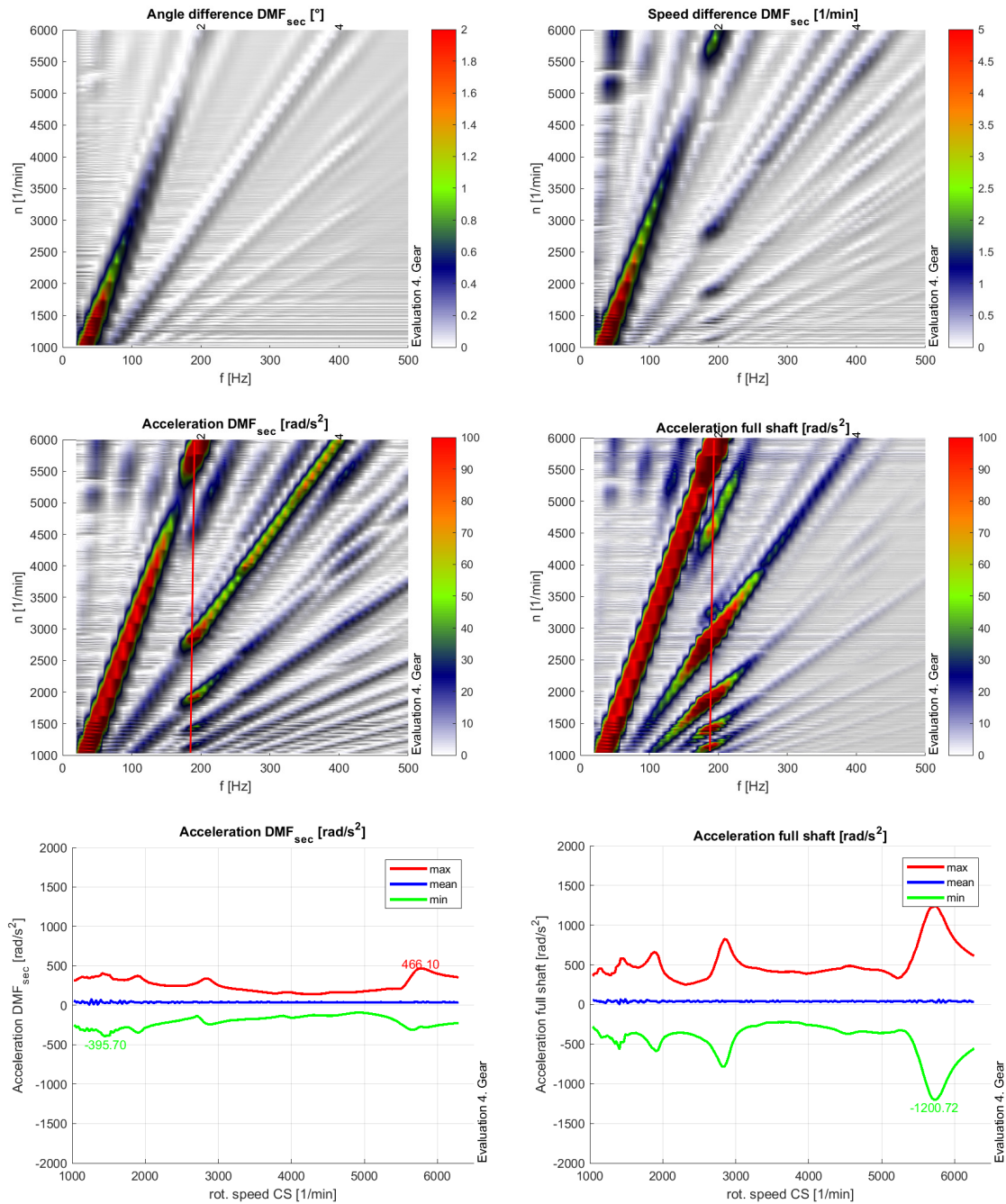


Figure 5.4.14 - 4th gear full load Campbell diagram (top and middle) for DMF secondary side angle difference (top - left), speed difference (top - right), acceleration (middle - left); full shaft acceleration (middle - right) and amplitude analysis (bottom) - DMF (left), full shaft (right)

In Figure 5.4.14 the Campbell diagram and amplitude analysis for a full-load run-up is shown. A clear increase of the amplitude is visible at 188 Hz confirming the previous theory. The influence of the 2<sup>nd</sup> engine order followed by the 4<sup>th</sup> and 6<sup>th</sup> order can be seen in Figure 5.4.15. Following is another excitation at ca. 51 Hz which is according to the modal analysis from section 5.3 caused by the wheel-floor contact. This frequency has greater influence on the angle difference as visible in Figure 5.4.15.

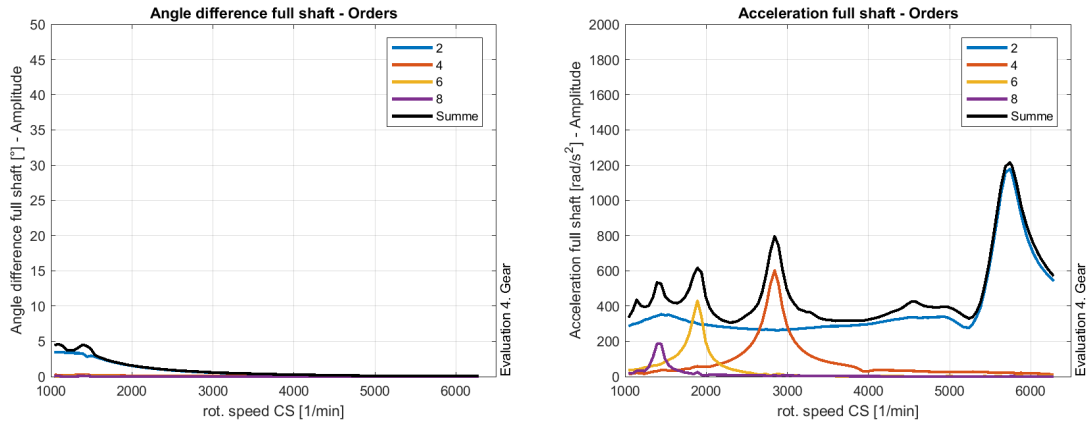


Figure 5.4.15 - 4th gear full load order analysis

Even though the amplitude caused by 2<sup>nd</sup> order oscillation has the highest value, the 4<sup>th</sup> and 6<sup>th</sup> order vibration are from bigger importance since they cause excitement at engine speeds lying in the usual operation range (1500-4000 rpm).

### Part Load

Similar are the results for part load run-up:

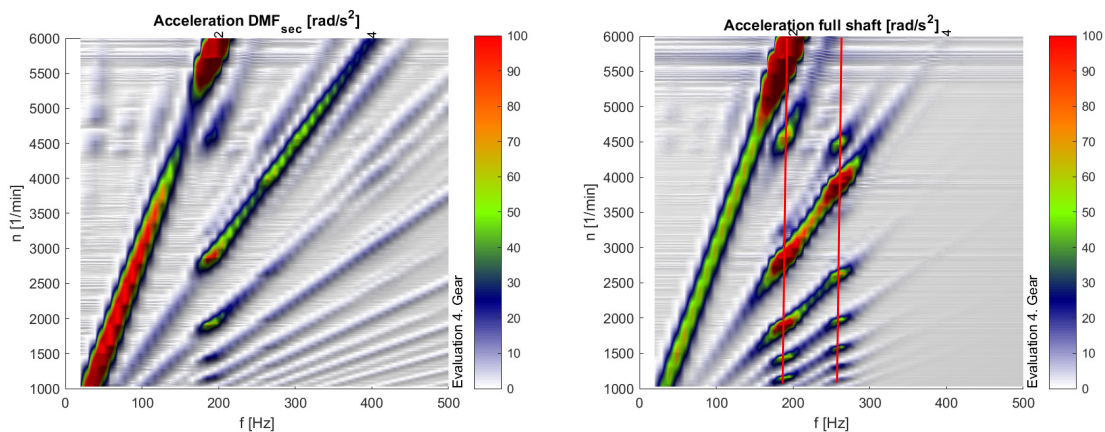


Figure 5.4.16 - 4th gear part load Campbell diagram - DMF (left), full shaft (right)

According to Figure 5.4.16, the excitement is as expected during full load stronger than during half load run-up. The frequency 188 Hz corresponds for the 2<sup>nd</sup> order to a speed of 5640 rpm and won't be reached often since normal vehicle operation usually occurs between 2000-4500 rpm. Because of this, the 4<sup>th</sup> and 6<sup>th</sup> order are of bigger importance, since they cause excitement at a speed of 2820 rpm and 1880 rpm.

### Fifth gear

#### Full load

In 5<sup>th</sup> gear is K1 engaged and the torque is being transmitted from the full shaft to the wheels over the second Hz output shaft OS2 according to Figure 5.4.17.

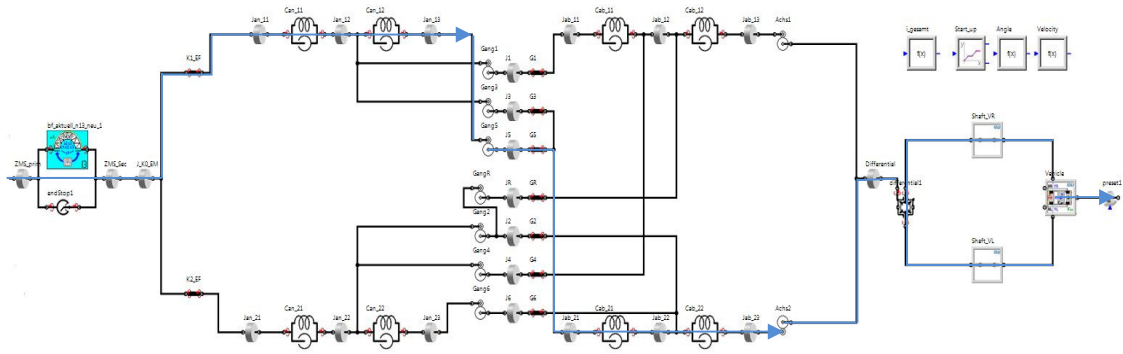


Figure 5.4.17 - Fifth gear power path

Excitation during 5<sup>th</sup> gear occurs at a frequency of 87 Hz corresponding to an engine speed of 2610 rpm for 2<sup>nd</sup> engine order.

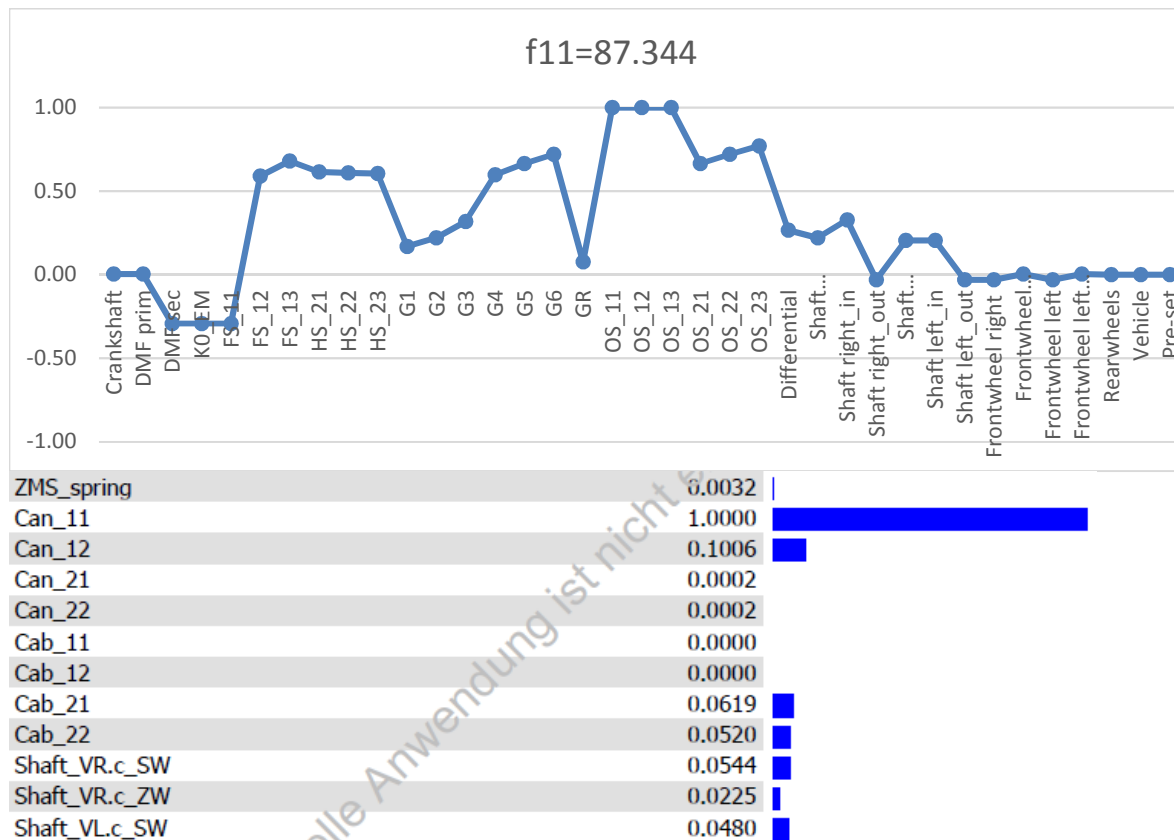


Figure 5.4.18 - Deflection and potential energy (5th gear)

The enlargement point of excitement is similarly as before the full shaft where torque is being transmitted and the deflection is then being increased by the second output shaft stiffness. Mainly affected are the first output shaft OS1 and second output shaft OS2. The transmission swings against the engine and side shafts. Since the excitement occurs at an engine speed lying in the usual operation range also for this gear an attempt for optimisation should be made.

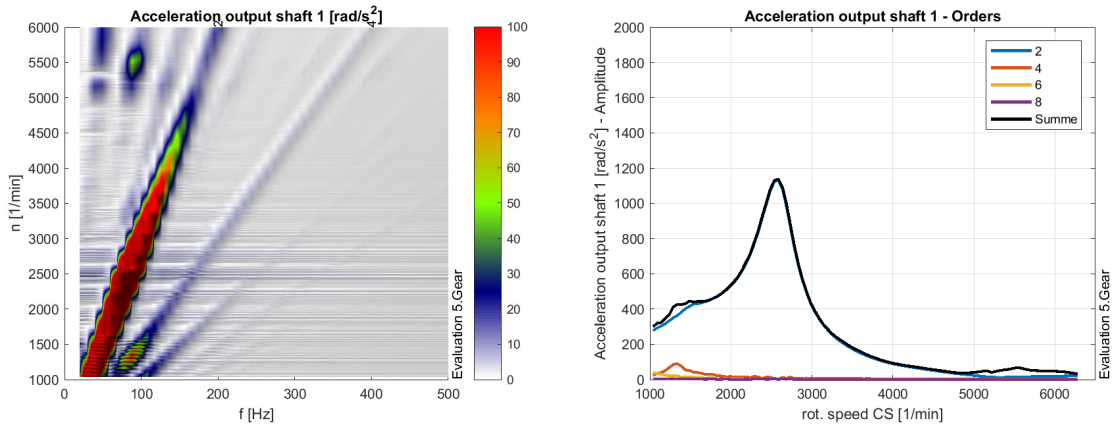


Figure 5.4.19 – 5<sup>th</sup> gear full load Campbell diagram (left) order analysis (right)

The highest vibration amplitude has been found at the output shaft and is mainly due to 2<sup>nd</sup> engine order. Its peak lies as mentioned before at 87 Hz. The 4<sup>th</sup> order has small influence at ca. 1300 rpm speed.

### Part Load

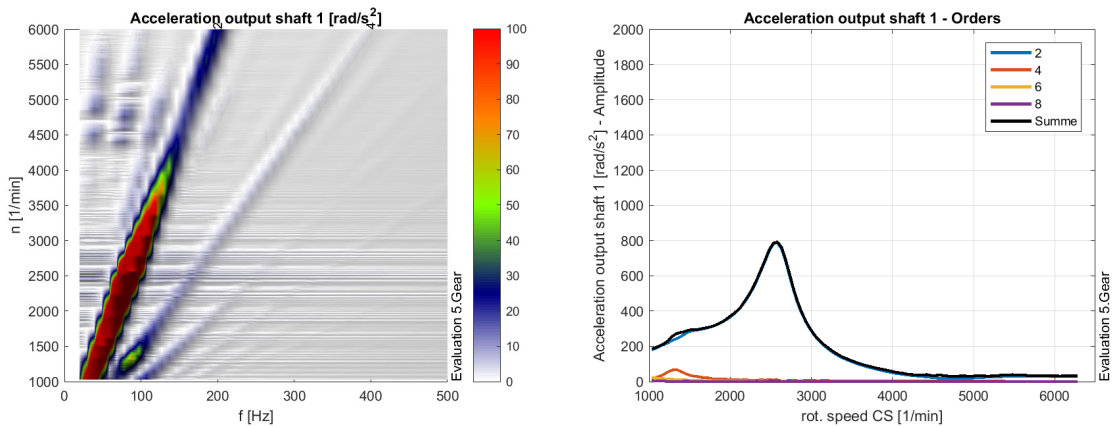


Figure 5.4.20 – 5<sup>th</sup> gear part load Campbell diagram (left) order analysis (right)

According to Figure 5.4.20 the excitement at part load is visibly lower than at full load. To confirm this assumption likewise the amplitudes will be compared.

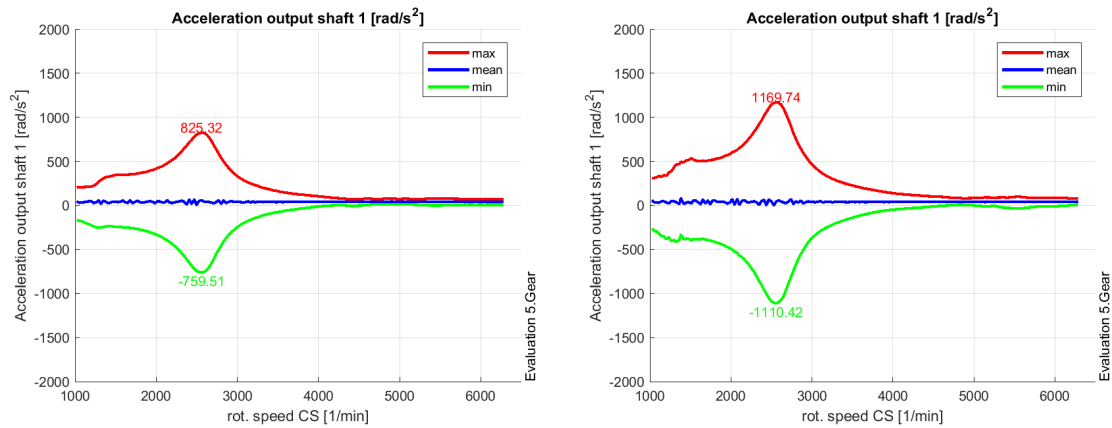


Figure 5.4.21 – 5<sup>th</sup> gear amplitude - part load (left) vs. full load (right)

The maximal acceleration value during part load is 825.32 rad/s<sup>2</sup>, during full load 1169.74 rad/s<sup>2</sup>.

In this case the 4<sup>th</sup> and 6<sup>th</sup> engine order have almost no influence on the excitement. The input shaft stiffness has a significant role in both gears and their reconstruction should be therefore considered.

#### 5.4.5. Run-up – rattle

Rattle has been also investigated for run-up again for the 2<sup>nd</sup> and 4<sup>th</sup> gear to compare the effect of the transmitted torque and drag torque on the system. The model for idle (appendix 3 and 4) can be used after removing the idle load-regulator and adding a velocity specification for normal run-up as described in section 5.2.4.

Since during run-up the main clutch and one of the two secondary clutches are closed, torque is being transmitted and all gears spin at a certain velocity given by the shifted gear pair. Likewise the connection allows transmission of engine oscillation in the powertrain.

As described in section 5.4.1, the normal force acting on the tooth flanks and the position difference have to be examined.

#### Second gear

For the second gear, different gear pairs for full load have been investigated to understand the effect of the gear pair resistance and velocity on rattle.

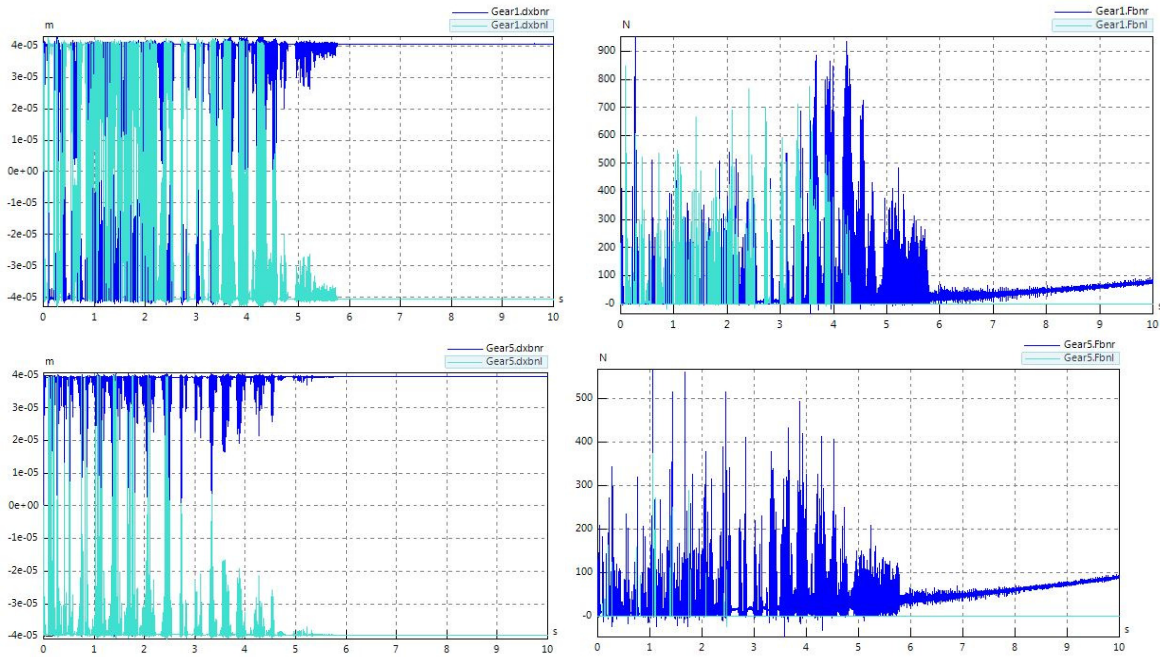


Figure 5.4.22 - Position difference (left) and normal tooth flank force (right) for the 1st gear pair (top) and 5th gear pair (bottom)

How to indicate whether rattle occurs has been described in section 5.4.1. The appearance of rattle is visible for both gear pairs in Figure 5.4.22. Position differences of bigger magnitude and bigger force acting on the left tooth flank is visible for the first gear pair. In the sixth second an angular velocity is being reached after which rattle settles and the normal force on the right tooth flank steadily increases indicating that the powertrain is being driven by the engine.

#### Fourth gear

In the fourth gear also the impact of load is being examined. Three different loads are being applied; 20%, 60% and 100% (Figure 5.4.23).

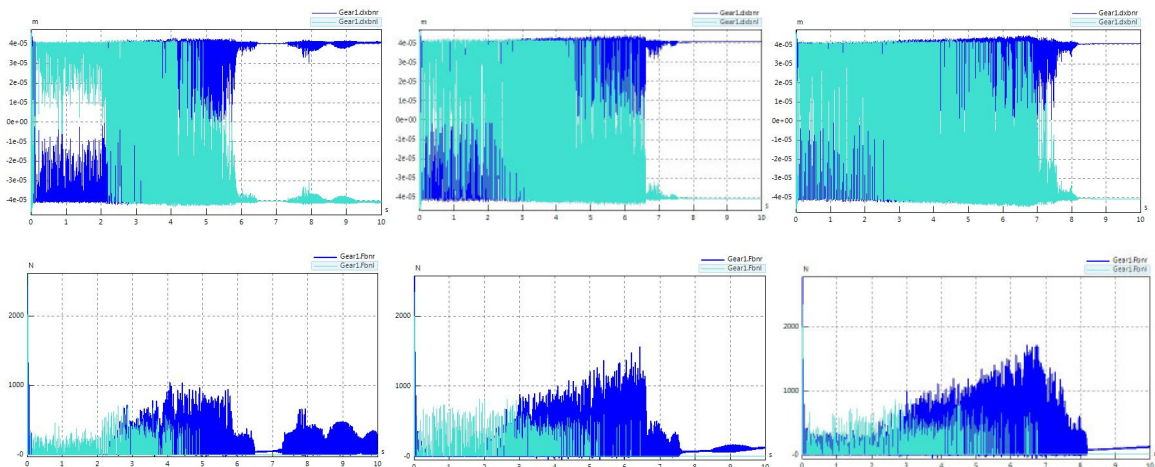


Figure 5.4.23 - Position difference (top) and normal tooth flank force (bottom) at 20% (left), 60% (middle) and 100% (right) 1st gear pair

## Comparison

When the 4<sup>th</sup> gear is shifted, all transmission shafts except of the hollow shaft (input shaft 2) rotate with a higher velocity than in 2<sup>nd</sup> gear. The bearing and synchro drag torque are dependent on the angular velocity difference between the gear wheel and output shaft. From this knowledge it can be concluded, that both drag torques have higher value in 4<sup>th</sup> gear than in 2<sup>nd</sup> gear and increase with higher angular velocity. Further they have higher value for the 1<sup>st</sup> gear pair than for the 5<sup>th</sup> gear pair. As already mentioned before, the splashing drag torque depends on the gear wheel tip radius, gear width and velocity. Although the loose gear velocity of the 1<sup>st</sup> gear is about 3.5 time lower than for the 5<sup>th</sup> gear, it has been found out that the splashing drag torque for the 1<sup>st</sup> gear pair is higher than for the 5<sup>th</sup> gear pair. The reason is the gear tip radius having a bigger impact on the splashing drag torque than the velocity. The bigger the gear tip radius, the more immerses the wheel into the oil causing higher resistance against the rotational movement.

The inertia acting on the output side of the transmission varies depending on the shifted gear. With increasing gear ratio likewise increases the inertia having a damping effect and lowering rattle.

Further dependence on load can be seen significant. Higher load causes an increase in the normal tooth flank force and also bigger position differences as visible in Figure 5.4.23.

From this insight it can be concluded that the normal force acting on the teeth flanks is dependent on the torque which is dependent on the shifted gear. On the first gear pair act bigger forces than on the 5<sup>th</sup> gear pair in all situation. Additionally it seems that the position difference has the same dependency on the angular velocity.

For the overall vehicle can be deduced that in 2<sup>nd</sup> gear rattle will occur at lower frequencies than in 5<sup>th</sup> gear and will be thus perceived as a humming noise whereas in 5<sup>th</sup> gear the transmitted noise will have a more sharp appearance.

## 5.5. Chapter Conclusions

The powertrain dynamic behaviour has been analysed in chapter 5. It has been found out, that the DMF with the initial settings is fulfilling its purpose. The excitement of the natural frequencies is mainly caused by input shaft 1 and could be therefore improved only by modifying its stiffness. In this case a higher stiffness would be favourable and could be achieved by moving the gears positioned in the middle of the shaft closer to the clutch, by increasing the shaft diameter or choosing a different material.

No significant negative impact has been found for hybrid start and idle rattle which also indicates a sufficient DMF setting.

For cycling in second gear the occurrence of jerking has been found, a for the passenger very inconvenient phenomena which can only be avoided by prolonging the load change gradient. Prolonging the load change would mean a slower vehicle reaction to the driving

demand and is insufficient for the driver. Further avoidance of jerking during load change can be only affected by the driver himself.

## 6. DMF optimization

---

The current goal in the automotive industry is as mentioned before lowering the fuel consumption. This can be achieved e.g. by variable displacement. Variable displacement is a technology which enables improvement of engine fuel economy by deactivating cylinders and is used in multi-cylinder engines during light-load operation. The deactivation is ensured by keeping the intake and exhaust valves closed for particular cylinders. Besides lowering the amount of fuel pumped into the cylinders, pumping losses are minimized.

The DMF will be optimized to ensure good decoupling in both operation with all cylinders working and during 2-cylinder activation.

Since in the analysis before a premium DMF has been used and its parameters for the four cylinder engine are already showing favorable behavior (the DMF natural frequency is not being excited during general operating states), optimization possibilities for the 4-cylinder engine are low.

To point out the difference in excitation between the 2-, and 4-cylinder engine, a comparison of the piston forces as function of the crankshaft angle behind the DMF will be made. The initial conditions are the same as for the 4-cylinder engine. After, the DMF will be adjusted for the 2-cylinder and 4-cylinder activation by modifying the given parameters. For 2-cylinder activation, the maximum engine static torque is half of the 4-cylinder static torque, i.e. 125 Nm. All parameters for the transmission and side shafts stay the same. The initial stiffness and torque ranges for the DMF are:

- $J_1 = 7.5e^{-2} \text{kgm}^2$
- $J_2 = 7.0e^{-3} \text{kgm}^2$
- $k_1 = 2.5 \text{ Nm/}^\circ$  from ca.  $1^\circ$
- $k_2 = 7.4 \text{ Nm/}^\circ$  from  $5.5^\circ/14 \text{ Nm}$
- $k_3 = 23.7 \text{ Nm/}^\circ$  from  $47.7^\circ/326 \text{ Nm}$

In general for torque fluctuation reduction the stiffness coefficients have to be reduced and the inertias increased. When increasing the inertia the natural frequency value decreases whereby the secondary inertia has a bigger influence than the primary one which could be due to the fact that for low values of inertia after an increase, the natural frequency value decreases exponentially (24). This cannot be done limitlessly. When increasing the inertia more space is needed and risk of flywheel wobble increases. When reducing the spring stiffness, the deflection angle increases and more installation space is needed for the spring.

For this example both inertias will be kept at the initial value. The number of stages, their action length and stiffness are going to be modified. The analyzed parameters to evaluate the modification proceeded are:

- the deflection angle between both flywheels

- acceleration of the secondary flywheel inertia
- the DMF characteristic curve

The influence of parameter modification will be compared for run-up since all frequencies are passed during it. The 5<sup>th</sup> gear will be analyzed since the DMF natural frequency achieves its highest value for it. Dynamic behavior at the DMF secondary side and thus its decoupling effect from engine oscillation is from importance and going to be inspected. The initial state will be analyzed to use it as a point for comparison for the modified values.

To design a DMF with reasonable parameters the DMF calculation tool presented in section 3.2.3 will be used.

## 6.1. Comparison 2-cylinder- and 4-cylinder activated IC engine

As already mentioned before, the excited order differs for the 2-cylinder and 4-cylinder engine. In 2-cylinder engines firing occurs once every revolution whereas in 4-cylinder engines twice every revolution. In case of cylinder deactivation act forces according to Figure 6.1.1, in both a segment of 720° (1 cycle) is shown:

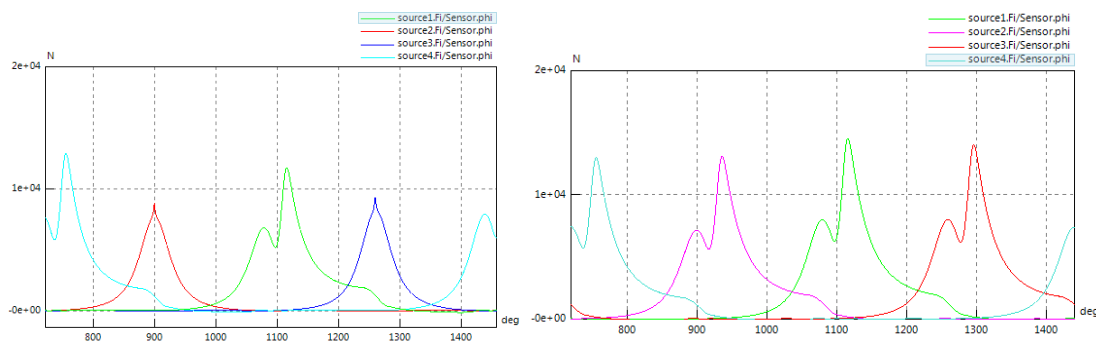


Figure 6.1.1 - Forces acting on the pistons for 2-cylinder activation (left) and 4-cylinder activation (right)

From this statement can be already deduced, that with a rising number of cylinders rotational irregularities decrease. Orders of higher value excited during run-up are usually multiples of the basic order (e.g. for the 4-cylinder engine 2,4,6,8 order). For excitation this means a negative influence on the system since especially the natural frequencies of lower value determined in the modal analysis in section 5.3 are shifted into the normal operating range and gain on importance. According to equation (5.3.2) are for the 4-cylinder activation all frequencies in Table 5.3-1 up to  $f_6$  only for the start-up process from relevance since they are in a speed range below 1000 rpm. Differently for 2-cylinder activation. All frequencies from 16 Hz have to receive attention.

Another important factor is the damping ratio. The 4-cylinder engine operation starts in the overcritical area (Figure 4.1.2– frequency ratio over  $\sqrt{2}$ ) whereas for 2-cylinder engines in the critical area where the magnification factor reaches its highest value. To show this effect, different diagrams for angle, velocity and acceleration will be compared. As already mentioned, the 5<sup>th</sup> gear has been chosen to check the for the DMF most critical setting.

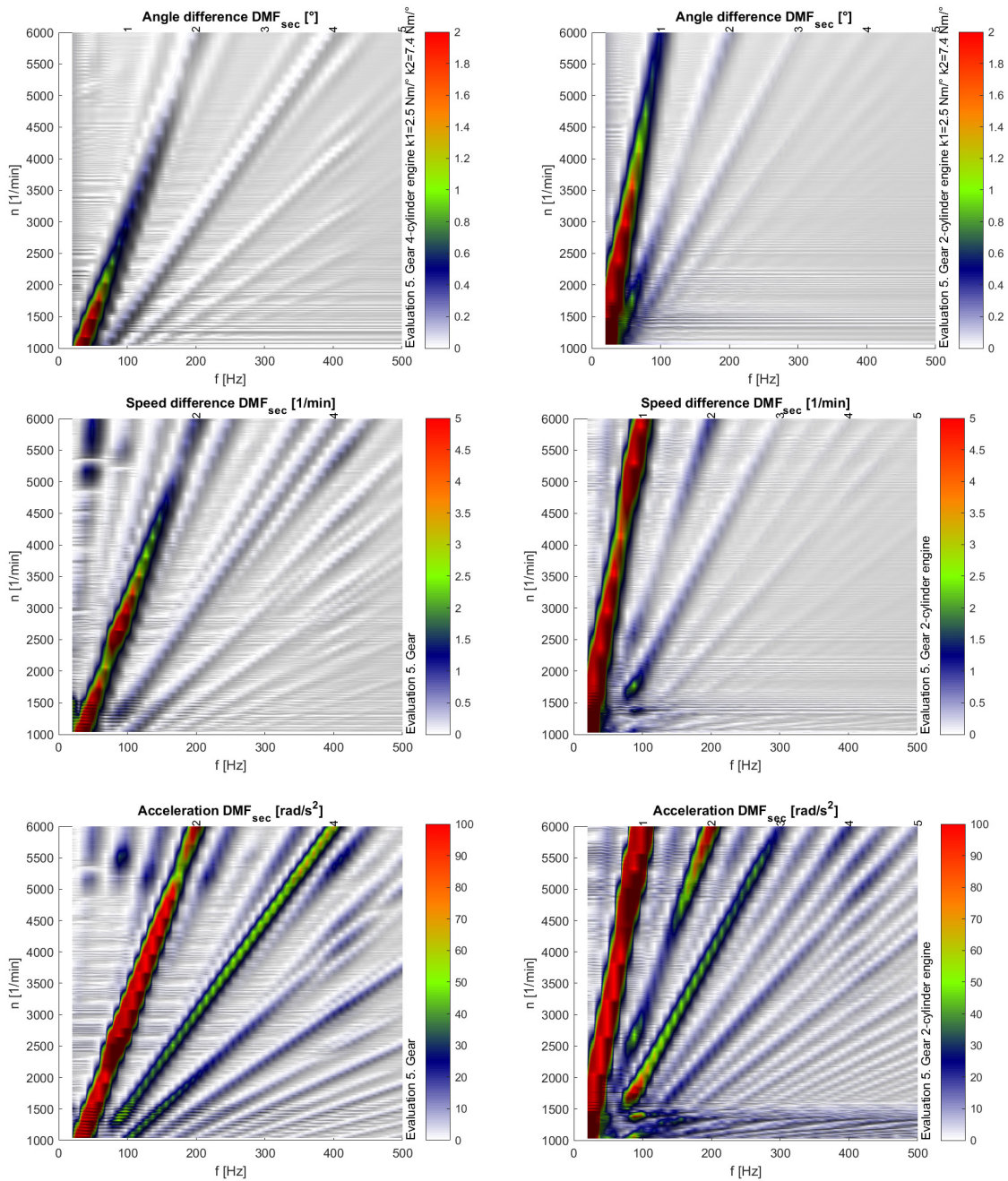


Figure 6.1.2 – 5<sup>th</sup> gear comparison of angle, velocity and acceleration Campbell diagram for 4-cylinder activation (left) and 2-cylinder activation (right)

In Figure 6.1.2 is the comparison of the angle difference amplitude between the primary and secondary DMF inertia for the 2-cylinder and 4-cylinder engine. According to it is the 1<sup>st</sup> engine order for the 2-cylinder engine and the 4<sup>th</sup> order for the 4-cylinder engine from greater importance. A significant increase of the amplitude is visible. The biggest influence of the engine order can be seen when comparing the angle difference amplitude of the 2-cylinder and 4-cylinder engine. A clear contrast is apparent in Figure 6.1.3.

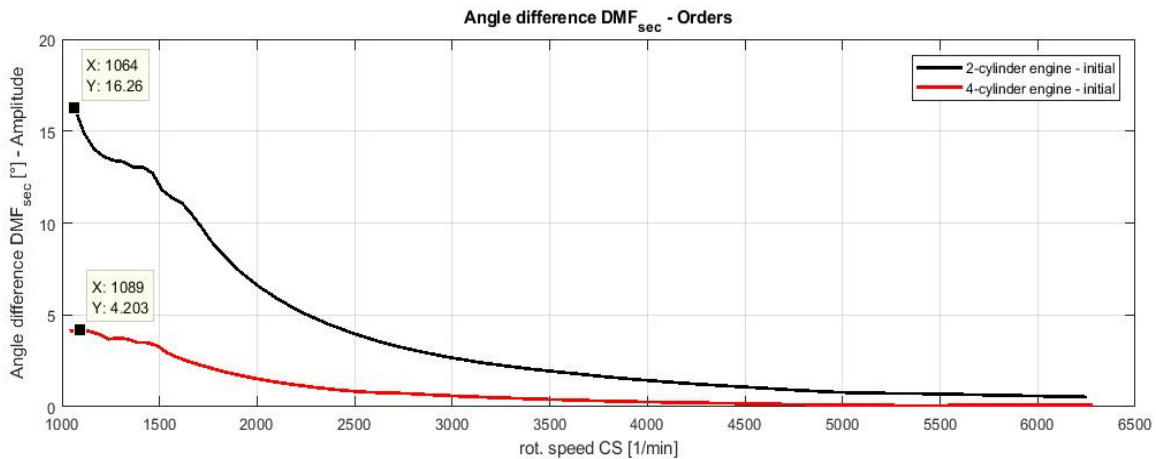


Figure 6.1.3 - 5th gear angle difference amplitude comparison for 2-cylinder and 4-cylinder activation

Irregularities at low engine speeds are even more significant for the 2-cylinder activation (about 25.85% higher amplitude according to the peak values visible in Figure 6.1.3) but even out with rising velocity.

In this case the natural frequencies analyzed before should stay the same since the inertias included in the simulation model were maintained and only firing was disabled. Otherwise for a conventional 2-cylinder engine an increase of the natural frequency values would be expected due to the lower inertia of the crankshaft.

The greatest risk sets the DMF natural frequency which should lay in a frequency range below idle. It has been found out to be in a range from 13.65-13.81 Hz for the 2<sup>nd</sup> to 5<sup>th</sup> gear according to Table 5.3-1. For the first engine order this means in the engine speed range from 818.94-828.42 rpm (equation (5.3.2)), which is still below the usual operating range and of relevance only during start-up.

When changing the stiffness for the first state, the related change of the natural frequency has to be taken into consideration. For a higher stiffness also the natural frequency is increasing and opposite for lower stiffness.

The excited frequency is according to Figure 6.1.4 (top) as expected for the 2-cylinder activation at the same value as for the 4-cylinder activation, 87 Hz. Its excitation amplitude can be lowered by optimizing the decoupling effect of the DMF. Besides the 1<sup>st</sup> engine order, which is from most significance with regard to the oscillation amplitude, also excitement of the 2<sup>nd</sup> and 3<sup>rd</sup> engine order is visible for the 2-cylinder engine.

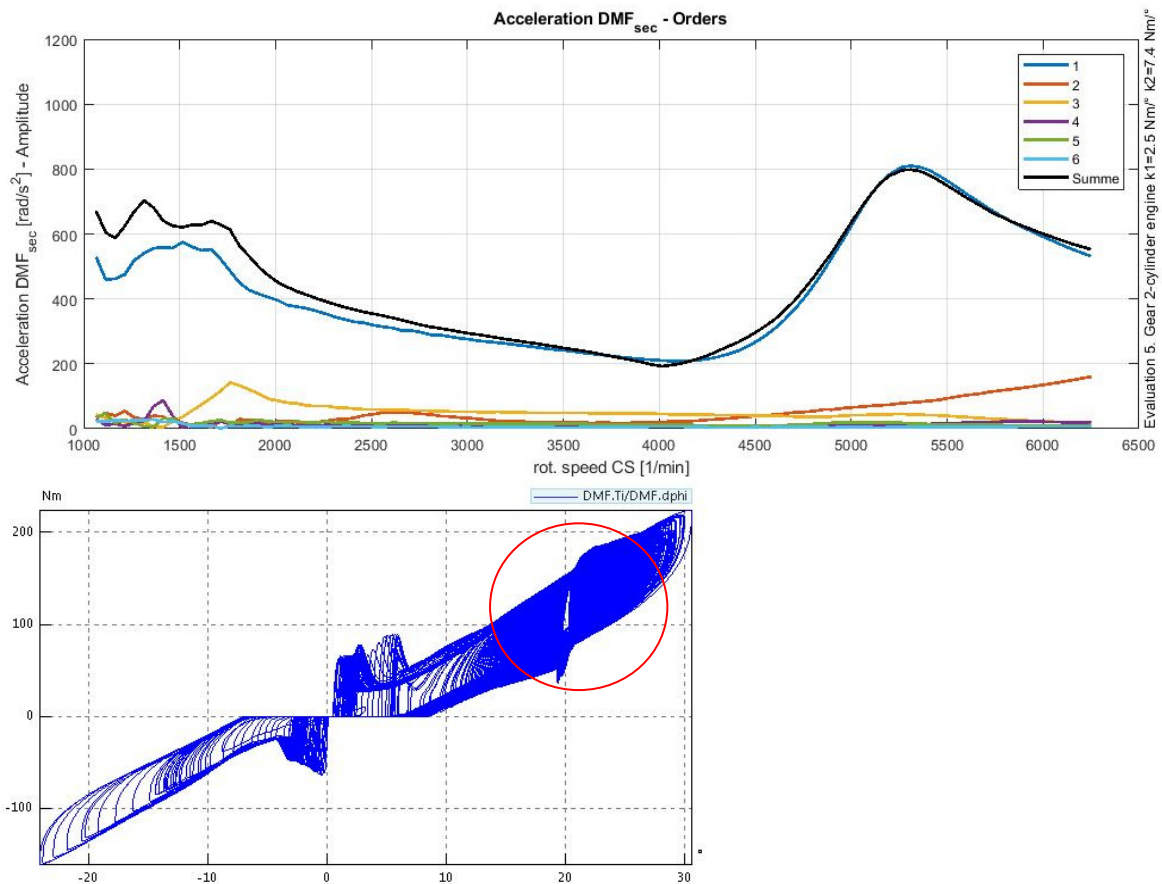


Figure 6.1.4 – 2-cylinder activation order analysis (top) of secondary inertia acceleration and DMF characteristic curve for initial values (bottom) 5<sup>th</sup> gear

The DMF characteristic curve (Figure 6.1.4 (bottom)) shows that the end stop is not being reached during run-up and its main operating point is in second stage (end stop stiffness starts at  $47.7^\circ$ ). The peaks in the first 10 seconds are due to the free angle between stopper and spring when the flange wings repeatedly hit the arc springs with unbraked force. As a countermeasure in some DMF additional friction devices are installed, which delays the rotation of the flange within a given working range.

For side shaft dimensioning is knowledge about the acting torque from importance. Comparison of the filtered engine and side shaft torque is in Figure 6.1.5.

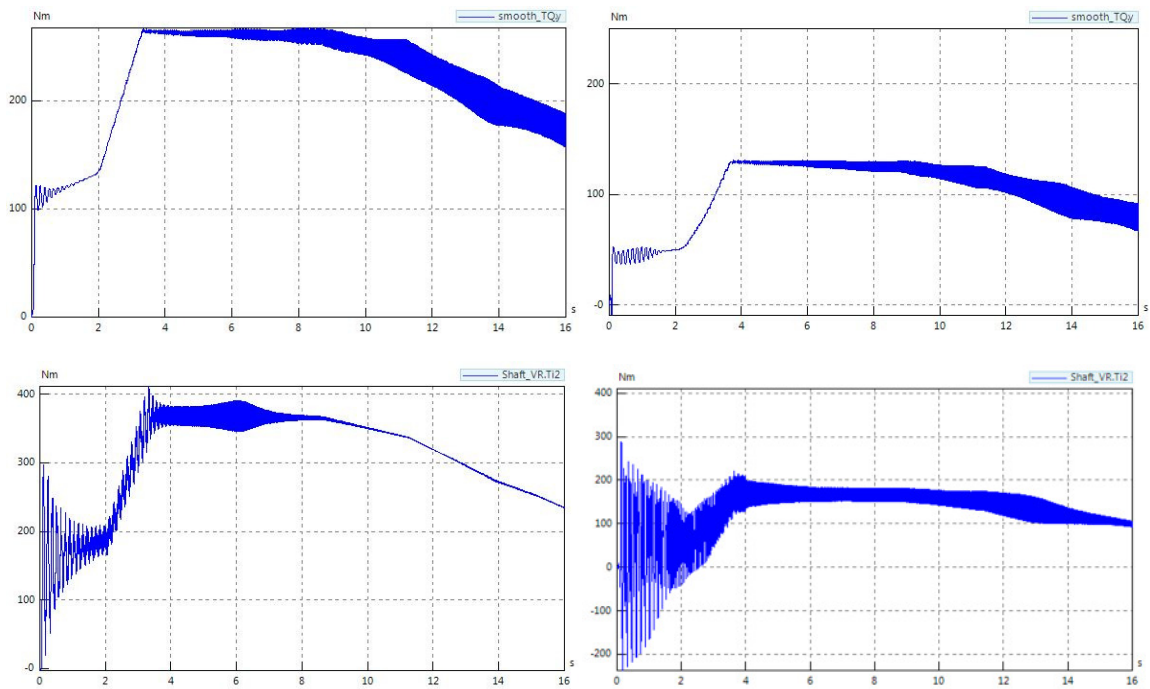


Figure 6.1.5 - Comparison engine torque (top) and right side shaft torque (bottom) for 4-cylinder (left) and 2-cylinder (right) activation

According to Figure 6.1.5 is the engine torque for the 2-cylinder activation as stated before half of the 4-cylinder torque, similarly for the right side shaft torque. The biggest difference is visible from the 14<sup>th</sup> second when almost the maximum engine velocity is reached. For 2-cylinder activation torque has a significantly flatter course at high engine velocities with in contrary higher amplitudes due to the acting gas forces and latter indicating insufficient decoupling from the engine vibration. An attempt to improve the DMF will be made to increase the decoupling effect for 2-cylinder, 4-cylinder activation first separately to find then a DMF setting sufficient for both, i.e. for an engine with variable displacement.

## 6.2. Adjustment for 2-cylinder activation

In general for run-up, lowering the stiffness has positive effect in terms of engine vibration decoupling from the transmission. A one stage DMF with lowest possible stiffness is going to be tested. Figure 6.1.4 (bottom) has shown, that the maximum dynamic torque acting on the DMF is ca. 220 Nm. The spring is going to be adjusted to it, reaching its maximum deflection at this value.

Using the Excel calculation file and considering the installation space parameters defined in section 3.2.3 a minimum stiffness value of 1.47 Nm/° for one spring results after adjusting the wire diameter to obtain a reasonable number of coils. Thus 3 Nm/° for the whole one stage DMF.

1<sup>nd</sup> modification 2-cylinder:

- $k_1=3 \text{ Nm/}^\circ$  from ca.  $1^\circ - 73.3^\circ/220 \text{ Nm}$

Results:	Windungsanzahl	
Wire diameter chosen (d)	5 mm	0.005 m
Wire diameter-tolerance (es)	0.2 mm	0.0002 m
Mean coil diameter (Dm)	30.00 mm	
Spring index	6	
Shear stress	708.37 N/mm <sup>2</sup>	
maximum coil number (active)	31.96	
Lowest reachable stiffness	1.47 Nm/°	84.221256 Nm/rad

Figure 6.2.1 - Determination of the lowest possible stiffness

Figure 6.2.2 shows how angle difference is influenced.

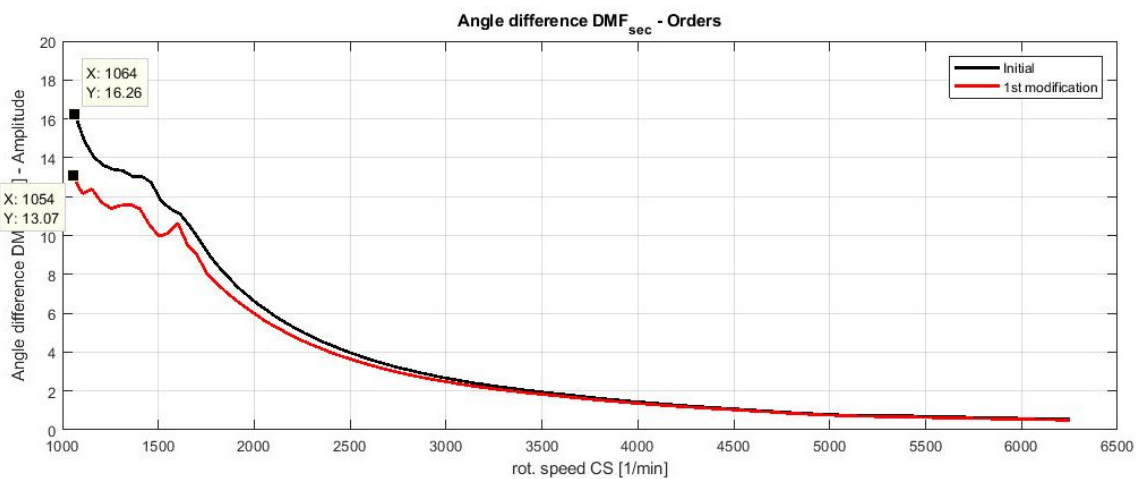


Figure 6.2.2 – Angle difference of the DMF sec. inertia with one stage DMF  $k=3 \text{ Nm/}^\circ$

The maximum amplitude for the initial DMF setting is as visible in Figure 6.2.2  $A_{init} = 16.26^\circ$  and after modification into a one stage DMF with  $k = 3 \text{ Nm/}^\circ$ ,  $A_{mod1} = 13.07^\circ$ . This means a 19.62% improvement of the dynamic behaviour.

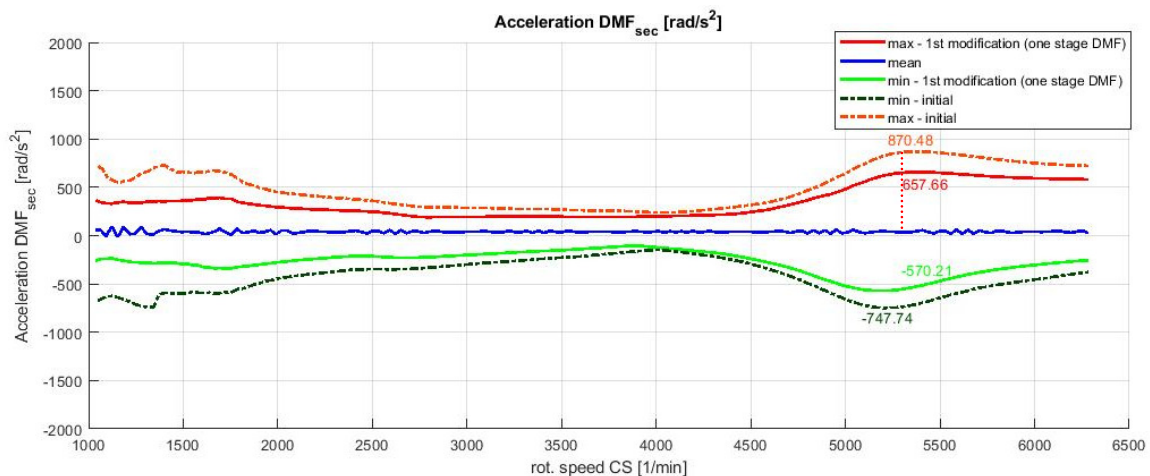


Figure 6.2.3 – Comparison of the acceleration of the DMF sec. inertia - initial DMF vs. one stage DMF with  $k=3 \text{ Nm/}^\circ$

In Figure 6.2.3 is the acceleration amplitude comparison. The amplitude occurring at the resonance frequency analysed in section 5.4.4 is marked with a dotted line. For the initial state is the maximum amplitude in the given spot  $A_{init\alpha} = 870.48 \frac{\text{rad}}{\text{sec}^2}$  and for the modified

DMF  $A_{mod1\alpha} = 657.66 \frac{rad}{sec^2}$  meaning a 24.45% improvement. Even bigger influence is apparent at low engine velocities; the acceleration amplitude lowers by ca. 30%.

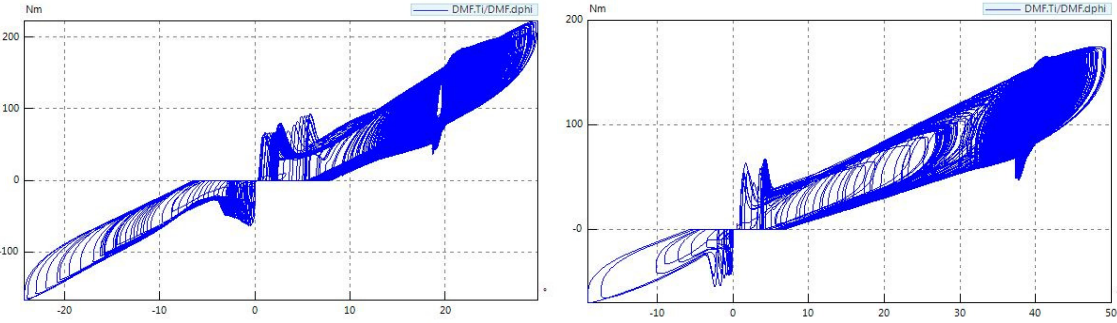


Figure 6.2.4 – Comparison DMF characteristic curve for initial state (left) and 1<sup>st</sup> modification (right) – 2-cylinder engine

In Figure 6.2.4 is visible how the characteristic curve changes with modification. The end stop (from 73.33°) is not being reached, the setting is sufficient.

### 6.3.Adjustment for 4-cylinder activation

Same as in section 6.2 will be proceeded for 4-cylinder activation. The 3 stage DMF will be replaced by a single stage DMF with the minimum stiffness value determined using the DMF Excel calculation file presented in section 3.2.3. For the initial state a maximal applicable torque of 450 Nm was set.

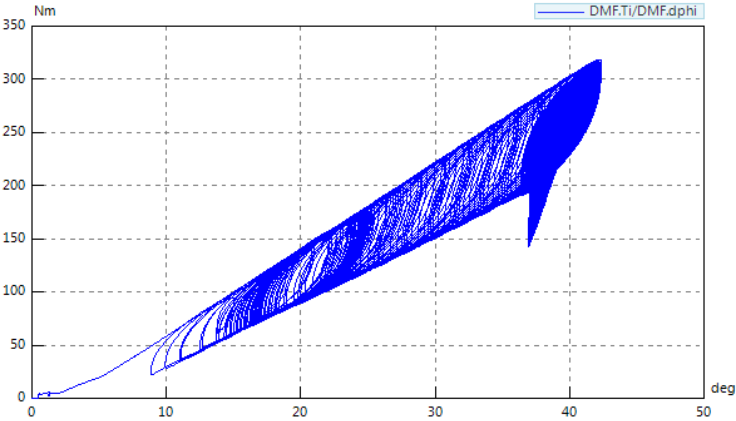


Figure 6.3.1 - Initial state DMF characteristic for 4-cylinder engine

According to Figure 6.3.1 is the maximal torque reached during full load run-up ca. 325 Nm. Due to this a new maximal applicable torque of 350 Nm will be set.

Results:		Windungszahl	
Wire diameter chosen (d)	5.50	mm	0.01
Wire diameter-tolerance (es)	0.03	mm	0.00
Mean coil diameter (Dm)	29.50	mm	
Spring index	5.36		
Shear stress	854.67	N/mm <sup>2</sup>	
maximum coil number (active)	30.38		
Lowest reachable stiffness	2.38	Nm/°	136.42
			Nm/rad

Figure 6.3.2 - Determination of the lowest possible stiffness for the 4-cylinder engine

The minimum stiffness is 2.38 Nm/°, i.e.  $k=4.8 \text{ Nm /}^\circ$  for the whole DMF.

1<sup>st</sup> modification 4-cylinder:

- $k_1=4.8 \text{ Nm/}^\circ$  from ca.  $1^\circ - 72.92^\circ/350 \text{ Nm}$

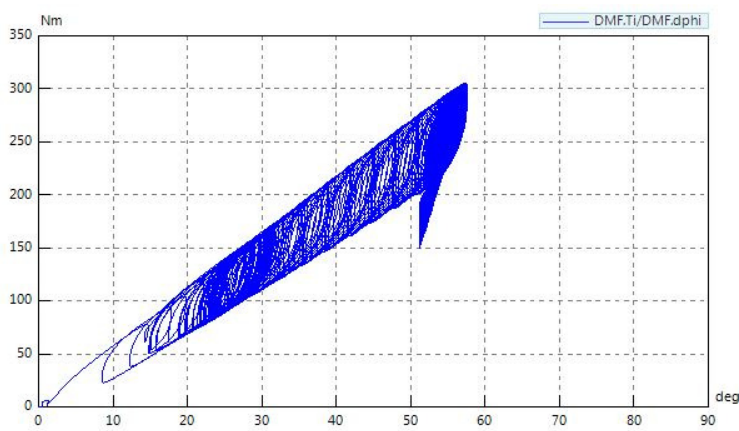


Figure 6.3.3 – 1<sup>st</sup> modification DMF characteristic for 4-cylinder engine

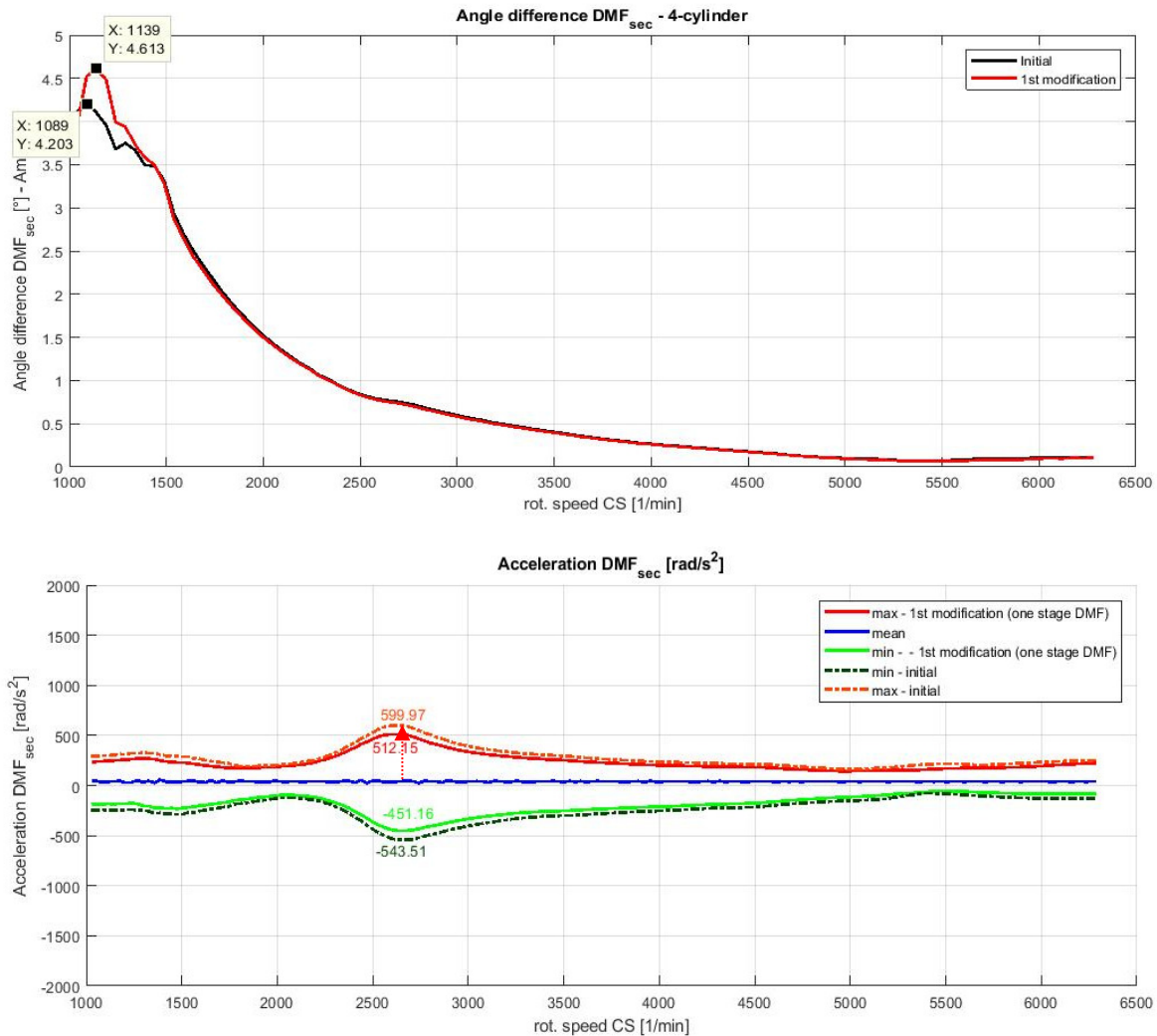


Figure 6.3.4- Comparison of the angle difference (top) and acceleration (bottom) for initial state vs. 1st modification (one stage DMF)

When comparing Figure 6.1.3 (bottom) and Figure 6.3.4 (top) deterioration of the angle difference between ca. 1000-1500 rpm and almost no improvement in the rest of the rotational speed range is visible. The overall acceleration is showing improvement after modification of around 14.64%.

#### 6.4. Adjustment for 2- and 4-cylinder activation, variable displacement

When combining the knowledge gained in the sections before, an attempt of adjustment for an engine with variable displacement can be made. In this case an optimisation to enable the deactivation of 2 of the 4 cylinders was chosen. The 3 stage DMF will be replaced by a 2 stage DMF to gain more deflection space for the first and second stage.

With addition of the second stage the lowest stiffness values for both stages have to be found similarly as in the previous section. The stage 2 torque will be first kept at the same value, i.e. 220 Nm. The minimal values are in Figure 6.4.1:

Results:	Windungszahl		Results:		
Wire diameter chosen (d)	5.10 mm	0.01 m	Wire diameter chosen (d)	3.00 mm	0.00 m
Wire diameter-tolerance (es)	0.03 mm	0.00 m	Wire diameter-tolerance (es)	0.02 mm	0.00 m
Mean coil diameter (Dm)	29.90 mm		Mean coil diameter (Dm)	21.75 mm	
Spring index	5.86		Spring index	7.25	
Shear stress	893.66 N/mm <sup>2</sup>		Shear stress	811.80 N/mm <sup>2</sup>	
maximum coil number (active)	29.34		maximum coil number (active)	14.61	
Lowest reachable stiffness	1.75 Nm/°	100.30 Nm/rad	Lowest reachable stiffness	1.71 Nm/°	97.76 Nm/rad

Figure 6.4.1 - Determination of the lowest possible stiffness for engine with variable displacement

With  $k_{s1} = 1.8 \text{ Nm/}^\circ$  for spring 1 and  $k_{s2} = 1.7 \text{ Nm/}^\circ$  for spring 2 are the final stiffness' deflection angles and torque stages due to the parallel arrangement ( $k_2 = k_{s1} + k_{s2}$ ):

2<sup>nd</sup> modification:

- $k_1=3.6 \text{ Nm/}^\circ$  from ca.  $1^\circ$
- $k_2=7 \text{ Nm/}^\circ$  from  $60.1^\circ/220 \text{ Nm}$

$k_1$  is higher than for the initial settings since an increase of stage 1 stiffness had to be made to be able to transmit the maximum torque (350 Nm) chosen and can have a negative impact during lower velocities.

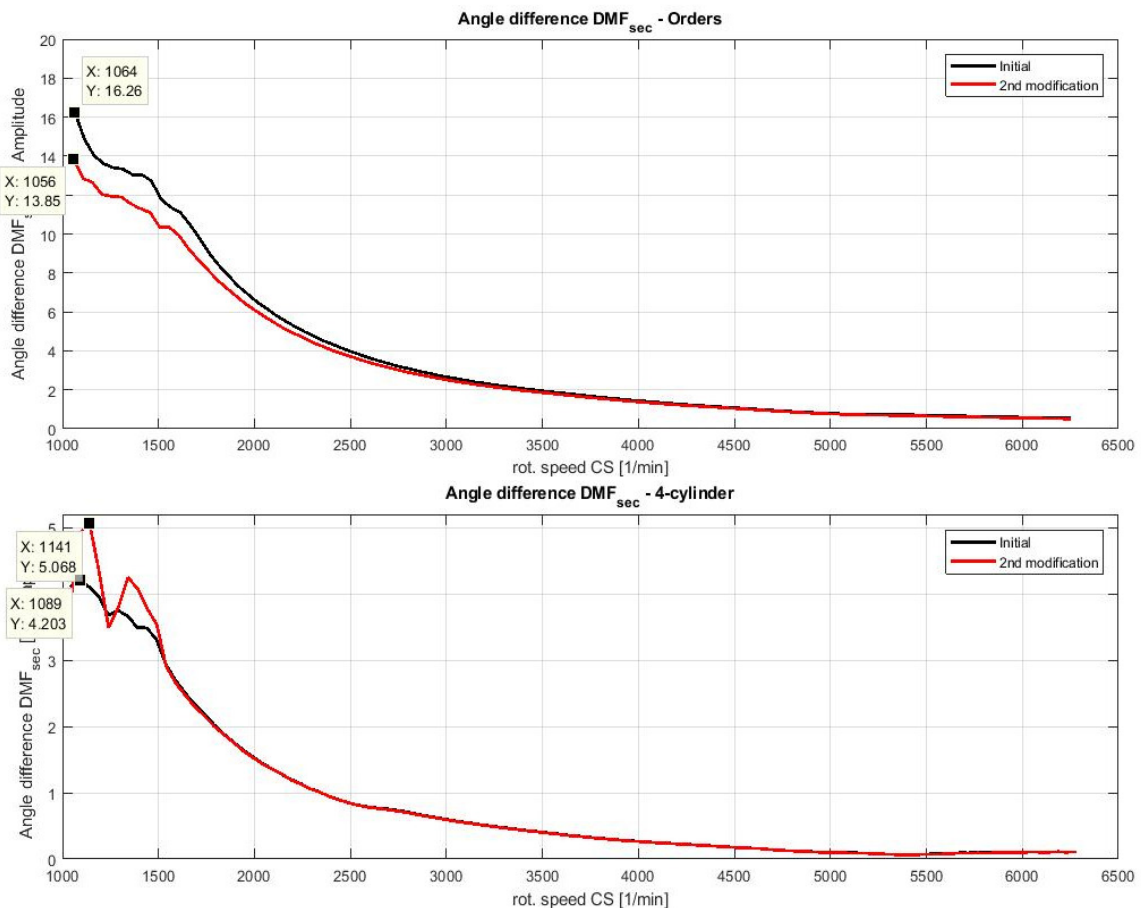


Figure 6.4.2 – Comparison of the angle difference of the DMF sec. inertia for 2-cylinder (top) and 4-cylinder activation (bottom) - initial setting vs. 2<sup>nd</sup> modification

In Figure 6.4.2 is the comparison of the angle difference of the initial DMF and the DMF after 2<sup>nd</sup> modification for 2-, and 4-cylinder activation. For the 2-cylinder activation 14.82%

improvement has been attained. When 4-cylinders are activated, a clear deterioration is visible between 1000-1500 rpm caused as mentioned before by the stage 2 stiffness.

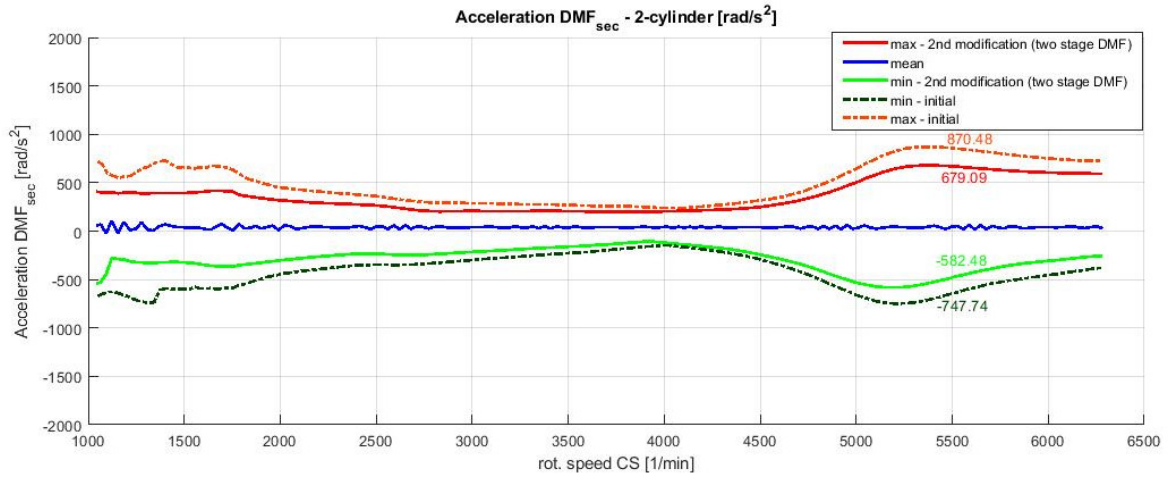


Figure 6.4.3 - Comparison of the acceleration for the DMF sec. inertia - initial vs. 2<sup>nd</sup> modification – 2-cylinder activated

Acceleration improves significantly according to Figure 6.4.3 for the 2<sup>nd</sup> modification when just 2 cylinders are activated. Significant improvement is visible especially during lower velocities up to 2000 rpm and during the resonance between 5000-6300 rpm. The lower stiffness ensures a better decoupling effect.

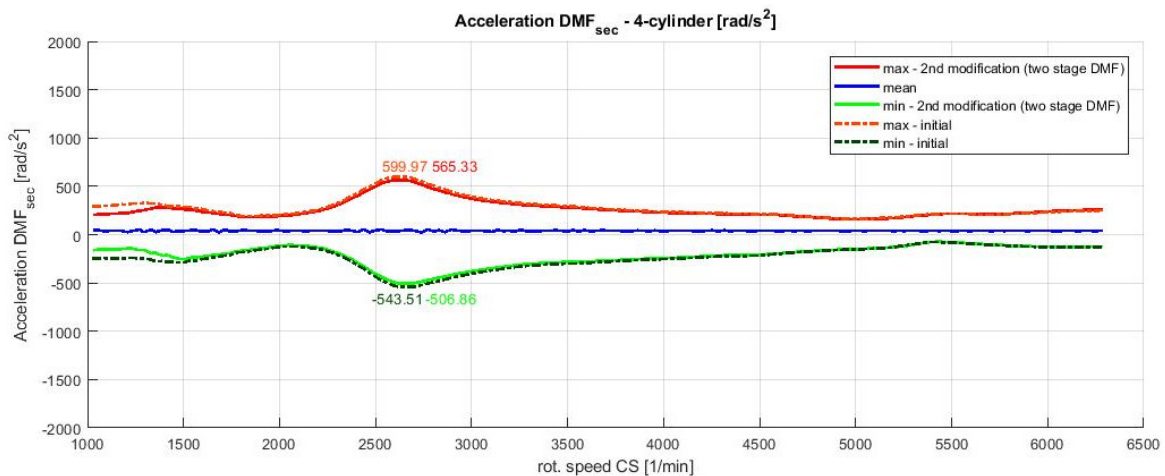


Figure 6.4.4 - Comparison of the acceleration for the DMF sec. inertia - initial vs. 2<sup>nd</sup> modification – 4-cylinder activated

As expected, almost no improvement has been made for the 4-cylinder engine and during low velocities the amplitude even worsens (Figure 6.4.4). The stiffness increase in stage one is given by the fact, that in case of the variable displacement option the overall applied torque increases limiting the minimum stiffness value. To be able to lower it again, stage 2 torque has to be varied. The static operating point is as mentioned before for the 4-cylinder engine at 250 Nm and for the 2-cylinder engine (or 2-cylinder activation) at 125 Nm. Stage 2 torque should be a value in between to avoid multiple stage to stage transitions during normal operation. Two options have been tested:

3<sup>rd</sup> modification:

- $k_1=2.8\text{Nm}/^\circ$  from ca.  $1^\circ$
- $k_2=6\text{ Nm}/^\circ$  from  $53.57^\circ/150\text{ Nm}$

4<sup>th</sup> modification:

- $k_1=2.4\text{ Nm}/^\circ$  from ca.  $1^\circ$
- $k_2=5.6\text{Nm}/^\circ$  from  $58.33^\circ/140\text{ Nm}$

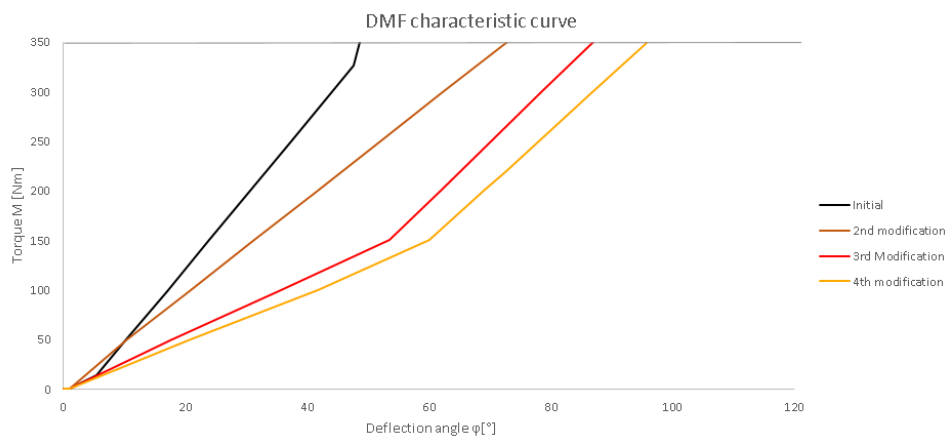


Figure 6.4.5 - DMF characteristic curve the initial state and all modifications

In Figure 6.4.5 are the characteristic curves for the initial state and all 3 modifications of the 2 stage DMF. The results for all of them will be compared in the sections bellow.

## 2-cylinder activation result comparison

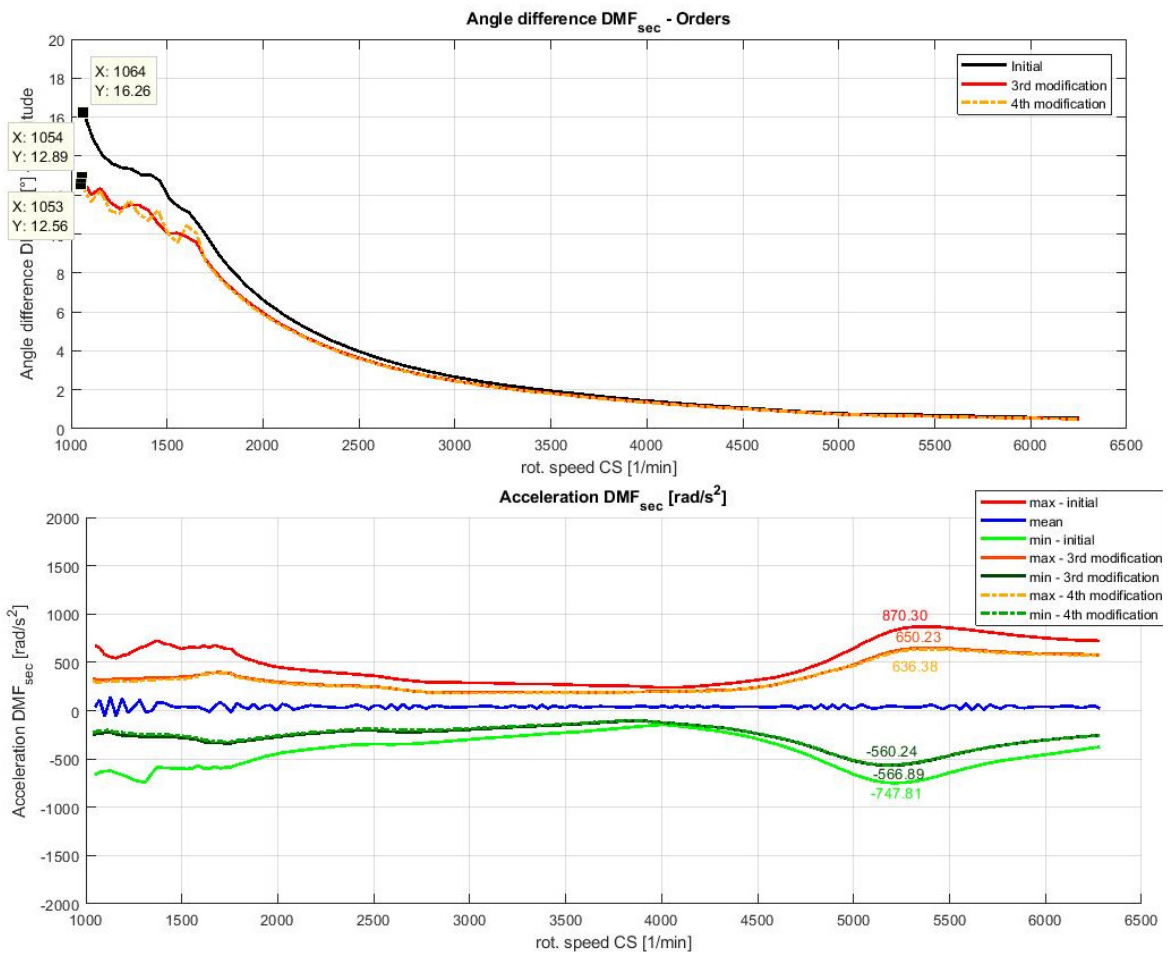


Figure 6.4.6 - Comparison of the angle difference (top) and acceleration (bottom) for the DMF sec. inertia - initial vs. 3<sup>rd</sup> and 4<sup>th</sup> modification- 2-cylinder activated

In Figure 6.4.6 is the comparison of the initial state with the 3<sup>rd</sup> and 4<sup>th</sup> modification for the angle difference and acceleration. A significant improvement compared to the initial state is visible for both values although the difference between the 3<sup>rd</sup> and 4<sup>th</sup> modification is very low. The 4<sup>th</sup> modification has in the amplitude comparison the lowest values and is therefore most suitable.

All maximum amplitude values and the improvement percentage compared to the initial state are collected in Table 6.4-1. For acceleration the maximum amplitude at the resonance frequency was used. During lower velocities even greater improvement of about 40% has been achieved:

Table 6.4-1 - Comparison of all modifications for 2-cylinders activated

2-cylinder act.	Angle difference [°]	Improvement [%]	Acceleration [rad/s <sup>2</sup> ]	Improvement [%]
Initial state	16.26	--	870.48	--
2 <sup>nd</sup> modification	13.85	14.82	679.09	21.99

3 <sup>rd</sup> modification	12.89	20.73	650.23	25.30
4 <sup>th</sup> modification	12.56	22.75	636.38	26.89

#### 4-cylinder activation result comparison

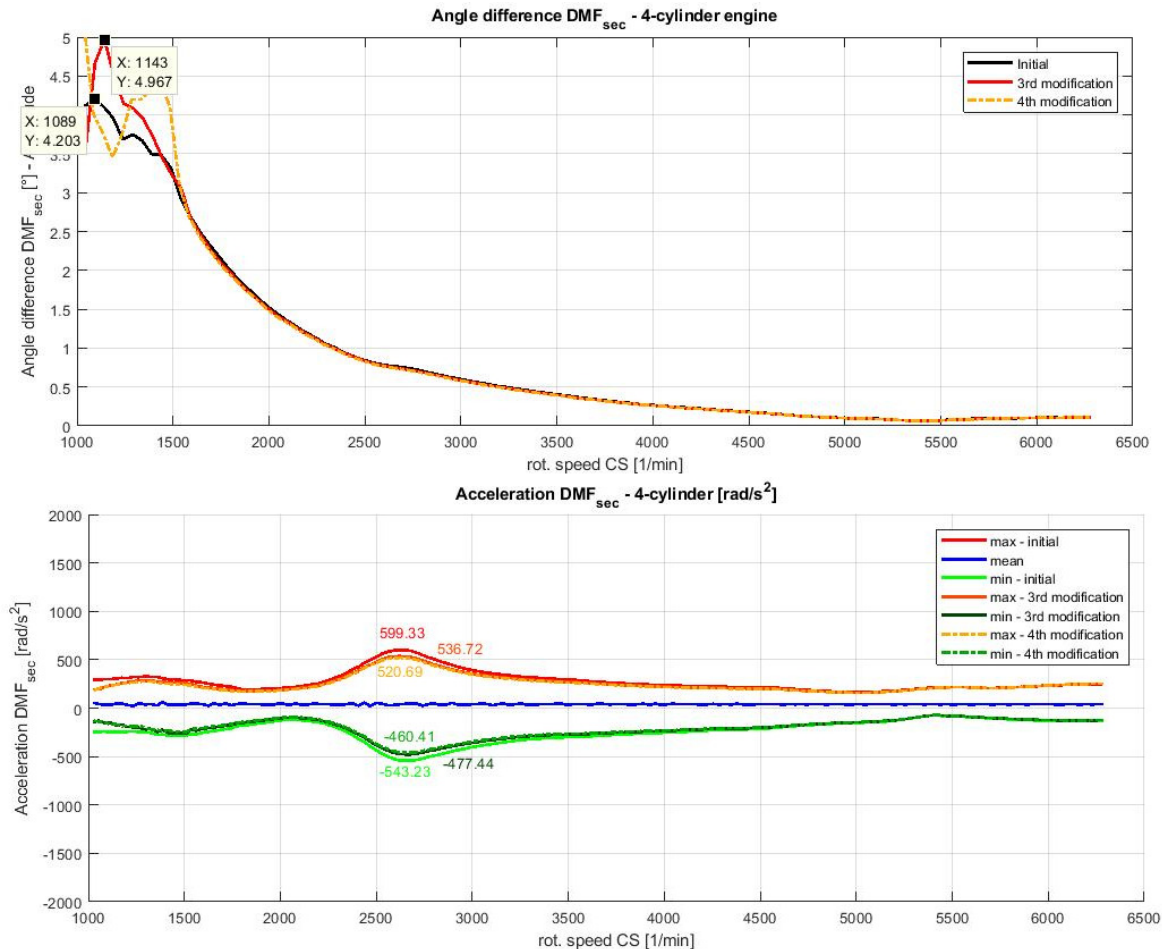


Figure 6.4.7 - Comparison of the angle difference (top) and acceleration (bottom) for the DMF sec. inertia - initial vs. 3<sup>rd</sup> and 4<sup>th</sup> modification- 4-cylinder activated

In Figure 6.4.7 (top) is the comparison of the angle difference, in the bottom of the acceleration for the initial state, 3<sup>rd</sup> and 4<sup>th</sup> modification for the 4-cylinder activation. Although the stiffness has been lowered considerably, for the angle difference is still a substantial deterioration visible. The best results for the angle difference between primary and secondary DMF inertia were achieved by the initial DMF settings with a first stage torque 14 Nm. This value is being overcome immediately after run-up and the DMF transfers to the second stage. Therefore for the 4-cylinder engine angle difference can be concluded that higher stiffness in the first stage is more favorable. Also the 1<sup>st</sup> modification with a higher stiffness in stage one was showing better results than the remaining modifications. The reasons will be discussed later. All modifications and the improvement compared to the

initial state are in Table 6.4-2. As before, for acceleration the maximum amplitude at the resonance frequency was used:

Table 6.4-2 - Comparison of all modifications for 2-, and 4-cylinders activated

4-cylinder act.	Angle difference [°]	Improvement [%]	Acceleration [rad/s <sup>2</sup> ]	Improvement [%]
Initial state	4.20	--	599.33	--
2 <sup>nd</sup> modification	4.60	-9.52	565.33	5.57
3 <sup>rd</sup> modification	4.97	-18.33	536.72	10.45
4 <sup>th</sup> modification	5.00	-19.04	520.69	13.12

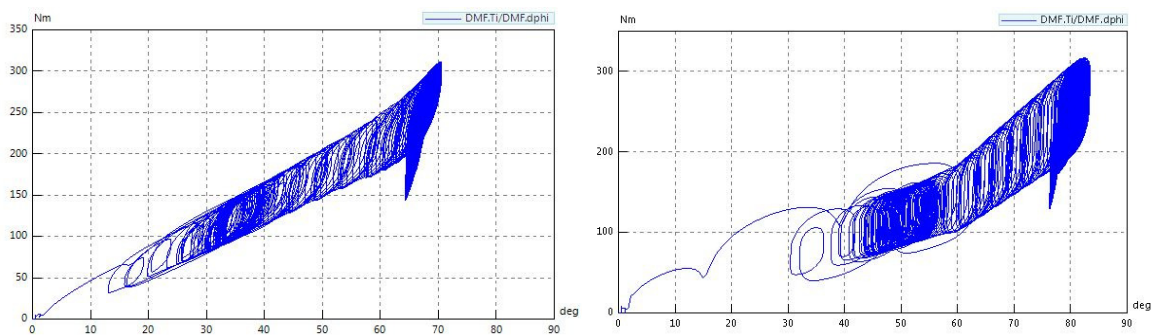


Figure 6.4.8 - 3<sup>rd</sup> (left) and 4<sup>th</sup> (right) modification DMF characteristic curve

The end stop has not been reached in neither of the modifications (Figure 6.4.8).

## 6.5. Chapter Conclusions

As expected are the optimization results for the 2-cylinder activation from bigger significance than for 4-cylinder activation. Improvement up to around 30% has been achieved by DMF modification and variation. For the 2-cylinder activation improvement for the angle difference between primary and secondary inertia is apparent as well as for acceleration. On the other hand for the 4-cylinder activation the result is somehow different. Angle differences have been found out to have better values for the initial DMF setting. This could be due to the two effects which start to emphasize when modifying the stiffness. When lowering the stiffness, the spinning movement between the primary and secondary DMF inertia increases. At the same time the natural frequency of the system is lowered resulting in a higher frequency ratio. This causes a shift of the powertrain in the overcritical area (Figure 4.1.2). For 2-cylinder activation is the described effect from bigger significance due to its initial position in the critical area. The 4-cylinder engine in contrast is already in the overcritical area. Decrease of the natural frequency has low potential effect and the increased spinning movement between primary and secondary DMF inertia starts to be from bigger importance. Resulting is a worsening angle difference as visible in Figure 6.3.4 (top), Figure 6.4.2 (bottom) and Figure 6.4.7 (top). Besides the angle difference a low improvement for the secondary inertia acceleration has been found.

For an engine with variable displacement, different settings have been tested. Even though a deterioration of 19% was noted for the 4<sup>th</sup> modification, for all other parameters greater improvement has been found. The angle differences during 2-cylinder activation are about three times larger compared to the 4-cylinder, therefore the degradation caused by the modification can be neglected. An average improvement of 15-20% has been achieved.

## 7. Conclusions

---

In the first part of the master thesis an introduction to hybrid vehicles, passenger vehicle side shafts and dual-mass flywheels has been made. Dimensioning for both side shaft and a three stage DMF has been conducted depending on a given installation space and an excel file for calculation created to ease the dimensioning process. For the DMF parameters provided by the company IAV have been used and for these the dimensions of the DMF springs have been calculated.

In the second part NVH in hybrid vehicle specific operating conditions (accounts mostly for the hybrid start) and components affecting NVH have been presented. A powertrain for 4-cylinder engine passenger P2-hybrid vehicle in the program SimulationX has been created to simulate these operating conditions and to subsequently perform a modal analysis highlighting all powertrain natural frequencies. Time domain analysis for the chosen operating conditions has been conducted:

- Idle (rattle)
- Hybrid start/tow launch
- Cycling
- Run-up part load/full load&rattle

During idle, two states with and without DMF have been tested to understand its influence. Although more oscillation and bigger forces acting on the teeth flanks are visible, no rattle for both has been detected. Therefore no action has to be taken.

For the hybrid start different parameters having influence on the dynamic development have been analyzed and evaluated. When the clutch starts to close and torque transmission begins, influence of the clutch transition time, clutch torque and extra tow torque supplied by the electric motor is visible. To obtain as favorable behavior as possible, a compromise for the clutch transition time and appropriate regulation has to be integrated. A practicable possibility is a simultaneous development of the tow- and clutch torque, while the clutch torque should be slowly increasing during the closing process and reach its maximum value necessary for the engine torque transmission after the clutch is already completely engaged. How fast torque rises has to be defined whilst considering the performance loss depending on it. High torques in the starting phases of the engagement process cause oscillation and higher losses due to conversion into frictional energy.

Cycling has been shown to excite vehicle jerking in both tip-in and tip-out situation in the second gear. As expected, the angular velocity amplitudes in the 2<sup>nd</sup> gear are much higher than for 5<sup>th</sup> gear. Dependency on the torque transmission to the wheels and gear dependent rising inertia can be used as an explanation. The easiest way to reduce these effects is to regulate the drivers wish before sending it to the actuator device to lower the load change gradient. This would have negative effect on the vehicle response dynamics and could be

negatively perceived by the driver. On the other hand jerking appears only during lower shifted gears in which the vehicle velocity is also low and a retard wouldn't have as much impact as during higher shifted gears and vehicle velocities.

A good method to detect natural frequencies affected and appearing during normal vehicle operation is the simulation of vehicle run-up. In this case the engine velocity range from 1000-6300 rpm has been analyzed for the fourth and fifth gear. In fourth gear excitation of the natural frequency at 188 Hz for the 2<sup>nd</sup>, 4<sup>th</sup> and 6<sup>th</sup> engine order have been detected. From these is the 2<sup>nd</sup> order from lowest importance since for 188 Hz it appears at an engine velocity of 5640 rpm and therefore won't be frequently reached during normal vehicle operation. The 4<sup>th</sup> and 6<sup>th</sup> engine order are in this case from bigger importance and modification should be considered. This could be done by increasing the hollow shaft (input shaft 2) and output shaft stiffness which have major influence.

In 5<sup>th</sup> gear excitement at 87 Hz appears in this case only for the 2<sup>nd</sup> engine order which corresponds 2610 rpm. Similarly as before is the full shaft (input shaft 1) stiffness responsible for this natural frequency. This is due to the distance between the clutch and gears on the input shafts. An increase of the stiffness could be simply achieved by either rearrangement of the gears on the shafts, by choosing a different material or by increasing the shaft diameter.

For the hybrid run-up rattle has been detected. Its cause has been analyzed in section 5.4.5. The biggest impact could be achieved by DMF modification. If the decoupling effect would be increased and thus the amplitude at the transmission input lowered also the loose gear movement could be decreased to a magnitude where no more rattle appears.

In the last part of the master thesis and attempt of optimization of the DMF has been made. The given parameters for the 4-cylinder passenger vehicle powertrain were already optimized for operation and therefore only low improvement can be achieved. For this, operation of an engine with variable displacement has been included. The lowest possible stiffness values for all modifications have been detected using the excel DMF calculation file presented in section 3.2. A single stage DMF for 2-cylinder and 4-cylinder activation has been tested. For 2-cylinder activation improvement up to 30% has been achieved by modification. Other for 4-cylinder activation. As expected, lower improvements could be made by up to 15%. When considering both operation possibilities, a two stage bow spring with three different stiffness and torque stage settings has been observed. Lowering stage 1 torque and the respective possibility to lower also stage 1 stiffness has shown even bigger improvement for 2-cylinder operation; about 40% compared to the initial setting. When all 4 cylinders are activated, deterioration of the angle difference increases with decreasing spring stiffness in stage 1. Since the angles compared to the 2-cylinder operation are significantly lower, this effect can be neglected. The acceleration amplitude has shown 13% improvement, a lower value than for the one stage DMF. This is due to the fact that the 4-cylinder engine operates in second stage at 250 Nm and in case of a one spring DMF a lower stiffness can be achieved than for the two stage DMF.

Another step would be to test the final DMF modification also for the remaining operating conditions mentioned in this thesis to inspect whether no deterioration occurs. Further optimization would show only slight improvement and other variants of DMF would have to be considered to improve the dynamic behavior especially during low engine velocities. DMFs are still a developed and researched component and probably many more varieties are going to be presented in the years to come.

## Bibliography

- [1.] Ramachandran, S. and Stimming, U. Royal Society of chemistry. [Online] September 2015. <http://pubs.rsc.org/en/content/articlehtml/2015/ee/c5ee01512j>.
- [2.] Stanford Edu. [Online] Stanford University, December 2011. <http://large.stanford.edu/courses/2011/ph240/goldenstein2/>.
- [3.] Crastan, V. *Elektrische Energieversorgung 2*. Berlin : Springer, 2009.
- [4.] hybrid-vehicle.org. [Online] <http://www.hybrid-vehicle.org/hybrid-vehicle-definition.html>.
- [5.] Jonasson, Karin. *Analysing Hybrid Drive System Topologies*. Sweden : s.n., 2002.
- [6.] Görke, D. *Untersuchungen zur kraftstoffoptimalen Betriebsweise von Parallelhybridfahrzeugen und darauf basierende Auslegung regelbasierter Betriebsstrategien*. Wiesbaden : Springer, 2016.
- [7.] Kirchner, E. *Leistungsübertragung in Fahrzeuggetrieben*. Berlin : Springer, 2007.
- [8.] Seherr-Thoss, H. Ch., Schmelz, F. and Aucktor, E. *Universal Joints and Driveshafts - Analysis, Design, Applications*. Berlin : Springer, 2006.
- [9.] Hughes, T. *Power Transmission and Bearing Handbook*. s.l. : Industrial Publishing Co., 1976.
- [10.] Dresig, H. and Holzweißig, F. *Maschinendynamik*. Berlin : Springer, 2006.
- [11.] Reik, W., Seebacher, R. and Kooy, A. *Das Zweimassenschwundgrad*.
- [12.] Schaeffler. *Dual Mass Flywheel - Technology/Failure Diagnosis, Special Tool/ User Instructions*. s.l. : Schaeffler Automotive Aftermarket GmbH, 2013.
- [13.] Kolomiets, A. *Rešerše použití karbonových poloos pro vůz Formula Student*. Prague : s.n., 2015.
- [14.] Patil, Ch., Imale, S., Hiware, K. und Tiwalkar, S. *Design and analysis of telescopic halfshaft for an all-terrain vehicle*. Aurangabad, India : s.n., 2016.
- [15.] Sauer, B. *Konstruktionselemente des Maschinenbaus 1*. Kaiserslautern : Springer, 2016.
- [16.] Semantic scholar. *Modeling and torque estimation of an automotive Dual Mass Flywheel*. [Online] June 2009. <https://pdfs.semanticscholar.org/3218/72358951ff30f97ed08bf28262a9cc152515.pdf>.
- [17.] Albers, A. *Advanced Development of Dual Mass Flywheel Design - Noise Control for Today's Automobiles*. Karlsruhe : s.n., 2016.
- [18.] Herbert Wittel, Dieter Muhs, Dieter Jannasch, Joachim Voßiek. *Roloff/Matek Maschinenelemente*. Wiesbaden : Vieweg+Teubner, 2011.

- [19.] Singh A., Bharadwaj S. and Narayan S. Engine oscillations [Online] 2016.  
<https://hrcak.srce.hr/file/238919>.
- [20.] Zeller, P. *Handbuch Fahrzeugakustik - Grundlagen, Auslegung, Berechnung, Versuch*. Munich : Springer, 2018.
- [21.] Mastinu, G., und Ploechl, M. *Road and OFF-Road Vehicle System Dynamics*. Boca Raton, Florida : CRC Press, 2014.
- [22.] Publications, Imech Event. *Vehicle Noise and Vibration*. s.l. : John Wiley&Sons Inc, 2002.
- [23.] *Analysis of various NVH sources of combustion engines*. Singh A., Bharadwaj S., Narayan S. India : s.n., 2016.
- [24.] Bourgois, G. *Dual Mass Flywheel for Torsional Vibrations Damping*. Sweden : s.n., 2016.
- [25.] Think Fast Engineering LLC. [Online] October 2012.  
<http://thinkfastengineering.com/2012/10/tripod-clocking/>.
- [26.] Huemer, M. *Akustische basis für Fahrzeugantriebe NVH Entwicklung*. Graz : s.n., 2017.
- [27.] Wiesinger, J. <https://www.kfztech.de/gast/schubert/dsg.htm>. [Online] march 2018.

List of tables

Table 3.2-1 – Torsion damper requirements ..... 33

Table 3.2-2 – spring 1 calculation parameters..... 35

Table 3.2-3 - spring 2 calculation parameters..... 41

Table 3.2-4 - spring 3 calculation parameters..... 43

Table 5.2-1 - parameters of the analysed vehicle..... 55

Table 5.2-2 - elements included in the simulation model ..... 60

Table 5.2-3- Simulation settings..... 61

Table 5.3-1 - natural frequencies (P2 hybrid) ..... 66

Table 6.4-1 - Comparison of all modifications for 2-cylinders activated ..... 101

Table 6.4-2 - Comparison of all modifications for 2-, and 4-cylinders activated..... 103

## List of figures

Figure 2.1.1- Series hybrid transmission scheme.....	15
Figure 2.1.2 - Parallel hybrid transmission scheme .....	15
Figure 2.1.3 - Parallel hybrid powertrain distinction depending on the EM position (6).....	17
Figure 2.2.1 - Hooke's jointed shaft in a Z-configuration and diagrammatic representation of the system elements .....	18
Figure 2.2.2-simple universal joint (left) and the double Cardan's joint concept (right).....	19
Figure 2.3.1 – Effect of the DMF (8) .....	21
Figure 2.3.2 – Planetary DMF (8).....	23
Figure 2.3.3- Components of a standard DMF .....	23
Figure 2.3.4- DMF with straight pressure springs on the outer (both) and inner radius (inner damper-right) .....	25
Figure 2.3.5 - From left: single-stage, two-stage and three-stage arc spring.....	26
Figure 2.3.6 – Initial position - Torque starts to act on the DMF -> spring 1 (yellow) starts to deflect.....	27
Figure 2.3.7 - Stage 1 torque reached -> spring 1 (yellow) has same length as spring 2 (red), when torque increases spring 1 and 2 start to deflect equally .....	27
Figure 3.2.1 – Radial forces acting on the spring guides (left) (12) and forces acting on spring coils and absorption areas (WFP) (right).....	31
Figure 3.2.2 –Torsion at different engine speeds (12).....	32
Figure 3.2.3 - Spring rate (left) and friction damping (right) as function of engine speed and vibration angle for a 2.5l diesel(13) .....	34
Figure 3.2.4 - DMF stopper and free angle (8).....	36
Figure 3.2.5 - Spring arrangement in stage 3 .....	37
Figure 3.2.6 - DMF characteristic curve .....	38
Figure 4.1.1 - Rotational speed and torque in hybrid specific operating conditions.....	46
Figure 4.1.2 - Ideal isolation for different damping values ( $V_2$ =amplification function, $\eta$ =frequency ratio).....	49
Figure 5.2.1 - P2 hybrid arrangement .....	55
Figure 5.2.2 - DMF settings in SimulationX .....	56
Figure 5.2.3 - MBS simulation model - engine side.....	57
Figure 5.2.4 - MBS simulation model - transmission side .....	58
Figure 5.2.5 - dual-clutch transmission with selected 2nd gear (25).....	59
Figure 5.2.6 - Engine pressure characteristic – zero load (left), full load (right) .....	62
Figure 5.2.7 - Clutch torque (left) and electric motor torque (right) timing.....	63
Figure 5.2.8 - Load change curve .....	64
Figure 5.2.9 - Run-up - Time settings .....	65
Figure 5.3.1 - f1 - for the 2 <sup>nd</sup> gear – jerking natural mode (top), potential energy (bottom) ..	67
Figure 5.3.2 - f2 - DMF natural mode (top), potential energy (bottom).....	68
Figure 5.3.3 - f3 – side shafts and wheels twist against each other (top), potential energy (bottom) .....	68

Figure 5.3.4 – f6 - Wheels oscillate against transmission (top), potential energy (bottom) ...	69
Figure 5.3.5 – f7 - Right and left side shaft and wheels twist against each other(top), potential energy (bottom).....	70
Figure 5.3.6 – f10 - Lower differential natural mode (top), potential energy (bottom).....	70
Figure 5.3.7 – f12 - Side shaft swing against each other (top), potential energy (bottom) ....	71
Figure 5.4.1 - Position difference and normal tooth flank force without DMF (left) and with DMF (right) .....	72
Figure 5.4.2 - Electric motor (light blue) and DMF secondary side (dark blue) angular velocity with 15 Nm (left) and 80 Nm (right) clutch torque.....	73
Figure 5.4.3 - Clutch torque withdrawal for 15 Nm (left) and 80 Nm (right).....	73
Figure 5.4.4 - Electric motor (light blue) and DMF secondary side (dark blue) angular velocity with 0.1 s (left) and 1 s (right) clutch closing time.....	74
Figure 5.4.5 - Power loss for 0.1 s (left) and 1 s (right) clutch closing time.....	74
Figure 5.4.6 - Electric motor angular velocity for 0 Nm (left) and 15 Nm (right) torque increase during clutch closure.....	75
Figure 5.4.7 - Cycling - angle difference DMF arc spring – second gear .....	76
Figure 5.4.8 - Cycling 2 <sup>nd</sup> gear - angular velocity at the DMF primary side and secondary side (left) and clutch (right) .....	76
Figure 5.4.9 - Cycling 2 <sup>nd</sup> gear - DMF torque (left) and DMF characteristic curve (right).....	77
Figure 5.4.10 – Cycling 4 <sup>th</sup> gear - angular velocity at the DMF primary side and secondary side (left) and clutch (right) .....	77
Figure 5.4.11 - Cycling 5th gear – clutch angular velocity (left) and DMF characteristic curve (right) with $c_2=3\text{Nm/deg}$ .....	78
Figure 5.4.12 - Fourth gear power path .....	78
Figure 5.4.13 - Deflection and potential energy (4th gear) .....	79
Figure 5.4.14 - 4th gear full load Campbell diagram (top and middle) for DMF secondary side angle difference (top - left), speed difference (top - right), acceleration (middle – left); full shaft acceleration (middle – right) and amplitude analysis (bottom) - DMF (left), full shaft (right).....	80
Figure 5.4.15 - 4th gear full load order analysis.....	81
Figure 5.4.16 - 4th gear part load Campbell diagram - DMF (left), full shaft (right).....	81
Figure 5.4.17 - Fifth gear power path.....	82
Figure 5.4.18 - Deflection and potential energy (5th gear) .....	82
Figure 5.4.19 – 5 <sup>th</sup> gear full load Campbell diagram (left) order analysis (right).....	83
Figure 5.4.20 – 5 <sup>th</sup> gear part load Campbell diagram (left) order analysis (right) .....	83
Figure 5.4.21 – 5 <sup>th</sup> gear amplitude - part load (left) vs. full load (right) .....	84
Figure 5.4.22 - Position difference (left) and normal tooth flank force (right) for the 1st gear pair (top) and 5th gear pair (bottom) .....	85
Figure 5.4.23 - Position difference (top) and normal tooth flank force (bottom) at 20% (left), 60% (middle) and 100% (right) 1 <sup>st</sup> gear pair .....	85

Figure 6.1.1 - Forces acting on the pistons for 2-cylinder activation (left) and 4-cylinder activation (right).....	89
Figure 6.1.2 – 5 <sup>th</sup> gear comparison of angle, velocity and acceleration Campbell diagram for 4-cylinder activation (left) and 2-cylinder activation (right).....	90
Figure 6.1.3 - 5th gear angle difference amplitude comparison for 2-cylinder and 4-cylinder activation.....	91
Figure 6.1.4 – 2-cylinder activation order analysis (top) of secondary inertia acceleration and DMF characteristic curve for initial values (bottom) 5 <sup>th</sup> gear.....	92
Figure 6.1.5 - Comparison engine torque (top) and right side shaft torque (bottom) for 4-cylinder (left) and 2-cylinder (right) activation.....	93
Figure 6.2.1 - Determination of the lowest possible stiffness.....	94
Figure 6.2.2 – Angle difference of the DMF sec. inertia with one stage DMF $k=3 \text{ Nm/}^\circ$ .....	94
Figure 6.2.3 – Comparison of the acceleration of the DMF sec. inertia - initial DMF vs. one stage DMF with $k=3 \text{ Nm/}^\circ$ .....	94
Figure 6.2.4 – Comparison DMF characteristic curve for initial state (left) and 1 <sup>st</sup> modification (right) – 2-cylinder engine.....	95
Figure 6.3.1 - Initial state DMF characteristic for 4-cylinder engine.....	95
Figure 6.3.2 - Determination of the lowest possible stiffness for the 4-cylinder engine.....	96
Figure 6.3.3 – 1 <sup>st</sup> modification DMF characteristic for 4-cylinder engine.....	96
Figure 6.3.4- Comparison of the angle difference (top) and acceleration (bottom)for initial state vs. 1st modification (one stage DMF).....	97
Figure 6.4.1 - Determination of the lowest possible stiffness for engine with variable displacement.....	98
Figure 6.4.2 – Comparison of the angle difference of the DMF sec. inertia for 2-cylinder (top) and 4-cylinder activation (bottom) - initial setting vs. 2 <sup>nd</sup> modification.....	98
Figure 6.4.3 - Comparison of the acceleration for the DMF sec. inertia - initial vs. 2 <sup>nd</sup> modification – 2-cylinder activated.....	99
Figure 6.4.4 - Comparison of the acceleration for the DMF sec. inertia - initial vs. 2 <sup>nd</sup> modification – 4-cylinder activated.....	99
Figure 6.4.5 - DMF characteristic curve the initial state and all modifications.....	100
Figure 6.4.6 - Comparison of the angle difference (top) and acceleration (bottom) for the DMF sec. inertia - initial vs. 3 <sup>rd</sup> and 4 <sup>th</sup> modification- 2-cylinder activated.....	101
Figure 6.4.7 - Comparison of the angle difference (top) and acceleration (bottom) for the DMF sec. inertia - initial vs. 3 <sup>rd</sup> and 4 <sup>th</sup> modification- 4-cylinder activated.....	102
Figure 6.4.8 - 3 <sup>rd</sup> (left) and 4 <sup>th</sup> (right) modification DMF characteristic curve.....	103

## List of appendices

Appendix 1

Appendix 2

Appendix 3

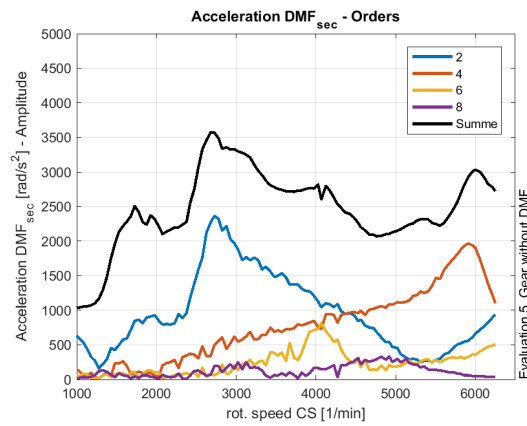
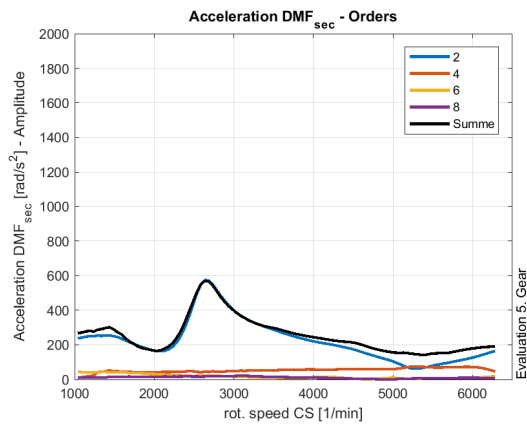
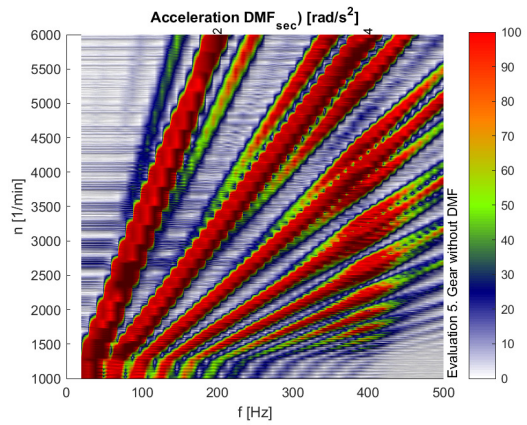
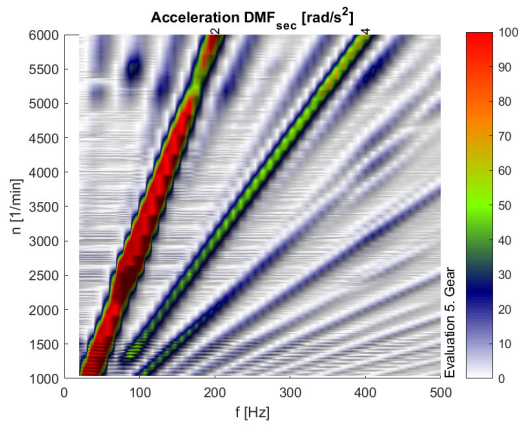
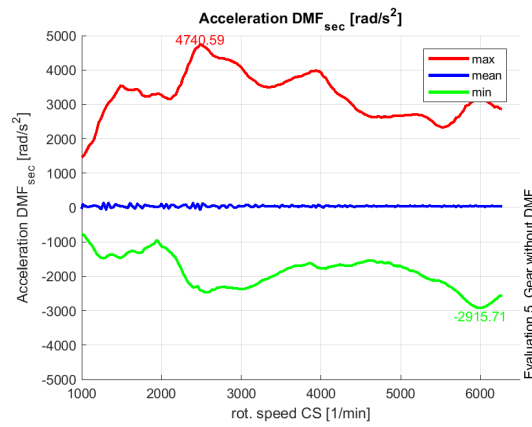
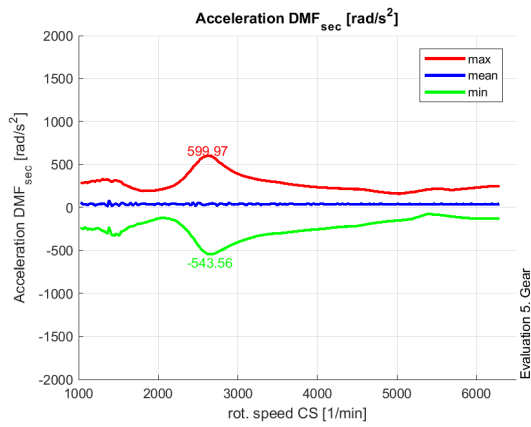
Appendix 4

For the elaboration of the work following software has been used:

- Microsoft Office Word and Excel 2010
- SimulationX 3.9
- MATLAB R2017b

# Appendix 1

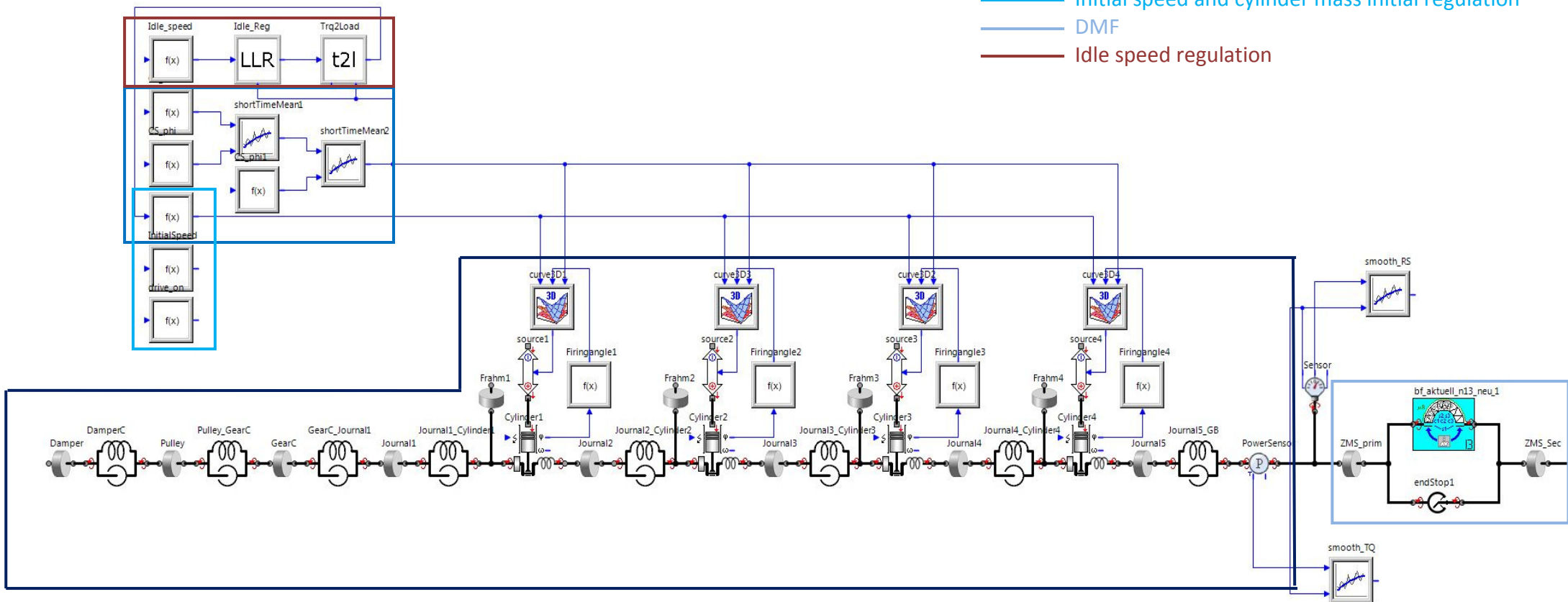
Comparison of run-up simulation in 5<sup>th</sup> gear of powertrain with and without DMF.



## Appendix 2

Simulation model for the operating condition – idle – rattle and run-up – rattle, engine side

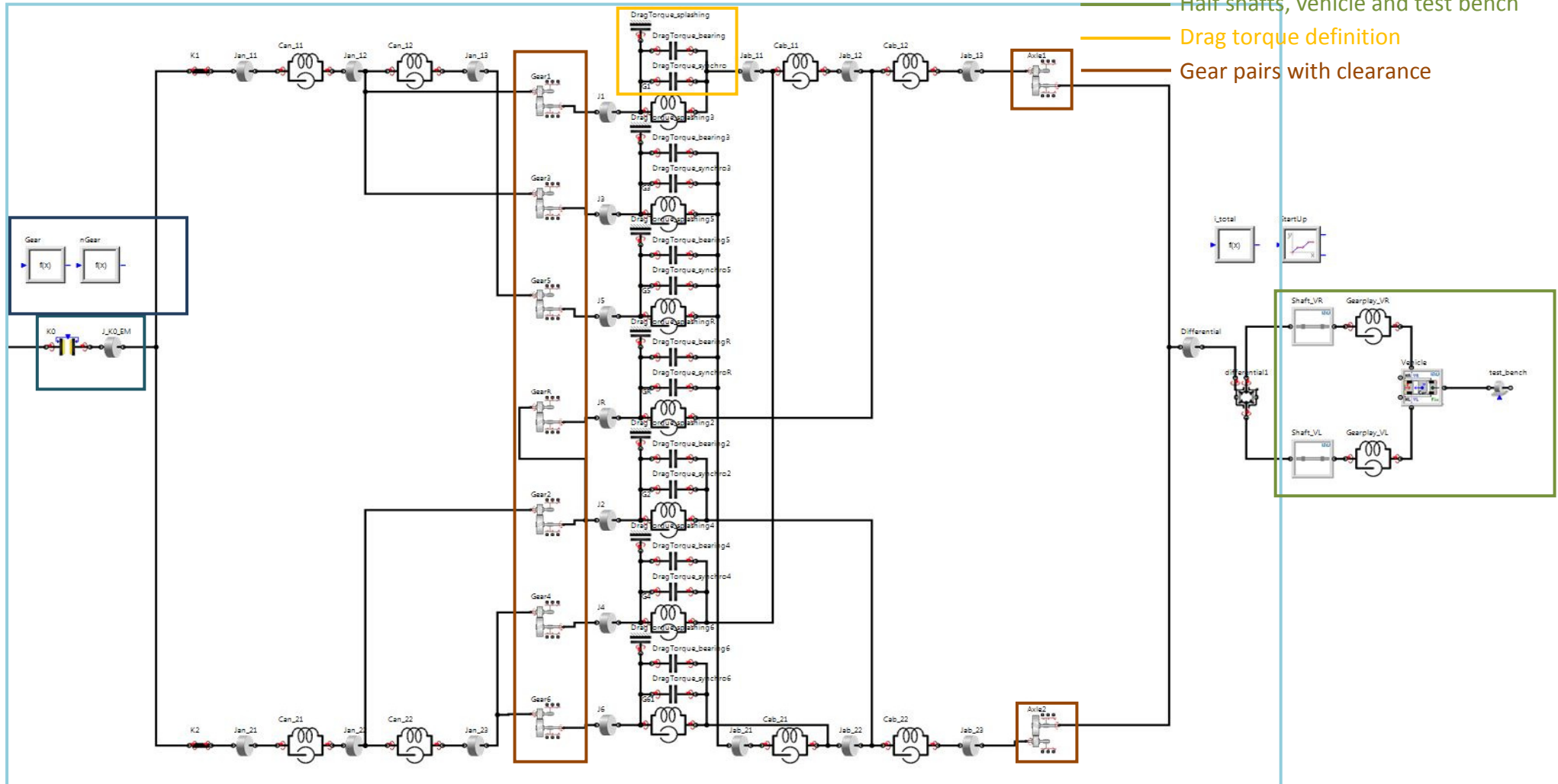
- Internal combustion engine
- Load regulation and angle signal
- Initial speed and cylinder mass initial regulation
- DMF
- Idle speed regulation



### Appendix 3

Simulation model for the operating condition – idle – rattle and run-up – rattle, transmission side

- Clutch and electric motor inertia
- Dual-clutch transmission
- Gear selection
- Half shafts, vehicle and test bench
- Drag torque definition
- Gear pairs with clearance



# Appendix 4

Simulation model for the operating condition – hybrid start, transmission side

- Clutch and electric motor inertia
- Dual-clutch transmission
- Gear selection
- Half shafts, vehicle and test bench
- Electric motor torque and clutch regulation

